Emergent symmetries in relativistic Quantum Phase Transitions

Inaugural-Dissertation
zur
Erlangung des Doktorgrades
der Mathematisch-Naturwissenschaftlichen Fakultät
der Universität zu Köln

vorgelegt von
Jesús Emilio Torres Ospina

aus
Bogotá, Kolumbien

Köln, 2019

Berichterstatter: PD Dr. Michael Scherer
Prof. Dr. Achim Rosch

Tag der mündlichen Prüfung: 03.05.2019

Abstract

This work deals with quantum phase transitions in Dirac systems where the symmetries involved play a key role in the nature of the transition and are enlarged at criticality. By using functional renormalization group (FRG) methods, we show that an emergent relativistic symmetry not present at the bare level is a common feature of several different kinds of phase transitions. In three different projects, the interplay of emergent symmetries and universality in critical phenomena are explored through FRG techniques. In the first project, we studied the relation between discrete symmetry breaking and the emergence of two diverging length scales with their respective critical exponents. A second project explored the relation between multicritical points where two adjacent symmetry-breaking phases are compatible and the possibility of a continuous, order-to-order transition. The third and final project was concerned with the persistence of chiral symmetry in three-dimensional quantum electrodynamics - here seen as an effective description of different condensed matter systems - for the lowest possible number of fermion flavours, as well as with a dual description that has the potential to provide exact results for this strongly correlated theory.

Kurzzusammenfassung

Diese Arbeit befasst sich mit Quantenphasenübergängen in Dirac-Systemen, bei denen die auftretenden Symmetrien eine entscheidende Rolle für das kritische Verhalten am Übergang spielen. Wir verwenden Funktionale Renormierungsgruppen Technicken (FRG) um zu zeigen, dass eine emergente relativistische Symmetrie ein gemeinsames Merkmal mehrerer verschiedener Arten von Phasenübergänge ist. In drei verschiedenen Projekten, wurde das Wechselspiel zwischen emergenten Symmetrien und Universalität durch FRG Technicken untersucht. Das erste Projekt befasste sich mit dem Zusammenhang zwischen diskreter Symmetriebrechung und dem Auftreten von zwei divergierenden Längenskalen sowie deren zugehörigen kritischen Exponenten. Im zweiten Projekt wurde die Verbindung zwischen multikritischen Punkten an denen zwei symmetriebrechende Phasen kompatibel sind und die Möglichkeit eines kontinuierlichen Ordnung-zu-Ordnung Übergangs beleuchtet. Das dritte und letzte Projekt befasste sich mit dem Bestehenbleiben chiraler Symmetrie in dreidimensionaler Quantenelektrodynamik, die hier gesehen werden kann als eine effektive Beschreibung verschiedener Festkörpersysteme, für die niedrigst mögliche Anzahl von Fermionenarten als auch mit einer dualen Beschreibung, die das Potenzial hat exakte Ergebnisse für die stark korrelierte Theorie zu liefern.

Contents

Chapter 1

Introduction

Understanding phase transitions and the critical phenomena associated to them has been a major driving force in the quest for unveiling which states of matter Nature allows and one part of fundamental physics that seems to continue to provide fruitful insights into the inner workings of our universe. The technological prowess of the last few decades has, moreover, allowed us to experiment with phenomena that were before, perhaps, thought to be only of academical interest, for they were not readily available in Nature. A prime example of this sort of development was the production in 2004 of a free standing two dimensional structure made of carbon atoms: graphene [1]. In fact, twenty years earlier, the first suggestions of an emergent relativistic low energy behaviour in graphite sheets had already been made [2, 3] and with these, the first attempts at understanding the possible phases in the system and the transitions between them.

Amongst the first interesting phenomena to be explored theoretically was that of breaking of chiral symmetry in graphene, and its related anomaly [3]. Chiral symmetry breaking is, however, a feature of strongly interacting systems (like QCD_4), and graphene's realization of a three dimensional Dirac fermion is known for being very good at screening the electromagnetic interaction (at charge neutrality), due to the vanishing of the density of states at the Dirac point [4]. Lucky for us, the condensed matter setting allows several different interactions to be induced. These can mimic the action of a gauge field [5–7] and indeed, chiral symmetry breaking in Dirac systems can be achieved in different ways [8, 9].

One way to induce chiral symmetry breaking in graphene is by including adsorbed atoms on its surface [10–12]. In this case, the mass generation for the massless fermions is concomitant with a Kekulé distortion, and the system goes into one of three equivalent ground states, each of which can be rightly called a Kekulé Valence Bond (KVB) configuration. The first experimental realization of this phenomenon [13] was achieved with graphene grown on a copper substrate, where the long range order was observed through scanning tunneling microscopy (STM) (see FIG 1.1). Once an experimental observation of the phase is achieved, it seems only natural to consider the phenomena related to the transition *into* this phase. In fact, although some of the features of the system when it is in a KVB phase had been proposed [10–12] and partially confirmed experimentally [13], there had been considerably less effort in understanding the transition itself and the universality (or lack thereof) associated to it.

The nature of the underlying lattice and the particular ordering formed in this case are unique to the condensed matter setting (when compared to e.g. the high-energy-inspired,

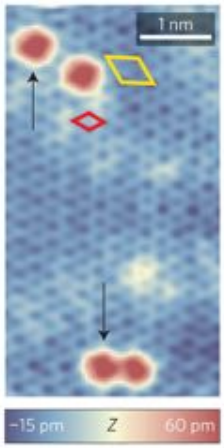

FIGURE 1.1: **Observation of Kekulé Valence Bond** patches on graphene grown on a copper substrate, as seen through STM. Figure adapted from [13].

emergent-gauge-field treatment), and play an important role for critical behaviour. Because these aspects had remained largely unexplored until recently [14–16], we set out to fill in some of the knowledge gaps in this area. In particular, we explored in detail questions like the nature of the transition (can it be considered as a first or second order transition? if the latter holds, under what conditions?) and features of the scaling behaviour of observables when the system transitions from one phase to the other. The results of this analysis comprises Chapter 3 of this work.

The critical point describing a transition into the KVB phase of graphene is only one example of what has been dubbed in the literature as a Fermion Induced Quantum Critical Point (FIQCP) [17]. As such, not only are similar symmetry breaking patterns in other Dirac systems possible, but different realizations of the kind of mass generation described here could also appear simultaneously. By this we mean that a similar mechanism as the one described above could be responsible for two *different* kinds of long range order in the *same* system. With this setting in mind, it becomes important to consider different ordering tendencies and how they interact with each other.

In the simplest setting, where the gapless, semimetallic Dirac phase could be adjacent to two gapped phases, the system exhibits a multicritical point (MCP) where all three phases meet. According to a Landau-Ginzburg description of the phase transition [18], when two adjacent phases have unrelated, independent symmetry properties, the transition between them is no longer generically[1] of second order (continuous), but is either of first order (discontinuous) or accompanied by an intermediate phase, as depicted in FIG. 1.2. One of the key features of FIQCPs is that a simple Landau-Ginzburg description in terms of order parameters *only* need not hold in a system where the low energy degrees of freedom are itinerant fermions, so the natural question arises as to whether or not these are the two only options.

Recent Quantum Monte Carlo (QMC) simulations [19] suggest that, indeed, a third option could be realized in Dirac systems: a *generic* direct, continuous, order-to-order transition. The findings in [19] moreover seem to indicate that the line separating the two phases (with broken $O(3)$ and $\mathbb{Z}_2$ symmetry, respectively) has an emergent $O(4)$ symmetry (see Fig. 4.1 in Chapter 4). A quick search through the literature points to another system where such a

[1] By this we mean, without the need to do some extra fine tuning in the parameters driving the transitions.

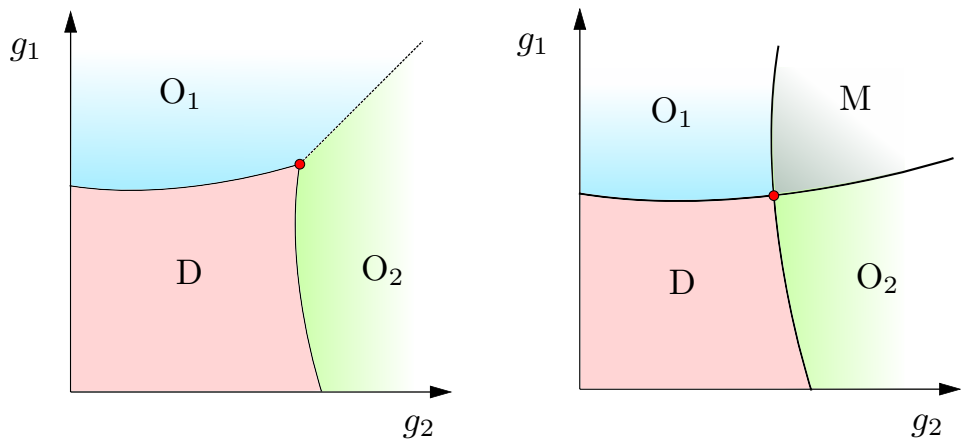

FIGURE 1.2: **Possible phase diagram** scenarios in the vicinity of a multicritical point (MCP) according to Landau-Ginzburg theory. A disordered phase (D) can reach the ordered phase $\mathrm{O}_{1/2}$ by tuning the parameter $g_{1/2}$, and these two phases meet at the MCP (the red dot). The boundary between ordered phases can be either a line of first order (discontinuous) transitions (left) or a region of coexistence (M) where both orders are mixed (right).

non-Landau transition is possible, namely a Deconfined Quantum Critical Point (DQCP) in spin-$\frac{1}{2}$ antiferromagnets on a square lattice. In that case, the critical point separating the Néel ordered phase (which breaks $O(3)$ symmetry) from the valence bond solid (VBS) phase (which breaks $O(2)$ symmetry) is more aptly described by emergent degrees of freedom (spinons) which couple to an emergent gauge field and render the transition continuous, while being confined in both of the ordered phases [20–22].

According to the numerical evidence [23], the transition there also shows an enlarged $O(5)$ symmetry at the critical point. Furthermore, recent developments in numerical simulations of similar models indicate that emergent $O(N)$ symmetries are an ubiquitous feature of DQCPs [24, 25]. One question that naturally arises is: could the emergent enlarged symmetry be a smoking gun signature for the kind of non-Landau transitions seen at DQCPs, namely, for the existence of a line of continuous order-to-order quantum phase transitions?

The first theoretical analysis of the kind of transition studied numerically in [19] confirmed [26, 27] that there is always[2] an MCP with emergent $O(N_1 + N_2)$ symmetry, if the adjacent phases break independent $O(N_1)$ and $O(N_2)$ symmetries, respectively. These works served as inspiration to explore the phase diagram of Dirac systems with two compatible, dynamically-generated masses that come about through the same mechanism as the chirality-breaking KVB phase. The results in Chapter 4 summarize our partial understanding of the phase diagram of the system.

As mentioned earlier, graphene's massless Dirac fermions can acquire a mass by the fluctuations from induced interactions, but its "natural" electromagnetic interactions are not strong enough to gap the system. This can be understood as a consequence of the fact that the system is only quasirelativistic, i.e. the velocity of fermions and of gauge degrees of freedom is not the same and the electromagnetic interactions are still allowed to propagate in 3+1 dimensions, while the emergent massless fermions are confined to move in 2+1 dimensions. In fact, the fully relativistic theory analogous to the one in graphene corresponds

[2] Terms and conditions apply. These can be found in Chapter 4.

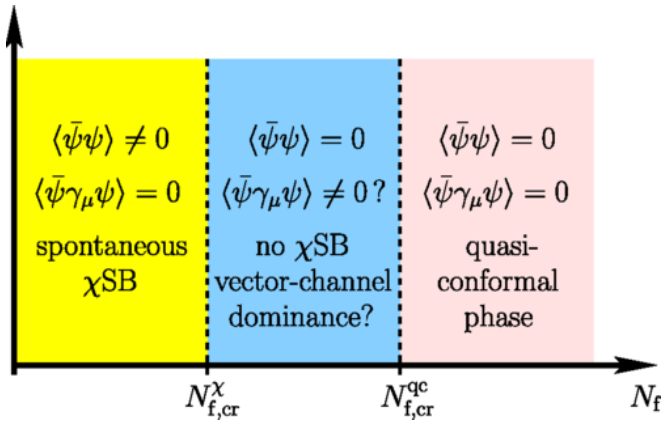

FIGURE 1.3: **Expected phase diagram of QED$_3$** as a function of number of flavours N_{f}, taken from [28]. Note that here N_{f} refers to 4-component fermions, of which the minimal number allowed is $N_{\mathrm{f}} = 1$.

to three dimensional quantum electrodynamics (QED$_3$) and is expected to exhibit spontaneous chiral symmetry breaking below a critical number of fermion flavours $N_{\mathrm{f}} < N_{\mathrm{f,c}} \sim 4.5$, as depicted in FIG. 1.3 (see e.g. [28] and references therein). Note that the low energy theory of a single sheet of graphene corresponds to a system with $N_{\mathrm{f}} = 2$ flavours of fermions.

To probe spontaneous chiral symmetry breaking in a $2+1$ dimensional Dirac system, it thus seems, we need a way to have a truly three dimensional gauge field mediated interaction. Nature[3], as luck may have it, has found a way to provide this to us in the form of an effective theory for the *surface states* of an interacting 3+1 dimensional topological insulator (TI) [29, 30]. This latter realization, however, differs in one key aspect from the usual setting where e.g. FIG 1.3 is believed to hold: where as in high energy conventions relativistic fermions are collected in *four* dimensional representations of the Clifford algebra of $\mathbb{R}^{d,1}$, their TI counterparts are made up of *two*-component fermions and, incidentally, only *one* of them. This situation can be loosely referred to as "$N_{\mathrm{f}} = 1/2$".

Because the field theory at hand (QED$_3$ at $N_{\mathrm{f}} = 1/2$) seems to also be an effective description of several condensed matter systems [31–33], it seems natural to ask: can we also expect spontaneous chiral symmetry breaking in this setting? Our attempts to provide an answer to this question are collected in the first part of Chapter 5.

The relation of QED$_3$ to one particular system, namely the half filled Landau level [33], is particularly interesting in our current setting since it more or less takes us back to square one but with "less" fermions. Concretely, it has been proposed [33–35] that the seemingly strongly interacting QED$_3$ shares the same low energy properties of (one quarter of) the free Dirac theory we started with[4]. We provide a simplified explanation of this equivalence as well as our attempt to extract universal information from it in the second part of Chapter 5.

Outline of the Thesis

The contents of this work have already been outlined in the above paragraphs and in exactly the order they appear in the thesis, with one small but important exception. Since

[3] Or theoretical physicists, depending on the point of view.

[4] Recall that the ground state of a normal graphene sheet can be described by an effective theory with $N_{\mathrm{f}} = 2$ flavours of free Dirac fermions.

the quantum phase transitions considered in Chapters 3 and 4 can be induced by diverse mechanisms, it is not at all clear from the outset that the degrees of freedom involved (i.e. the bosonic order parameters) have a low energy description in terms of relativistic dynamics. In the theoretical models used in those chapters, however, we do start from a Lorentz invariant Ansatz for the effective actions involved in which bosonic and fermionic degrees of freedom have the same velocity, $v_{\mathrm{f}} = v_{\mathrm{b}} = 1$ (in approppriate units). The justification for this choice is found in the final part of Chapter 2, right after a short recap on critical phenomena meant to set up notations and conventions and a recap of the variant of renormalization group tool used in all other chapters. Concluding remarks are gathered in Chapter 6. Appendix A contains detailed formulas used in the main text, and appendix B is a supplement to Chapter 5 and contains an alternative way to compute one of the main equations in that chapter.

Chapter 2

Phase transitions and relativistic invariance

In this chapter we discuss some of the common features that will be found in all of the problems dealt with in later chapters. In Sec. 2.1 we introduce the common language we will use to describe phase transitions, starting with a recap of widely known facts. The discussion here therefore borrows heavily from standard textbooks (e.g. [36, 37]) and is by no means extensive since it serves mainly as a way to introduce the formalism that will be applied later on. In Sec. 2.2.2 we describe our weapon of choice to tackle quantum phase transitions involving strongly interacting fermionic systems, namely the functional renormalization group. Again, the discussion is kept brief and the reader is advised to consult the literature for a more in depth treatment [38, 39]. Finally, Sec. 2.3 presents a first application of the formalism: a nonperturbative argument for emergent Lorentz symmetry at criticality in Dirac systems in $d = 2$ spatial dimensions. The contents of section 2.3 are original, unpublished work by the author and are a crucial part of the setup in later chapters.

2.1 Symmetry breaking and order parameters

A quantum system whose ground state does not have the full symmetries of the hamiltonian describing it is said to exhibit spontaneous symmetry breaking [37]. Just as in thermal phase transitions, the onset of spontaneous symmetry breaking in quantum many-body systems is accompanied by the nonanalytic behaviour of some observable quantity [36]. Let the symmetry transformations of the system be denoted by G. If the ground state $|\Psi\rangle$ is not invariant under the action of a symmetry element $g \in G$, then one can find an operator $\mathcal{O}$ transforming nontrivially under g and such that

$$\phi = \langle \mathcal{O} \rangle \neq 0 \,, \tag{2.1}$$

where $\langle \mathcal{O} \rangle := \langle \Psi | \mathcal{O} | \Psi \rangle$ is the expectation value on the ground state. The quantity ϕ will be called an order parameter for the symmetry g. If the hamiltonian depends on a dimensionless parameter $\tilde{g}$ such that the ground state is symmetric ($\phi = 0$) for values of $\tilde{g} > \tilde{g}_c$ but has broken symmetry ($\phi \neq 0$) for $\tilde{g} < \tilde{g}_c$ then the phase transition at $\tilde{g} = \tilde{g}_c$ is signaled precisely by the nonanalytic behaviour of ϕ.

Order parameters thus serve as labels to identify different phases and are therefore key to understand the phase transitions between them. Consequently, they will be the main

focus of a considerable part of this work and it will prove useful to get an intuitive feel for them. To this end, we consider a fermionic system whose time evolution is determined by the second quantised microscopic hamiltonian

$$H = H_0 + V \,, \tag{2.2}$$

where H_0 is the free part and V a two body interaction, i.e.

$$H_0 = \sum_{\alpha} \epsilon_\alpha c_\alpha^\dagger c_\alpha \tag{2.3a}$$

$$V = \sum_{\alpha_i} V_{\alpha_1,\alpha_2,\alpha_3,\alpha_4} c_{\alpha_1}^\dagger c_{\alpha_2}^\dagger c_{\alpha_4} c_{\alpha_3} \,, \tag{2.3b}$$

with α a multi-index collecting all degrees of freedom including e.g. band and/or sublattice indices and $c_\alpha^\dagger$ is an operator that creates a fermion in state α. For spinful fermions on a simple lattice, for example, $\alpha = (\vec{k}, s)$, with $\vec{k} \in U \subset \mathbb{R}^d$ is a momentum vector in the first Brillouin zone U and $s \in \{\pm 1\}$ denotes the spin projection on the z axis in units of $\hbar/2$.

Order parameters of interest for such a system can be defined as expectation values of bilinears of the original fermions, namely, combinations of the form

$$\mathcal{O}_{\alpha,\beta} = \sum_{\delta,\gamma} \widetilde{V}_{\alpha,\beta}^{\delta,\gamma} c_\delta^{(\dagger)} c_\gamma^{(\dagger)} \,, \tag{2.4}$$

where the coefficients $\widetilde{V}_{\alpha,\beta}^{\delta,\gamma}$ can be thought of as a partial decomposition of the kernel of the interacting potential V. To illustrate this last point, consider a translation invariant system of spin $1/2$ fermions, for which the bare interaction V is $SU(2)$ conserving, then $\alpha = (\vec{k}, s)$ and $V_{\alpha_1,\alpha_2,\alpha_3,\alpha_4}$ can be split as

$$V_{\alpha_1,\alpha_2,\alpha_3,\alpha_4} = U(\vec{k}_1, \vec{k}_2, \vec{k}_3)(2\pi)^d \delta(\vec{k}_1 + \vec{k}_2 - \vec{k}_3 - \vec{k}_4) S(\{\vec{\sigma}_i\}). \tag{2.5}$$

where S is a function depending on the product of spin-rotation invariant combinations $\vec{\sigma}_i \cdot \vec{\sigma}_j$ for $i, j \in \{1, \cdots, 4\}$. An analytic function S with these properties depends on the products of such combinations so that it can be further decomposed into parts commuting or anticommuting with the components of the spin operators. The coefficients of such a decomposition correspond to a choice of $\widetilde{V}$ and lead to the order parameters

$$\rho(\vec{q}) := \left\langle \sum_{\vec{k},s} c_s^\dagger(\vec{k} + \vec{q}) c_s(\vec{k}) \right\rangle \,, \tag{2.6a}$$

$$\vec{M}(\vec{q}) := \left\langle \sum_{\vec{k},s,s'} c_s^\dagger(\vec{k} + \vec{q}) (\vec{\sigma})_{s,s'} c_s(\vec{k}) \right\rangle \,, \tag{2.6b}$$

i.e., to order parameters for staggered charge density or staggered spin magnetization [40, 41]. It is worth pointing out that also order parameters of the form $\sim c^\dagger c^\dagger$ (e.g. accounting for the formation of Cooper pairs) can be written in the aforementioned form. Alternatively, one can consider order parameters starting from a given fermion bilinear and considering the kind of interactions that could give rise to nonvanishing expectation values for it. This approach, in turn, provides a way to identify the kind of interaction that leads to a breaking

of the symmetry.

First hint of universality and field theory description When the phase transition is such that $\phi = 0$ at $\tilde{g} = \tilde{g}_c$ the transition is said to be continuous or of second order. Close to $\tilde{g}_c$, the correlation length ξ associated to the observable $\mathcal{O}$, defined as the exponent in

$$\langle \mathcal{O}(x)\mathcal{O}(0)\rangle \sim e^{-|x|/\xi} , \tag{2.7}$$

diverges as a power law, that is

$$\xi^{-1} \sim |\tilde{g} - \tilde{g}_c|^{\nu} , \tag{2.8}$$

for ν a positive number. Because of this divergence, all other intrinsic length and energy scales in the system play no role and the onset of nonzero ϕ depends only on the general features of the system, like the dimensionality and the symmetry properties that $\mathcal{O}$ breaks/preserves. A description of the transition is thus possible in terms of a coarse grained theory for the order parameter - a continuous field - since changes at microscopic scales become irrelevant (in the nontechnical sense) and one can expect only these universal aspects to be of importance.

2.1.1 Landau-Ginzburg-Wilson theory

Let us start by considering a thermal phase transition in spatial dimension D, where the parameter that needs to be tuned to reach said transition is temperature (i.e. $\tilde{g} = T$). A good starting point to understand the vicinity of the critical point $T = T_c$, is to describe the dynamics of the space dependent order parameter $\varphi(x)$, where $x \in \mathbb{R}^D$, by the Landau-Ginzburg free energy $F[\varphi] = k_B T S[\varphi]$, with

$$S[\varphi] = \int \mathrm{d}^D x \left(\frac{\kappa}{2}(\partial_i \varphi)^2 + V(\varphi) \right) , \tag{2.9}$$

where $V(\varphi)$ is an analytic function of φ, and $i = 1, \cdots, D$. In the action Eq. (2.9), κ, as well as the coefficients of V in an expansion in powers of φ, contain all microscopic details of the system and can be thought of as phenomenological parameters that can, in principle, be determined from, e.g. experimental or numerical data. In the simplest scenario, where the only relevant symmetry is $\varphi \to -\varphi$ one can truncate V to the lowest nontrivial order, that is,

$$S[\varphi] = \int \mathrm{d}^D x \left(\frac{\kappa}{2}(\partial_i \varphi)^2 + \frac{r}{2}\varphi^2 + \frac{u}{4!}\varphi^4 \right) \tag{2.10}$$

where $r \sim T - T_c$ changes sign at the critical point. The inclusion of a spatially varying order parameter is an improvement on the mean field treatment (corresponding to $\kappa = 0$) and can be further improved by considering all possible field configurations in a path integral formalism. One thus sets $F = -\ln(\mathcal{Z})$, where

$$\mathcal{Z} = \int \mathscr{D}\varphi \, \exp(-S[\varphi]) . \tag{2.11}$$

is the partition function of the system.

From the partition function $\mathcal{Z}$ in Eq. (2.11) one can now obtain the n-point functions which provide information about e.g. the susceptibility and other observable quantities.

2.2 Renormalization Group

Renormalization group techniques combine the idea that the properties of a system depend on the energy scale at which it is probed with the scale invariance and universality implied by the divergence of the correlation length. Although the method has proven to be useful in a variety of contexts [42], we will be mainly interested in its use in describing critical phenomena and consequently our discussion of the method will go straight to this particular aspect.

The basic idea of the renormalization group transformation is to perform an iterative evaluation of the partition function Eq. (2.11) where in each step one integrates out or decimates certain degrees of freedom only, in such a way that at the end of the iteration process all degrees of freedom have been considered. In a lattice system of spins, for example, this could be adding the contributions of spins in a given block to define a new coarse grained spin variable [43].

The form of decimation we will be interested in consists of integrating out high energy degrees of freedom and is closely related to the so called momentum-shell RG which we now describe. Consider a system whose energy is a monotonic increasing function of momentum $p := |\vec{p}|$, e.g. a quadratic in momentum dispersion, then one can distinguish between low and high energies by spliting momenta into "fast" and "slow" modes, i.e. $\Lambda/b < p < \Lambda$ or $0 < p < \Lambda/b$, respectively, where $b > 1$ and Λ is the UV cutoff of the theory (for a lattice, this would be the inverse lattice spacing). This induces a spliting of the field variables as $\varphi = \varphi^+ + \varphi^-$, where $\varphi^\pm$ only contains fast/slow Fourier components.

The effective action S_{eff} is now defined as

$$\exp(-S_{\text{eff}}[\varphi^-]) := \int \mathscr{D}\varphi^+ \ \exp(-S[\varphi^+ + \varphi^-]) \ , \tag{2.12}$$

and by rescaling the fields and couplings, one can rewrite the latter so that it takes the same form of the bare action, thus producing a mapping in the set of couplings,

$$x_i \to \tilde{x}_i(b, \{x_j\}) \ . \tag{2.13}$$

If the procedure is performed n times, the limit $n \to \infty$, corresponds to integrating out all degrees of freedom, so that the field independent part so obtained would correspond to the free energy density of the system. Considering the decimations by the factor b to be made up of infinitesimal steps of size δt, i.e. $b \simeq 1 + \delta t$ for $\delta t \ll 1$, one obtains from Eq. (2.13) a system of differential equations of the form

$$\frac{\mathrm{d}}{\mathrm{d}\, t} x_i = \beta_i(\{x_j(t)\}) \ , \tag{2.14}$$

and it is at this point that the divergence of the correlation length comes into play again. Indeed, the procedure just described is nothing but a rescaling of the momentum scales of the system, and close to the phase transition, the fact that there is a divergent length scale

in the system leads to scale invariance. From this it follows that a stationary point of the differential rescaling transformation Eq. (2.14), i.e. the so called *beta functions*, describes the behaviour of the couplings at the phase transition.

For interacting field theories, however, obtaining an exact beta function is as complicated as solving the full theory so that this procedure is often impossible to carry out, and one must resort to approximations. Within perturbation theory, one thus identifies some control parameter and the approximation takes the form of a series of Feynman diagrams in said parameter.

Although it is beyond the scope of this work to describe in detail the methods devised for this purpose, it is worth mentioning two common approximation methods whose results often serve to compare the results obtained with the nonperturbative method that will be described in Section 2.2.2: The first one, the ϵ-expansion, uses the fact that the scaling of fields depends on the dimension of spacetime D in such a way that there is a dimension D_u such that for $D > D_u$ all couplings not present in the free theory get reduced with each successive RG step, and thus become unimportant. Low order expansions in terms of the difference $\epsilon := D_u - D$ should thus provide trustworthy results close to $\epsilon \sim 0$. Unfortunately, the systems of interest to us are such that $\epsilon = 1$, so that high order expansions are required to obtain sensible results and even then, the validity of the results in the limit $\epsilon \to 1$ cannot be ensured without further independent checks and/or complicated resummation schemes. The second common method is applicable whenever there is a large number N of some degrees of freedom of the theory (e.g. components of the order parameter or flavours of fermions), in which case a similar expansion can be performed in powers of $1/N$. This method suffers from the same disadvantage as the ϵ-expansion, namely that the systems of interest to us usually lie in the range of $N \sim 1$, so that results obtained within a large N expansion usually need to be complemented by other methods. Nevertheless, and as stated above, both methods serve as a valuable guide to benchmark some of the results obtained by nonperturbative methods where no obviously small control parameter is available and we will make use of this observation in chapters 3 and 5.

2.2.1 Critical behaviour from RG fixed points

In the vicinity of a continuous phase transition, the free energy density, and consequently several physical quantities of interest of the system, display scaling behaviour similar to that of the correlation length ξ in equation Eq. (2.8). The scaling properties of the different observables like susceptibilites and other correlators of the theory should thus be accessible from information about the fixed point that describes said phase transition, as discussed in the previous section. We now describe how to extract this information from knowledge of the beta functions.

The set of beta functions for all the couplings of the theory are the prototypical example of a dynamical system [44], for which there are extensive results and analogies that can not only be carried over almost verbatim, but can also provide useful insights [45]. Of particular interest for us is the stability analysis, i.e. the description of properties close to the stationary points of the flow.

In the following, we rephrase the discussion in terms of the renormalization time t, which is defined as

$$t := \ln\left(\frac{k}{\Lambda}\right) \leq 0 \,, \tag{2.15}$$

with Λ the UV cutoff of the theory. Denoting the full set of couplings by a vector as $\vec{x}$, a stationary point is then just an element in coupling space $\vec{x}^*$ such that

$$\vec{\beta}(\vec{x}^*) = \vec{0} \,, \tag{2.16}$$

and for analytic beta functions we can linearize the system of equations Eq. (2.14) to study deviations from this point. Denoting these as $\vec{y} := \vec{x} - \vec{x}^*$, the linearized system takes the form

$$\frac{\mathrm{d}}{\mathrm{d}\,t}\vec{y} = \mathbb{M}\vec{y} \,, \tag{2.17}$$

where

$$\mathbb{M}_{ij} := \frac{\partial \beta_i}{\partial x_j}\Big|_{\vec{x}=\vec{x}^*} \,, \tag{2.18}$$

is the *stability matrix* of the critical point. The solutions of equation Eq. (2.17) are given by

$$\vec{y} = \exp(\mathbb{M}t)\vec{y}_0 \,, \tag{2.19}$$

from where the following physical picture of the vicinity of the critical point in terms of the spectrum of $-\mathbb{M}$ - denoted by $\sigma(-\mathbb{M})$ - emerges: all directions with positive eigenvalue correspond to couplings that are driven away from their critical values when the scale is changed, while those with negative eigenvalues correspond to couplings flowing towards their critical values. Directions in the kernel of $\mathbb{M}$ correspond to couplings that freeze at different values depending on the initial conditions. Couplings satisfying these conditions will be called *relevant, irrelevant* and *marginal*, respectively. Since $\sigma(\mathbb{M})$ is in general complex, the previously introduced classification should be understood to apply to the real parts of the eigenvalues.

A continuous phase transition can now be identified with a stable saddle point, i.e. a stationary point that has only one relevant direction. In this case, one can obtain the correlation length exponent, ν, from the scaling hypothesis and the assumption that close to criticality ξ is the most important length scale. Concretely, if one denotes the momentum scale by k, and if the parameter corresponding to the relevant direction is denoted by g, the singular part of the free energy density scales as

$$f_{\mathrm{sing}}(g(k)) \sim \xi^{-(d+z)} \sim |g - g_c|^{(d+z)\nu} \sim k^{(d+z)/\theta_1} \,, \tag{2.20}$$

where z is the dynamical exponent relating frequency and momentum as $\omega \sim k^z$, and

$$\theta_1 := \max\{\sigma(-\mathbb{M})\} \,; \tag{2.21}$$

is the largest eigenvalue[1] of the stability matrix.

Away from the critical point and in the disordered phase where $\langle\varphi\rangle = 0$, the correlations in the system will fall off as $C(x) \sim e^{-|x|/\xi}$, so the scaling behaviour *exactly* at criticality is characterized by another exponent, namely the anomalous dimension of the order parameter. The anomalous dimension η measures the algebraic decay of the two point correlator of the order parameter,

$$G(x) := \langle\varphi(x)\varphi(0)\rangle \sim \frac{e^{-|x|/\xi}}{|x|^{d-2+\eta}} \,, \tag{2.22}$$

and, together with ν, they provide all scaling exponents of response functions of the system [39].

Saddle points with more than one relevant direction will be identified with a first order transition or with a multicritical point joining three or more different phases. In the latter case, and when the fixed point involves only two relevant directions, we say the multicritical point is stable.

2.2.2 Functional Renormalization Group

The renormalization group transformation described in the previous section can be implemented exactly in terms of a functional closely related to the generator of one particle irreducible diagrams, Γ, also known as the effective action. This is particularly useful, since $n-$point correlators depend solely on these diagrams. The effective action is obtained from the generating functional by adding a source term J, as

$$\exp(W[J]) := \int \mathscr{D}\varphi \, \exp(-S[\varphi] + \int J\varphi) \,, \tag{2.23}$$

and then taking a Legendre transformation of this quantity, i.e.

$$\Gamma[\phi] := \sup_J \left\{ \int J\phi - W[J] \right\} \,. \tag{2.24}$$

To implement the renormalization group on the effective action we construct a new scale dependent functional by introducing an infrared cutoff at the scale k, denoted by $\Gamma_k^W[\phi]$, in such a way that at any given scale k, only fluctuations with momenta $q^2 \geq k^2$ are included in Γ_k^W. In the limit $k \to 0$ all fluctuations are included so that $\Gamma_0^W = \Gamma$ is the full effective action. At the UV cutoff scale Λ no fluctuations are included and $\Gamma_\Lambda^W = S$ is the classical action. Such a functional interpolating between the full (effective) and bare actions can be constructed by following the same procedure used in contructing Γ, but with the replacement $S \to S + \Delta S_k$, where

$$\Delta S_k[\varphi] := \frac{1}{2} \int \frac{\mathrm{d}^D q}{(2\pi)^D} \varphi(q) R_k(q) \varphi(-q) \,, \tag{2.25}$$

and $R_k(q)$ is a regulator function that satisfies three properties:

[1] Note that we assumed, as is actually the case in spacetime dimension $D > 2$, that the space of non-irrelevant couplings is of finite dimension so that for all fixed points, $\sigma(-\mathbb{M})$ is compact and can be ordered by ordering its real parts.

(i) $\lim_{k\to 0} R_k(q) = 0$ for fixed q.

(ii) $\lim_{k\to\infty} R_k(q) = \infty$.

(iii) $R_k(q)$ does not explicitly break any global symmetries in S.

With a regulator satisfying the above properties, the flow equation for Γ_k^W, usually referred to as the Wetterich equation, is given by [42, 46]

$$\partial_t \Gamma_k^W[\Phi] = \mathrm{STr}\left(\frac{\partial_t R_k}{\Gamma_k^{W(2)} + R_k}\right) , \tag{2.26}$$

where

$$\Gamma_k^{W(2)} = \frac{\overrightarrow{\delta}}{\delta\Phi}\Gamma_k^W\frac{\overleftarrow{\delta}}{\delta\Phi} , \tag{2.27}$$

is the functional Hessian and STr denotes the super trace, i.e. a trace that includes a negative sign for each fermionic component of the (column) vector of fields Φ. The notation here is merely used to distinguish the functional just defined from the effective action generating the one particle irreducible diagrams Γ. From now on we will drop the superscript and refer to this functional simply as the effective action.

For a given regulator R_k, properties of the flow are nonuniversal and scheme dependent at intermediate scales, but the conditions imposed on R_k ensure that they approach the scheme-independent and therefore physically relevant quantities of interest. For this reason, one has a lot of freedom in choosing the regulators. In particular, given that Eq. (2.26) has a one loop structure, one can choose a regulator that simplifies the required loop integrals. A convenient choice in relativistic systems that we will often use is the linear optimized Litim regulator [47]. For bosons, it takes the form

$$R_k(q) = Z_k(k^2 - q^2)\Theta(k^2 - q^2) , \tag{2.28}$$

where $Z_k := k^{-\eta}$ is the "wavefunction normalization" including the anomalous dimension η, and Θ is the Heaviside step function. For fermions a similar regulator can be defined by including the spinor/band structure. These form of regulator has some convenient convergence properties while allowing analytic evaluation of the loop integrals involved in computing Eq. (2.26).

Truncations

The exact equation Eq. (2.26) is usually impossible to solve for nontrivial models and approximation schemes have to be devised. These take the form of an infinite hierarchy of integro-differential equations that can be truncated to a given order to make them a closed system. The main approaches involve either a vertex or a derivative expansion, both of which we will now briefly describe.

The vertex expansion consists of, as the name suggests, expanding both sides of Eq. (2.26) in powers of the involved fields and matching the resulting coefficients. This kind of approximation is particularly useful when extracting information about instabilities in condensed matter systems, for it gives an unbiased way to probe the momentum dependence of, e.g. competing order parameters.

Derivative expansions are particularly useful when the momentum dependence of interacting vertices is known beforehand and one is interested in long-wavelength physics, i.e. where the order parameter fields can be expected to vary smoothly in spacetime. In this case, an expansion in gradients of the order parameter fields is sensible. To implement this approximation, an Ansatz for Γ is made, which for an $O(N)$-symmetric theory takes the form

$$\Gamma_k = \int d^D x \Big[\frac{1}{2} Z_k(\rho)(\partial_\mu \phi_\alpha)^2 + U_k(\rho) + \frac{1}{4} Y_k(\rho)(\partial_\mu \rho)^2 + \cdots \Big], \tag{2.29}$$

with $\rho := \phi_\alpha^2/2$. When one further sets $Y = 0$, and considers Z to be field independent this approximation is known as the improved local potential approximation, or LPA'. It is this approximation that we will use in the following chapters, where we further expand the potential $U(\rho)$ in a Taylor series around a running minimum, and truncate up to some power of the field ϕ.

Convergence and validity of results The FRG method does not rely on any parameter being small (like e.g. ϵ or $1/N$) and for any particular truncation there is, in principle, no clear cut method to control the range of validity of the results obtained. For the particular truncations described above, one way to check for the consistency of results is to include all symmetry allowed couplings (in LPA') or vertices (in the vertex expansion) up to a given power of the fields, and neglect the flow of higher order terms.

In LPA' the approximation of considering powers of the field up to order N is aptly referred to as LPA'N. The reliability of the obtained results can thus be measured by the convergence of observable quantities when increasing the order of truncation. For this reason, in the next chapters we will always include all allowed couplings up to some N (high but, of course, finite) where it is already clear that the results for, e.g., critical exponents converge.

2.3 The case for Lorentz symmetry

As a first application of the formalism reviewed in Section 2.2.2, we provide a simple and fairly general argument for the emergence of Lorentz symmetry at criticality in certain phase transitions of interacting Dirac systems. Specifically we will argue that, at the critical point, the velocities of fermions and of bosons reach the same value and that the difference of velocities is an irrelevant parameter in the system.

Our starting assumption is that the bare action possesses relativistic *covariance* in the separate bosonic and fermionic sectors. This assumption, in turn, consists of two separate statements:

(i) All spatial directions are equivalent.

(ii) The (bare) dynamical exponent controlling the frequency momentum relation $\omega \sim k^z$, satisfies $z = 1$.

To proceed, we consider a system of gapless Dirac fermions that interact with an N_b-component order parameter field $\vec{\varphi}$. The final assumption will be that the interaction is such that a nonvanishing expectation value for the order parameter corresponds to the opening of a

fermionic mass gap, and such that it anticommutes with the kinetic terms of the fermions[2]. Concretely, we consider the system described by the microscopic action

$$S = \int d^D x \Big[\overline{\psi}(i\gamma_0\partial_0 + iv_{\mathrm{f}}\gamma_j\partial_j)\psi + \bar{h}\overline{\psi}\left(\gamma_\alpha\varphi_\alpha\right)\psi \\ - \frac{1}{2}\varphi_\alpha(\partial_0^2 + v_{\mathrm{b}}^2\partial_j^2)\varphi_\alpha + \frac{\bar{m}^2}{2}|\vec{\varphi}|^2 + \frac{\bar{\lambda}}{4!}|\vec{\varphi}|^4 + \cdots \Big] , \tag{2.30}$$

where repeated indices are summed over, $j = 1, \cdots, d$, $\alpha = d+1, \cdots, d+N_b$ and the gamma matrices appearing in Eq. (2.30) are a 4-dimensional representation of the euclidean Clifford algebra, i.e.

$$\{\gamma_\mu, \gamma_\nu\} = 2\delta_{\mu\nu} , \tag{2.31}$$

for all $\mu, \nu \in \{0, 1, \cdots, d+N_b\}$. The bosonic and fermionic velocities are represented by v_{b} and v_{f} respectively, and $\bar{h}$ is the Yukawa coupling between bosons and fermions. The dots in Eq. (2.30) refer to either higher order terms in $|\vec{\varphi}|^2$ (corresponding to self-interactions consistent with $O(N_b)$ symmetry) or terms mixing different components of the bosonic fields (corresponding to anisotropy terms explicitly breaking $O(N_b)$ symmetry). The bosonic mass $\bar{m}^2$ serves as a tuning parameter to reach the transition and the quartic coupling $\bar{\lambda}$ determines, as usual, the curvature at a minimum of the potential. We generalize the previous bare action by considering N_{f} flavours of fermions and the most general bosonic potential analytic in φ_α. The corresponding LPA' Ansatz for the efective action thus has the form

$$\Gamma_k[\vec{\varphi}, \overline{\Psi}, \Psi] = \int d^D x \Big[Z_{\psi,k}\overline{\Psi}(i\gamma_0\partial_0 + iv_{\mathrm{f},k}\gamma_j\partial_j)\Psi + \bar{h}_k\overline{\Psi}\left(\gamma_\alpha\varphi_\alpha\right)\Psi \\ - \frac{1}{2}Z_{\varphi,k}\varphi_\alpha(\partial_0^2 + v_{\mathrm{b},k}^2\partial_j^2)\varphi_\alpha + U_k(\vec{\varphi}) \Big] , \tag{2.32}$$

where we defined $\Psi = \oplus_{i=1}^{N_{\mathrm{f}}}\psi$. In the following, it will prove convenient to define the dimensionful momentum vectors

$$q := (q_0, \vec{q}) , \tag{2.33a}$$

$$q_{\mathrm{x}} := (q_0, v_{\mathrm{x},k}\vec{q}) \qquad \text{for } \mathrm{x} \in \{\mathrm{f}, \mathrm{b}\} , \tag{2.33b}$$

In the previous equation we made explicit that $v_{\mathrm{b/f}}$ are running couplings, but from now on we will omit the explicit k dependence. As mentioned before, for each physical situation, the choice of regulator should be such that it does not explicitly break the symmetries under consideration in order to avoid artificial regulator-induced symmetry breaking. Using the notation just introduced, and the Feynman slash notation $\gamma_\mu v_\mu =: \not{v}$we can take the regulators to be of the form

$$R_{\varphi,k}(q_0, \vec{q}) = Z_{\varphi,k}q_{\mathrm{b}}^2 r_\varphi\left(\frac{q_{\mathrm{b}}^2}{k^2}\right) , \tag{2.34}$$

$$R_{\psi,k}(q_0, \vec{q}) = Z_{\psi,k}\not{q}_{\mathrm{f}} r_\psi\left(\frac{q_{\mathrm{f}}^2}{k^2}\right) , \tag{2.35}$$

[2] A detailed discussion of the kind of physics described by such a system, for $N_{\mathrm{f}} = 2, d = 2$ and $N_b = 2$, is performed in chapter 3. The conditions required to define this model for general d, N_{f} and N_b, can be found in chapter 4 where a detailed analysis of the transitions is performed for the case where all OPs involved have rotational symmetry.

where $r_{\varphi/\psi}(\cdot)$ are *arbitrary* "shape functions" such that the regulator satisfies the requirements stated in Section 2.2.2. We could, for example, use the linear Litim regulator introduced in Eq. (2.28), whose shape function is

$$r_\varphi = \left(\frac{1}{x} - 1\right)\Theta(1-x)\ , \tag{2.36a}$$

$$r_\psi = \left(\frac{1}{\sqrt{x}} - 1\right)\Theta(1-x)\ . \tag{2.36b}$$

However, in the following we avoid restricting to a particular regulator shape function, to ensure our argument remains as general as possible, and only use this particular form to make provide some estimates later on. The choice of the functional dependence of the regulator on momenta ensures that we do not introduce any bias towards either bosonic or fermionic degrees of freedom. We note, however, that this is not the only possible choice and, in principle, a momentum-only regulator should allow one to obtain the same results as we will present below, at least in the low energy limit $k \to 0$.

The vector of fields in momentum space is given by

$$\Phi(q)^T = \left(\vec{\varphi}(q), \overline{\Psi}(q), \Psi(-q)^T\right)\ , \tag{2.37}$$

so the regulator matrix is represented as

$$R_k(q) = \begin{pmatrix} R_{\varphi,k}(q)\delta_{\alpha\beta} & 0 & 0 \\ 0 & 0 & R_{\psi,k}(q) \\ 0 & -R^T_{\psi,k}(-q) & 0 \end{pmatrix}\ . \tag{2.38}$$

To formulate the beta functions applying the Wetterich equation, Eq.(2.26) to the LPA' Ansatz, Eq.(2.32), it is necessary to compute the dressed propagator. We thus split the Hessian of Γ_k into field dependent and independent parts as $\Gamma^{(2)}_k = \Delta\Gamma^{(2)}_k + \Gamma^{(2)}_{k,0}$, with $\Gamma^{(2)}_{k,0}$ the hessian of Γ_k at zero fermionic fields and at the minimum of the bosonic potential U_k. The field independent part of the dressed propagator then takes the form

$$\mathcal{P}^{-1}_k(p,q) := \left(\Gamma^{(2)}_{k,0} + R_k\right)^{-1}(p,q) = \begin{pmatrix} D(q) & 0 & 0 \\ 0 & 0 & -G^T(-q) \\ 0 & G(q) & 0 \end{pmatrix}\delta^D(p-q)\ , \tag{2.39}$$

where the $N_b \times N_b$ matrix D, and G, are the bosonic and fermionic propagators respectively. Their entries are given by

$$\left(D^{-1}(q)\right)_{\alpha\beta} := Z_{\varphi,k}q_{\rm b}^2(1 + r_\varphi(q_{\rm b}^2))\delta_{\alpha\beta} + \left.\frac{\partial^2 U}{\partial\varphi_\alpha\partial\varphi_\beta}\right|_{\rm min}\ , \tag{2.40a}$$

$$G^{-1}(q) := Z_{\psi,k}\not{q}_{\rm f}(1 + r_\psi(q_{\rm f}^2)) + \bar{h}\gamma_\alpha\varphi_{\alpha,\rm min}\ . \tag{2.40b}$$

The β-functions of the velocities can now be obtained from the following projections

$$\partial_t Z_\varphi = \lim_{q\to 0}\frac{\partial}{\partial q_0^2}\partial_t\Gamma_{\varphi\varphi}(q)\ , \tag{2.41a}$$

$$\partial_t(Z_\varphi v_{\mathrm{b}}^2) = \lim_{q\to 0}\frac{\partial}{\partial \vec{q}^2}\partial_t\Gamma_{\varphi\varphi}(q)\ , \tag{2.41b}$$

$$\partial_t Z_\psi = \frac{1}{4N_{\mathrm{f}}}\lim_{q\to 0}\mathrm{tr}\left(\gamma_0\frac{\partial}{\partial q_0}\partial_t\Gamma_{\overline{\psi}\psi}(q)\right)\ , \tag{2.41c}$$

$$\partial_t(Z_\psi v_{\mathrm{f}}) = \frac{1}{4N_{\mathrm{f}}d}\lim_{q\to 0}\mathrm{tr}\left(\gamma_j\frac{\partial}{\partial q_j}\partial_t\Gamma_{\overline{\psi}\psi}(q)\right)\ . \tag{2.41d}$$

In the previous equation we used the notation

$$\begin{aligned}\partial_t\Gamma_{\Phi_a\Phi_b} &= \frac{\overrightarrow{\delta}}{\delta\Phi_a}\partial_t\Gamma_k\frac{\overleftarrow{\delta}}{\delta\Phi_b}\ ,\\ &= \frac{\overrightarrow{\delta}}{\delta\Phi_a}\left(\mathrm{STr}\left(\frac{\partial_t R_k}{\Delta\Gamma_k^{(2)}+\mathcal{P}}\right)\right)\frac{\overleftarrow{\delta}}{\delta\Phi_b}\ .\end{aligned} \tag{2.42}$$

The anomalous dimension and the velocity anomalous dimension can now be defined as

$$\eta_\varphi := -\partial_t\ln Z_\varphi\ ,\qquad \widetilde{\eta}_\varphi := \partial_t\ln Z_\varphi v_{\mathrm{b}}^2\ , \tag{2.43a}$$

$$\eta_\psi := -\partial_t\ln Z_\psi\ ,\qquad \widetilde{\eta}_\psi := \partial_t\ln Z_\psi v_F\ , \tag{2.43b}$$

from where we finally obtain the flow equations for the velocities

$$\partial_t v_{\mathrm{b}} = \frac{v_{\mathrm{b}}}{2}\left(\eta_\varphi+\widetilde{\eta}_\varphi\right) = \left(1-\left(\frac{v_{\mathrm{f}}}{v_{\mathrm{b}}}\right)^2\right)\frac{v_{\mathrm{b}}}{2v_{\mathrm{f}}^d}\ell_2(\mathbf{g})\ , \tag{2.44a}$$

$$\partial_t v_{\mathrm{f}} = v_{\mathrm{f}}\left(\eta_\psi+\widetilde{\eta}_\psi\right) = v_{\mathrm{f}}\widetilde{\ell}_1(v_{\mathrm{f}},v_{\mathrm{b}};\mathbf{g})\ , \tag{2.44b}$$

where g denotes all other (dimensionless) flowing couplings, and ℓ_i are dimensionless threshold functions that, of course, depend explicitly on the regulator shape functions. The one entering the bosonic velocity is given by

$$\ell_2(\mathbf{g}) = \frac{2h^2N_{\mathrm{f}}v_D}{D}\int_0^\infty \mathrm{d}\,y\ y^{\frac{D}{2}}\widetilde{\partial}_t\left[y\left(\left(\frac{1+r_\psi(y)}{P_\psi(y)}\right)'\right)^2+\left(\left(\frac{M_\psi^2}{P_\psi(y)}\right)'\right)^2\right]\ . \tag{2.45}$$

while the one entering the fermion velocity is given by

$$\begin{aligned}\widetilde{\ell}_1(v_{\mathrm{f}},v_{\mathrm{b}};\mathbf{g}) = 2h^2\int\frac{\mathrm{d}^D p}{(2\pi)^D}\Bigg[&\mathrm{tr}(D'(p_{\mathrm{b}}^2))\widetilde{\partial}_t\left(\frac{1+r_\psi(p_{\mathrm{f}}^2)}{P_\psi(p_{\mathrm{f}}^2)}\right)\left(\frac{v_{\mathrm{b}}^2\vec{p}^2}{d}-p_0^2\right)\\ &+\mathrm{tr}(\widetilde{\partial}_t D(p_{\mathrm{b}}^2))\left(\frac{1+r_\psi(p_{\mathrm{f}}^2)}{P_\psi(p_{\mathrm{f}}^2)}\right)'\left(\frac{v_{\mathrm{f}}^2\vec{p}^2}{d}-p_0^2\right)\Bigg]\ ,\end{aligned} \tag{2.46}$$

In both equations, the prime stands for the derivative with respect to the argument, since all functions involved depend only on squares of momenta p_x^2 and the scale derivative $\widetilde{\partial}_t$ is defined to act only on the regulators $R_{\varphi,\psi}$. Moreover, we introduced the notation $M_\psi^2 = h^2\vec{\varphi}_{\min}^2$ for the (dimensionless) generated mass of the fermions and $P_\psi(y) = y(1+r_\psi(y))^2 + M_\psi^2$, while v_D is the geometric factor coming from integration over the d sphere, $v_D = (\Gamma(D/2)2^{D+1}\pi^{D/2})^{-1}$.

Remarkably, Eq. (2.45) does not depend on the velocities at all[3]. The dependence on the

[3]Because of the dressed fermionic propagator, the equation does depend on η_ψ and $\widetilde{\eta}_\psi$, but it does so *linearly*, so the discussion that follows still holds.

velocities is just the prefactor of Eq. (2.44a). From this it follows that the only zero of this beta-function (for nonnegative v_i) corresponds to equal velocities. The line in parameter space $v_\mathrm{f} = v_\mathrm{b}$ would consist of fixed points of the RG flow equations if it is also a zero of the beta function for v_f, that is, if $\widetilde{\ell}_1(v_\mathrm{f} = v_\mathrm{b}; \mathbf{g}^*) = 0$, with all couplings at their fixed point values $\mathbf{g} = \mathbf{g}^*$.

That this is true follows, in turn, from the fact that for $v_\mathrm{f} = v_\mathrm{b} = c$ we can perform the following substitutions in Eq.(2.46) (by homogeneity of the arguments and the integration region)

$$\frac{v_\mathrm{x}^2 \vec{p}^2}{d} \to \frac{c^2 \vec{p}^2}{d} \to \frac{p^2}{D} \tag{2.47}$$

$$p_0^2 \to \frac{p^2}{D} \,, \tag{2.48}$$

which merely introduces an overall prefactor of c^{-d} and evidently cancels the contributions on both lines of Eq. (2.46). Therefore $\widetilde{\ell}_1$ vanishes for $v_\mathrm{f} = v_\mathrm{b} = c$ and we can try to extract the leading behaviour with respect to the velocities close to the line of fixed points in order to perform a stability analysis of this line. In the vicinity of $v_\mathrm{f} = v_\mathrm{b} = c$, and by the same homogeneity argument leading to Eq. (2.48), we obtain

$$\widetilde{\ell}_1(v_\mathrm{f}, v_\mathrm{b}; \mathbf{g}) = \left(\left(\frac{v_\mathrm{b}}{v_\mathrm{f}} \right)^2 - 1 \right) \frac{\ell_1^{(\mathrm{f})}(\mathbf{g})}{2 v_\mathrm{f}^d} + \left(\left(\frac{v_\mathrm{f}}{v_\mathrm{b}} \right)^2 - 1 \right) \frac{\ell_1^{(\mathrm{b})}(\mathbf{g})}{2 v_\mathrm{b}^d} \,, \tag{2.49}$$

with the new threshold functions given by

$$\ell_1^{(\mathrm{f})}(\mathbf{g}) := \frac{2h^2 v_D}{D} \int_0^\infty \mathrm{d}\, y\, y^{\frac{D}{2}} \left[\mathrm{tr}(D'(y)) \widetilde{\partial}_t \left(\frac{1 + r_\psi(y)}{P_\psi(y)} \right) \right] \,, \tag{2.50a}$$

$$\ell_1^{(\mathrm{b})}(\mathbf{g}) := \frac{2h^2 v_D}{D} \int_0^\infty \mathrm{d}\, y\, y^{\frac{D}{2}} \left[\mathrm{tr}(\widetilde{\partial}_t D(y)) \left(\frac{1 + r_\psi(y)}{P_\psi(y} \right)' \right] \,. \tag{2.50b}$$

Before we continue, it is worth pointing out that these equations hold regardless of the form of the flowing bosonic potential U_k. The particular dependence of U_k on $\vec{\varphi}$ as well as the number of components N_b are "hidden" in the matrix propagator D. Moreover the simple form of the beta functions of velocities, namely Eqs. (2.44) with the approximation Eq. (2.50), depend solely on the assumed isotropic nature of the LPA Ansatz, i.e., of the fact that we assume the velocities in all spatial directions to flow identically.

We now proceed with the stability analysis. Considering the flow of only this sector of the theory while all other couplings are at their critical values, i.e. $\mathbf{g} = \mathbf{g}^*$, the stability matrix at a fixed point with $v_\mathrm{f} = v_\mathrm{b} = c$ has the eigenvalues

$$\lambda_1 = 0 \,, \tag{2.51a}$$

$$\lambda_2 = -\frac{1}{c^d} (\ell_1^{(\mathrm{b})}(\mathbf{g}^*) - \ell_1^{(\mathrm{f})}(\mathbf{g}^*) + \ell_2(\mathbf{g}^*)) \,. \tag{2.51b}$$

so the fixed point has no relevant directions coming from this sector if the sum of threshold functions in Eq. (2.51b) is non-negative.

Without an explicit choice of $r_{\varphi,\psi}$, we cannot say much about the positivity of the different ℓ_i, but we can get an estimate for them if we approach the critical point from the disordered

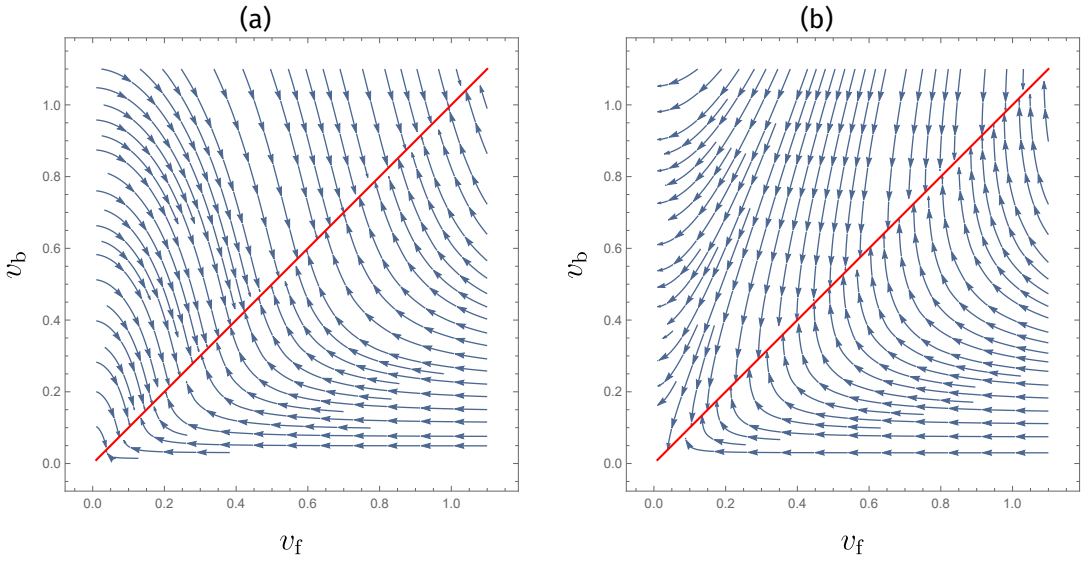

FIGURE 2.1: **Flow of the velocities** cf. Eqs. (2.44) for $\ell_1^{(\mathrm{b})}(\mathbf{g}^*) = 0.1$, $\ell_2(\mathbf{g}^*) = 0.7$ and (a) negative or (b) positive $\ell_1^{(\mathrm{f})}$ in spatial dimension $d = 2$. The stream lines point to the infrared, i.e. in both cases the line of fixed points $v_\mathrm{f} = v_\mathrm{b}$ is attractive when $k \to 0$.

side. In that case we the minimum of the bosonic potential $U(\rho)$ lies at $\rho_0 = 0$, and the function ℓ_2 satisfies

$$\eta_\varphi = \ell_2(\mathbf{g}^*) \,, \tag{2.52}$$

where η_φ is the anomalous dimensions of the bosonic two-point correlator. The latter is expected to be nonnegative in integer dimension and for any interacting field theory that leads to a well defined underlying Hilbert space, i.e. where no negative norm states are allowed (that this is not necessarily true for noninteger dimensions has been argued for in [48]). We can thus expect ℓ_2 to be positive and of order unity [49, 50]. To get an estimate for the other two threshold functions we have no choice but to use a particular regulator shape function. With the choice of (2.36), for example, we obtain

$$\eta_\psi = \ell_1^{(\mathrm{b})}(\mathbf{g}^*) \,, \tag{2.53a}$$
$$0 = \ell_1^{(\mathrm{f})}(\mathbf{g}^*) \,, \tag{2.53b}$$

i.e. we can expect $\ell_1^{(\mathrm{b})}$ to be a small positive number. With these values of threshold functions and different values for $\ell_1^{(\mathrm{f})}$ (since its vanishing in Eq. (2.53b) seems to depend strongly on our choice of regulator), the flow of the velocities is as depicted in FIG. 2.1.

The physical significance of Eqs. (2.44a) and (2.44b) is perhaps best understood by switching to the variables

$$\Delta_\pm := \frac{v_\mathrm{f} \pm v_\mathrm{b}}{2} \,, \tag{2.54}$$

where it is clear that the difference Δ_- corresponds to an irrelevant direction and the sum Δ_+ to the marginal direction. This means that velocities will always flow to a common value. Our results also indicate that the value of c, controlled by the flow of the sum Δ_+, is not universal but freezes at some value that depends on the initial conditions $v_{\mathrm{b},0}$ and $v_{\mathrm{f},0}$.

The form of Eq. (2.44a) seems to indicate that there are no further fixed points with $v_{\mathrm{f}} \neq v_{\mathrm{b}}$ in Dirac systems in any spacetime dimension. Note that chiral $O(N_b)$ universality classes for $N_{\mathrm{f}} \geq 1$ are expected to satisfy the conditions leading to Eq. (2.52), namely, the fixed point describing the transitions are well defined and can be found from an expansion starting in the symmetric regime [49, 50]. We can thus expect the flow of the velocities close to the quantum critical points of interest in this work to be as described here.

For Lorentz invariance to be reached in a particular simulation of the given phase transition or in an experiment (where the system sizes are finite), the velocities would have to flow to the common value at a faster pace than the leading correction to scaling exponent as obtained from a Lorentz invariant analysis, θ_2. The rate at which the velocities approach each other is given by the negative eigenvalue of the stability matrix, Eq.(2.51b), which we denote by θ_-. Since for universal critical behaviour we require only θ_1 to be positive, the previous statement translates to $0 > \theta_2 > \theta_-$.

Note that without specifying a particular regulator shape function, it is not possible to tell how fast the velocities approach their common terminal value $c = v_{\mathrm{f}} = v_{\mathrm{b}}$. Additionally, since Eq. (2.51b) depends on the nonuniversal fixed point value c, it also depends on the initial conditions on the velocities. With the choice leading to Eq. (2.53), however, we can obtain an estimate for the chiral $O(N_b)$ transitions by assuming c to be of the order of $v_{\mathrm{f},0} = 1$. These estimates for $N_{\mathrm{f}} = 2$ can be found in Table 2.1.

TABLE 2.1: **Stability exponents:** Numerical values for the largest two critical exponents of chiral $O(N_b)$ transitions and the exponent controlling the approach to Lorentz invariance θ_- for $N_{\mathrm{f}} = 2$ and different N_b in $D = 2 + 1$ in LPA$12'$. $N_b = 2_3$ corresponds to an XY model with cubic terms, i.e. the model studied in Chapter 3. In all cases except for the Chiral Ising model ($N_b = 1$) the leading corrections to scaling (shown in boldface) are larger than θ_-.

N_b	θ_1	θ_2	θ_-
1	0.9819	-0.8723	**-0.7916**
2	0.8623	**-0.8779**	-0.9376
3	0.7717	**-0.9239**	-1.099
4	0.7333	**-1.017**	-1.251
5	0.7374	**-1.132**	-1.374
2_3	0.8623	**-0.00497**	-0.942

Finally, our generic argument can be compared to results from an ϵ-expansion, where the approach to Lorentz invariance was studied for $O(2)$ order parameters without charge [51]. There it was found that in the absence of fluctuating gauge fields, the bosonic and fermionic velocities indeed approach a common terminal velocity c whose value lies between the initial values of $v_{\mathrm{f/b}}$. We further stress the key role played by the assumed isotropy of the velocities in obtaining our results, since there is evidence that there is no common velocity if e.g. anisotropic gauge fields are taken into account [52]. We moreover note that the results derived here stand in stark contrast to quantum phase transitions in two spatial dimensions involving gapless fermions *with a Fermi surface*, in which both assumptions are invalid [53, 54]. In such a system, directions parallel and perpendicular to the Fermi surface have different momentum dependence and $z > 1$.

Chapter 3

Emergent length scales from discrete symmetry breaking: the Kekulé Valence Bond Solid

The quantum phase transition from a Dirac semimetal to a $\mathbb{Z}_3$-ordered Kekulé Valence Bond Solid (KVBS) in two spatial dimensions is discussed in this chapter. This is an example of a fermion-induced quantum critical point, in which the presence of the gapless fermions becomes crucial to observe universal critical behaviour in what would otherwise be a discontinuous transition. In terms of symmetry breaking, the phase transition corresponds to a crystalline system going from having a C_6 to a C_3 point symmetry. As such, this phenomenon is relevant for e.g. graphene, as its honeycomb layer structure allows both the presence of gapless fermions as well as the particular symmetry breaking patterns of interest. The dimerized pattern that results in a KVBS state has been recently observed in graphene grown on a copper substrate in [13].

As will be discussed in more detail below, the low energy efffective theory of this transition corresponds partially to that of a breaking of chiral symmetry for Dirac fermions and accordingly, there have been considerable theoretical efforts to understand such a phenomenon, even in the context of condensed matter [3, 7–9]. However, given the particular nature of a lattice system setting, there are two important aspects which are rather unique to it: The first one is the fact that starting from a miscroscopic model possessing only $\mathbb{Z}_3$ symmetry, the phase transition is characterised by an emergent $U(1)$ symmetry at criticality. The second is that, unlike the usual picture of second order phase transitions where only the correlation length ξ diverges, the symmetry broken regime has a second diverging length scale ξ' induced by the discreteness of the nontrivial leftover symmetry in the symmetry-broken regime. We discuss both of these aspects in more detail below. Our results include a detailed examination of the emergence of the second length scale, improved estimates for the value of corresponding critical exponent ν', as well as general characterization of the symmetric and symmetry-broken phases of Dirac fermions in spatial dimensions $1 < d < 3$ and for general numbers of fermions.

The outline of this chapter is as follows: We introduce the dimerization pattern and discuss its symmetry properties in Sec. 3.1. This includes a discussion of the systematics of fermion-induced QCPs and some of the recent findings and evidence which support this scenario, which justifies the introduction of the Gross-Neveu-Yukawa theory of interest to describe

the quantum phase transition of gapless Dirac fermions towards a Kekulé valence bond solid (VBS) in Sec. 3.1.3. In this model the Kekulé VBS transition is captured by a complex-valued and $\mathbb{Z}_3$-symmetric order parameter field which is coupled to the fermions. In Sec. 3.3 we discuss our results for the renormalization group flows in the vicinity of the FIQCP. In particular, we describe the flow of the system from the symmetric into the symmetry-broken regime which is subject to the influence of various fixed-points. Technical details on the flow equations are given in Appendix A.

Disclaimer The contents of this chapter have been published in [55] and some parts of the text and figures here are identical to that manuscript. Changes with respect to the published manuscript include the addition of Sec. 3.1.1, the substantial modification of the discussion of Fermion-Induced Quantum Critical Points in Sec. 3.1.2 and several minor changes in other sections, where detailed explanations have been added or expanded for improved readability.

3.1 Kekulé Valence Bond Solid on the honeycomb lattice

3.1.1 Kekulé dimerization and related symmetries

To describe what a Kekulé dimerization pattern is, we start with the simplest tight binding model describing the motion of spinless fermions on the honeycomb lattice [56], which takes the form of the second quantized hamiltonian

$$\hat{H}_0 = -t \sum_{\vec{R},i} \left(\hat{u}(\vec{R})^\dagger \hat{v}(\vec{R} + \vec{e}_i) + \text{h.c.} \right) , \tag{3.1}$$

where the operator $\hat{u}(\vec{R})$ ($\hat{v}(\vec{R})$) annihilates an electron at position $\vec{R}$ of the triangular sublattice A (B), $\vec{e}_i$ are the position vectors of the nearest neighbours, and the hopping parameter t satisfies $t > 0$ [57]. This hamiltonian can be diagonalized in fourier space to yield the single particle energy dispersion

$$\epsilon(\vec{k}) = \pm t \left| \sum_{i=1}^{3} \exp(i\vec{k} \cdot \vec{e}_i) \right| , \tag{3.2}$$

with $\vec{k}$ in the first Brillouin zone. The two inequivalent points in the Brillouin zone at which the dispersion vanishes, denoted by $\vec{K}$ and $\vec{K}' = -\vec{K}$, provide the main contribution to low energy excitations above the ground state. We thus retain only Fourier modes close to these points, i.e. $|\vec{k} \pm \vec{K}|a = |\vec{q}|a \ll 1$ with a the lattice constant, and define the spinor

$$\widehat{\psi}(\vec{q})^T := (\hat{u}(\vec{K} + \vec{q}), \hat{v}(\vec{K} + \vec{q}), \hat{v}(-\vec{K} + \vec{q}), \hat{u}(-\vec{K} + \vec{q})) , \tag{3.3}$$

with $\hat{u}(q), \hat{v}(q)$ the corresponding annihilation operators in the momentum representation. In terms of these, the Hamiltonian takes the form

$$\hat{H}_0 = \sum_{|\vec{q}|a \ll 1} \widehat{\psi}(\vec{q})^\dagger h(\vec{q}) \widehat{\psi}(\vec{q}), \tag{3.4}$$

with

$$h(\vec{q}) = v_{\mathrm{f}}\vec{\alpha}\cdot\vec{q}\,, \tag{3.5}$$

for $\vec{\alpha} = \sigma_z \otimes \vec{\sigma}$, and $v_{\mathrm{f}} = 3ta/2$. The advantage of this representation for the spinors ψ is that they can be clearly seen to be composed of two Dirac cones with opposite "chiralities" given by eigenvalues of the operator $\sigma_z \otimes \mathbb{1}_2$. Of the many different kinds of interactions that can open a gap in the spectrum [58–64], we will be concerned with those that break this chiral symmetry.

The simplest terms connecting the two Dirac points [13, 65–69] take the form of anticommuting mass terms for the spinors. Concretely, adding to $h(q)$ a term of the form

$$\delta h = \phi_1\alpha_3 + \phi_2\alpha_5\ , \tag{3.6}$$

where $\phi_{1/2} \in \mathbb{R}$, $\alpha_3 := \sigma_i \otimes \mathbb{1}_2$ and $\alpha_5 := \sigma_2 \otimes \mathbb{1}_2$, corresponds to opening a $2\sqrt{\phi_1^2+\phi_2^2}$ gap in the one particle spectrum and clearly $\{\vec{\alpha}, \alpha_{3/5}\} = 0$.

The complex quantity $\phi(\vec{R}) := \phi_1(\vec{R}) + i\phi_2(\vec{R})$ is a Kekulé texture. Whenever $\phi(\vec{R})$ is nonzero we will say that the system is Kekulé ordered or that the system is in a Kekulé Valence Bond (KVB) phase. The microscopic effect of the added term can be seen by going back to the real-space representation, where ϕ corresponds to a modulation of the hopping parameter with a wavevector connecting the $\vec{K}$ and $\vec{K}'$ Dirac points, i.e. $t \to t + \delta t(\vec{R}, j)$, with

$$\delta t(\vec{R}, j) = \phi(\vec{R})e^{i\vec{K}\cdot\vec{e}_j}e^{i(\vec{K}-\vec{K}')\cdot\vec{R}}/3 + \text{ c.c.}\ , \tag{3.7}$$

which means ϕ induces a dimerization pattern in the honeycomb lattice and thus doubles the size of the unit cell or, in other terms, turns the C_6 symmetry of the original lattice into a smaller C_3 symmetry. This is depicted in FIG. 3.1.

We used the linearization of the hopping hamiltonian, Eq. (3.5), to introduce the Kekulé order parameter but the latter can be considered without discussing the former and both descriptions should, of course, be consistent. Because of the lattice origin of the Kekulé ordering as a modulated hopping amplitude, it is important to ensure that all other symmetries of the microscopic hamiltonian in Eq. (3.1) are preserved when we add interactions to the continuum limit of the linearized version Eq. (3.5). In this sense, the most relevant symmetry with respect to the Kekulé order is time reversal (TRS) symmetry, which basically amounts to demand that the modulation induced by ϕ is real. TRS is implemented in the linearized hamiltonian Eq. (3.5) by the transformation $\widehat{\psi} \to T\mathscr{K}\widehat{\psi}$ where $\mathscr{K}$ is complex conjugation and T is a matrix exchanging $\vec{K}$ and $\vec{K}'$ but leaving the sublattices invariant. In our representation, this matrix is given by

$$T = \sigma_x \otimes \sigma_x\ , \tag{3.8}$$

which, combined with the interpretation of ϕ as an order parameter, leads to the following transformation rule under TRS

$$\phi_1(\vec{R}) = \langle\widehat{\psi}^\dagger(\vec{R})\alpha_3\widehat{\psi}(\vec{R})\rangle \to +\phi_1(\vec{R})\ , \tag{3.9}$$

$$\phi_2(\vec{R}) = \langle\widehat{\psi}^\dagger(\vec{R})\alpha_5\widehat{\psi}(\vec{R})\rangle \to -\phi_2(\vec{R})\ . \tag{3.10}$$

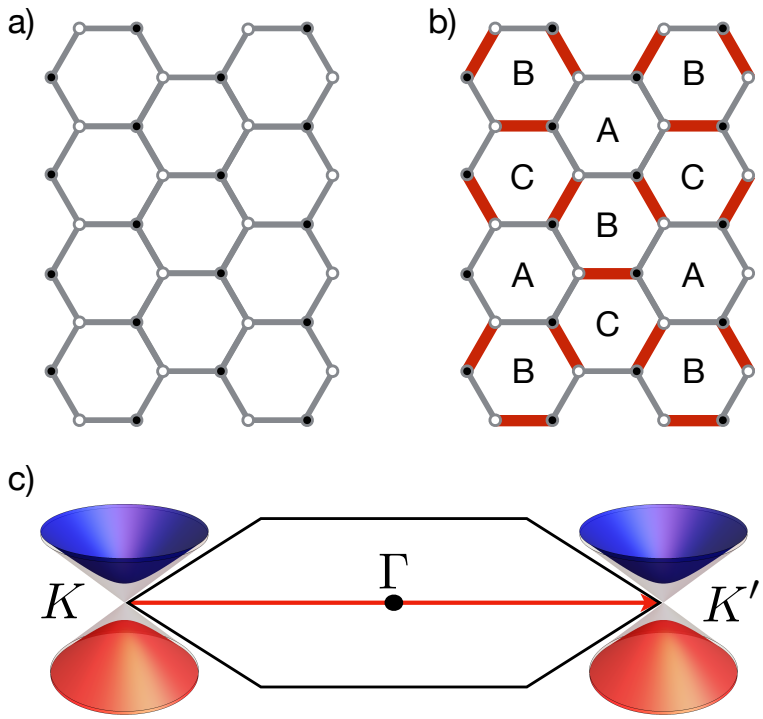

FIGURE 3.1: **Honeycomb lattice and Kekulé dimerization**. (a) Sublattices A and B are represented by the open and filled circles. (b) One of the three possible dimerization patterns of the Kekulé VBS state, where thick red lines mark stronger bonds and thinner gray lines mark weaker bonds. (c) Brillouin zone of the honeycomb lattice with the Dirac points K, K' where the Kekulé pattern opens a mass gap.

3.1.2 Fermion-induced quantum critical points

The Kekulé ordering can be any of three different but equivalent patterns observed in FIG. 3.1. Thus, ϕ is a complex-valued order parameter whose physics is invariant under rotations of $2\pi/3$ on the complex plane. Within the Landau-Ginzburg-Wilson approach and to study the onset of this order, one would define a free energy functional $F[\phi]$ possessing a discrete $\mathbb{Z}_3$ symmetry, i.e. $F[\phi]$ should include terms proportional to ϕ^3. A mean-field Landau-Ginzburg approach then suggests that the minimum of $F[\phi]$ discontinuously jumps from $\phi = 0$ to $\phi \neq 0$ when the system is tuned through the transition, see FIG. 3.2. This simple assessment, however, underestimates the impact of fluctuations which can become essential for an appropriate description of a system, when the dimensionality is decreased or when additional degrees of freedom are relevant. In fact, even beyond this mean field picture (as will be discussed below in Sec. 3.2.3 and in particular FIG. 3.3), a description in terms of a $\mathbb{Z}_3$ order parameter field alone appears to be inadequate for the Kekulé VBS transition in Dirac systems at zero temperature, as the fluctuations of the gapless Dirac fermions can strongly affect the nature of the phase transition.

For instance, it is known that the critical behaviour of $O(N)$-symmetric order parameters gets strongly modified by the inclusion of gapless fermion fluctuations and define the chiral universality classes [70–74]. That massless degrees of freedom affect the physics of this particular problem has already been hinted at in Refs. [14–17, 75], where evidence that the expected discontinuous Kekulé transition is rendered continuous in 2+1 dimensions is presented.

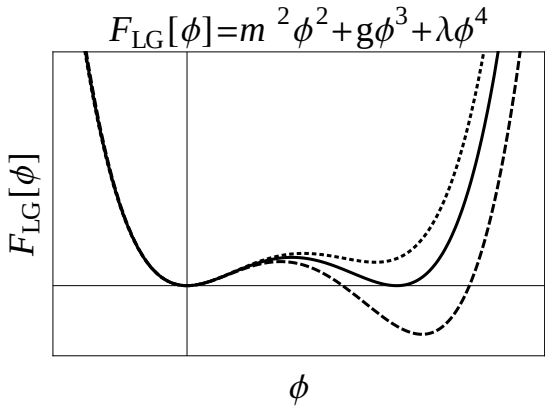

FIGURE 3.2: Landau-Ginzburg free energy for nonzero cubic terms $g \neq 0$. Across the transition, the minimum of $F[\phi]$ jumps from its value at the origin $F[\phi = 0] = 0$, to a nonzero value $F[\phi = \phi_{\min}] \neq 0$.

From a RG point of view, the fact that the phase transition changes from being discontinuous to continuous can be understood by considering the scaling dimensions of the coupling constant g corresponding to the cubic order-parameter term, i.e. $g\phi^3$. At the Gaußian, non-interacting fixed point, its presence suggests a second RG relevant direction with sizable power-counting dimension $[g] = 3 - D/2$ where the spacetime dimension is D. At a non-trivial interacting fixed point, fluctuation corrections modify the RG scaling of all couplings as compared to the scaling suggested by dimensional analysis [76, 77]. Whether the phase transition is first order or continuous then depends on whether the direction corresponding to the cubic coupling remains relevant or becomes irrelevant at the fixed point that describes this transition. This means when the fluctuations from the gapless Dirac fermions are strong enough to render the canonically relevant direction from the cubic coupling irrelevant, a continuous transition is induced. In this case, only one relevant direction remains, i.e. a single tuning parameter is sufficient to drive the system to the non-trivial fixed point and universal critical behavior can be observed [16].

3.1.3 Effective model for the Kekulé transition

In the previous section, it was established that a description of the KVBS transition requires considering the fluctuations of the gapless fermionic degrees of freedom. We now consider the continuum limit of the previously described theory and rephrase the main ingredients of the low energy effective theory in the path integral formalism. As a generalization we consider N_{f} pairs of independent Dirac points, to account for e.g. spin ($N_{\mathrm{f}} = 2$), so the euclidean Lagrangian corresponding to Eq. (3.5) takes the form (in units where $v_{\mathrm{f}} = 1$),

$$\mathscr{L}_0 = \sum_{\nu=1}^{N_{\mathrm{f}}} \overline{\psi}_\nu (-i\gamma^\mu \partial_\mu)\psi_\nu \ , \tag{3.11}$$

where we defined $\overline{\psi}_\nu := \gamma^0 \psi_\nu^\dagger$ for $\gamma^0 := \sigma_x \otimes \mathbb{1}_2$ and $\gamma^i := \gamma^0 \alpha_i$. Considering the Kekulé order parameter as a dynamical bosonic field, its coupling to the fermions corresponds to the Yukawa coupling

$$\mathscr{L}_y := h \sum_{\nu=1}^{N_f} \overline{\psi}_\nu \left(\phi_1 \gamma^3 + \phi_2 \gamma^5\right) \psi_\nu \ , \tag{3.12}$$

with $\gamma^{3/5} := \gamma^0 \alpha_{3/5}$. Note that in the Lagrangian for the fermions and the Yukawa interaction alone, cf. Eqs. (3.11) and (3.12), the chiral symmetry is the same as the $U(1)$ symmetry generated by $\gamma_{35} := -i\gamma^3\gamma^5$:

$$\psi \to e^{i\theta\gamma_{35}/2}\psi\,, \qquad \phi \to e^{i\theta}\phi\,. \tag{3.13}$$

This symmetry is, however, reduced by the transformation properties of ϕ under rotations of $2\pi/3$. Since any of the three dimerization patterns of FIG. 3.1 represents the same phase transition, the effective theory should be invariant under these rotations. For later convenience, we define $\phi = \frac{\phi_1+i\phi_2}{\sqrt{2}}$, so the dynamics of the order parameter are thus described by a lagrangian

$$\mathscr{L}_b = -|\partial\phi|^2 + V(\phi,\phi^*)\,, \tag{3.14}$$

in which the potential $V(\phi,\phi^*)$ contains all bosonic self-interaction terms allowed by $\mathbb{Z}_3$ symmetry. Since this includes all $U(1)$ symmetric terms, this means that V depends (only) on the rotationally invariant quantity $\rho := \phi^*\phi \propto \phi_1^2+\phi_2^2$, as well as a $\mathbb{Z}_3$-invariant quantity τ'. In principle, this means that we have two choices for τ':

$$\phi^3 + \phi^{*3} = \phi_1^3 - 3\phi_1\phi_2^2\,, \tag{3.15}$$

$$\text{or} \quad i(\phi^3 - \phi^{*3}) = \phi_2^3 - 3\phi_2\phi_1^2\,. \tag{3.16}$$

but due to Eq. (3.10) terms of odd degree in ϕ_2 alone are not time reversal symmetric, and should not enter the effective theory. This leads us to conclude that the most general potential describing the transition is a real function of the two invariants

$$\begin{aligned}\rho(\phi,\phi^*) &:= \phi^*\phi = \frac{\phi_1^2+\phi_2^2}{2}\,,\\ \tau'(\phi,\phi^*) &:= \phi^3 + (\phi^*)^3 = \frac{\phi_1^3 - 3\phi_1\phi_2^2}{\sqrt{2}}\,,\end{aligned} \tag{3.17}$$

that is $V(\phi,\phi^*) = U(\rho,\tau')$. The full low-energy effective theory for the transition is thus given by the Gross Neveu Yukawa theory with lagrangian [3, 67]

$$\mathscr{L} = \mathscr{L}_0 + \mathscr{L}_y + \mathscr{L}_b\,. \tag{3.18}$$

3.2 FRG analysis of the symmetry broken regime

3.2.1 Truncation

Our FRG analysis of the KVBS transition is based on an ansatz for the effective average action Γ_k, inspired by the original form of the microscopic lagrangian, Eq. (3.18). Denoting dimensionful quantitites by a bar, we have explicitly

$$\begin{aligned}\Gamma_k = \int d^Dx \Big[& Z_{\psi,k}\overline{\Psi}(-i\gamma^\mu\partial_\mu)\Psi + \bar{h}_k\overline{\Psi}\left(\Phi_1\gamma^3 + \Phi_2\gamma^5\right)\Psi\\ & - \frac{1}{2}Z_{\phi,k}(\Phi_1\partial_\mu^2\Phi_1 + \Phi_2\partial_\mu^2\Phi_2) + U_k(\bar{\rho},\bar{\tau}')\Big]\,,\end{aligned} \tag{3.19}$$

where $Z_{\psi,k}$ and $Z_{\phi,k}$ are the running wavefunction renormalization constants, $\bar{\rho}, \bar{\tau}'$ are the bosonic field invariants defined in Eq. (3.17) and (3.20), and $\bar{h}_k$ is the running Yukawa coupling. To simplify notation, we defined $\Psi := \oplus_i \Psi_i$, so that our gamma matrices are now of size $N_{\mathrm{f}} d_\gamma$, with d_γ the dimension of the chosen representation of the Clifford algebra of $\mathbb{R}^{2+1}$ (namely $d_\gamma = 4$). The potential $U_k(\bar{\rho}, \bar{\tau}')$ is defined as $\Gamma_k[\Phi, \Phi^*] =: \Omega\, U_k(\bar{\rho}, \bar{\tau}')$, where the fields Φ, Φ^*, Ψ are held constant and where Ω is the volume of the system.

In the symmetry-broken regime, the potential $V(\Phi, \Phi^*)$ exhibits three equivalent minima and the physics is generally determined by the global minimum of the potential and its surrounding. Consequently, we use an expansion around one of these three minima in the following. Additionally, to simplify some of the resulting expressions, we introduce another time reversal symmetric $\mathbb{Z}_3$-invariant quantity, which is a combination of ρ and τ':

$$\bar{\tau} := \bar{\tau}' + 2\bar{\rho}^{3/2} \,. \tag{3.20}$$

With this definition, we find that $\bar{\tau} = 0$ when evaluated at a minimum of $V(\Phi, \Phi^*)$. We note that the whole procedure could also be carried out in terms of monomials of the original fields,so that there are no introduced nonanalytic terms by using this new invariant.

3.2.2 Flow equations

The different threshold functions $l^{\cdots}_{\cdots}, m^{\cdots}_{\cdots}$ can be all evaluated explicitly and are presented in App. A.1

Mass terms and bosonic potential

To discuss fixed point properties, it is necessary to switch to dimensionless variables, denoted without the bar, and defined as

$$\rho := \frac{k^{D-2}}{Z_{\phi,k}} \bar{\rho} \,, \quad \text{and} \quad \tau := \frac{k^{3(D-2)/2}}{Z_{\phi,k}^{3/2}} \bar{\tau} \,, \tag{3.21}$$

for the bosonic invariants and

$$h^2 := \frac{\bar{h}^2}{k^{4-D} Z^1_{\phi,k} Z^2_{\psi,k}} \,, \tag{3.22}$$

for the Yukawa coupling.

Moreover, to study the FIQCP from both sides of the transition we now expand the dimensionless potential $u := k^{-D} U_k$ around $\rho = \tau = 0$ for the symmetric phase and around one of its running minima, $\kappa_{\rho,k} := \rho^{\min}_{j,k} \neq 0$ for the symmetry broken regime. Here, $j \in \{1, 2, 3\}$ enumerates the three equivalent minima of the potential. We use the freedom in choosing any of the three minima by choosing one in which τ vanishes, which is equivalent to the choice $\phi_1^{\min} = -\sqrt{2\rho}, \phi_2^{\min} = 0$.

The expansion of the potential in the symmetric regime then reads explicitly

$$u_k(\rho, \tau) = \sum_{m+n=1}^{N_{\max}} \frac{\lambda_{m,n;k}}{m!n!} \rho^m \tau^n \,, \tag{3.23}$$

with

$$\lambda_{m,n;k} := \frac{\partial^{m+n} u_k}{\partial \rho^m \partial \tau^n}\Big|_{\rho=\tau=0} ; \tag{3.24}$$

while in the symmetry-broken regime, the expansion is given by

$$u_k(\rho,\tau) = \Lambda_{0,1;k}\tau + \sum_{m+n=2}^{N_{\max}} \frac{\Lambda_{m,n;k}}{m!n!}(\rho-\kappa_{\rho,k})^m \tau^n , \tag{3.25}$$

where

$$\Lambda_{m,n;k} := \frac{\partial^{m+n} u_k}{\partial \rho^m \partial \tau^n}\Big|_{\rho=\kappa_\rho,\tau=0} , \tag{3.26}$$

$$0 = \frac{\partial u_k}{\partial \rho}\Big|_{\rho=\kappa_\rho,\tau=0} , \tag{3.27}$$

and $N_{\max}$ denotes the order of the truncation.

The flow equations are functions of the second and third derivatives of the bosonic potential. Of particular importance is the Hessian of the potential, for its eigenvalues define the longitudinal and transversal masses. We denote the derivatives with respect to the components of ϕ with a subindex and the derivatives with respect to the invariants Eqs. (3.17) and (3.20) by a superindex, i.e. $u_{ij} = \frac{\partial^2 u}{\partial\phi_i \partial\phi_j}$ and analogously for u_{ijk} and $u^{(m,n)} = \frac{\partial^{m+n} u}{\partial\rho^m \partial\tau^n}$. With these conventions, the general expression for the masses in terms of the invariants ρ and τ is

$$\begin{aligned} m^2_{L,T} = {} & \rho u^{(2,0)} + \frac{9}{2}\sqrt{\rho} u^{(0,1)} + u^{(1,0)} + \tau\left(2u^{(0,2)} + 3u^{(1,1)}\right) \pm \\ & \Bigg[\left(\rho u^{(2,0)} - \frac{9}{2}\sqrt{\rho}u^{(0,1)}\right)^2 + 3\tau\left(2u^{(0,1)} + 3(\tau - 2\rho^{3/2})u^{(0,2)} + 2\rho u^{(1,1)}\right) u^{(2,0)} \\ & + \frac{9\tau}{\sqrt{\rho}}(u^{(0,1)})^2 + \frac{9\tau}{2\sqrt{\rho}}\Big(\left(3(6\rho^{3/2}+\tau)u^{(0,2)} + 10\rho u^{(1,1)}\right) u^{(0,1)} \\ & + 2\rho\left(9\sqrt{\rho}\tau(u^{(0,2)})^2 + 6\tau u^{(1,1)}u^{(0,2)} + 4\rho(u^{(1,1)})^2\right)\Big)\Bigg]^{1/2} . \end{aligned} \tag{3.28}$$

which simplify substantially when evaluated at the minimum of our choice to

$$m^2_{L,\min} = 2\kappa_\rho \Lambda_{2,0} , \tag{3.29}$$

$$m^2_{T,\min} = 9\sqrt{\kappa_\rho}\Lambda_{0,1} . \tag{3.30}$$

From Eqs. (3.29) and (3.30), it can be seen that there are no Goldstone modes in the system for any nontrivial dependence of u on τ, which is to be expected given that only a discrete symmetry is broken. In other terms, the masses m^2_L, m^2_T are always different and nonzero except exactly at the phase transition. The appearance of a nonzero transversal mass is the reason behind the emergence of a second length scale in the symmetry-broken regime. Note, moreover, that this phenomenon can only be seen when $\kappa_\rho \neq 0$ and, in particular, observing its effect depends crucially on the fact that we can follow the evolution of the system for arbitrarily large values of κ_ρ, which is not a feasible task in a perturbative approach. In

terms of these masses, the flow equation for u is given by

$$\partial_t u = -Du + \frac{1}{2}(D-2+\eta_\phi)\left(2\rho u^{(1,0)} + 3\tau u^{(0,1)}\right) + 2\left(l_B(m_L^2) + l_B(m_T^2)\right) - 2N_{\mathrm{f}} d_\gamma l_F(\omega_\psi), \tag{3.31}$$

where $\omega_\psi = 2h^2\rho$, and the anomalous dimension η_ϕ will be defined below. Flow equations for the individual bosonic couplings λ/Λ are obtained by acting with ∂_t on both sides of Eqs. (3.26) and (3.27). Further terms appearing in the flow equations below are given by the expressions

$$u_{11} = 2\rho u^{(2,0)} + u^{(1,0)}\,, \tag{3.32}$$
$$u_{12} = u_{21} = 0\,, \tag{3.33}$$
$$u_{22} = 9\sqrt{\rho}u^{(0,1)} + u^{(1,0)}\,, \tag{3.34}$$
$$u_{111} = -\sqrt{2\rho}\left(3u^{(2,0)} + 2\rho u^{(3,0)}\right)\,, \tag{3.35}$$
$$u_{112} = u_{121} = u_{211} = u_{222} = 0\,, \tag{3.36}$$
$$u_{221} = u_{212} = u_{122} = \frac{9u^{(0,1)} + 18\rho u^{(1,1)} + 2\sqrt{\rho}u^{(2,0)}}{-\sqrt{2}}\,. \tag{3.37}$$

Yukawa Coupling

To obtain a projection for the Yukawa coupling, we expand the fields as a sum of their expectation value plus a fluctuating part, i.e. $\Phi_1 = \Phi_{1,0} + \Delta\Phi_1$, $\Phi_2 = \Delta\Phi_2$. We choose the following projection for the Yukawa coupling,

$$\bar{h}_k = \frac{1}{N_f d_\gamma}\mathsf{Tr}\left[\gamma_5 \frac{\delta}{\delta\Delta\Phi_2(p')}\frac{\delta}{\delta\bar{\Psi}(p)}\Gamma_k\frac{\delta}{\delta\Psi(q)}\right]\,, \tag{3.38}$$

leading to the flow equation

$$\partial_t h^2 = (D-4+\eta_\phi+2\eta_\psi)h^2 - 8h^4\left(l_{11}^{FR_2} - l_{11}^{FR_1}\right) - 16\sqrt{2\kappa_\rho}h^4 u_{122} l_{111}^{FR_1R_2}\,. \tag{3.39}$$

Anomalous dimensions

The anomalous dimensions, are defined as

$$\eta_\phi = -\partial_t \ln Z_{\phi,k}\,, \qquad \eta_\psi = -\partial_t \ln Z_{\psi,k}\,, \tag{3.40}$$

and to compute them, we evaluate the Wetterich equation for momentum dependent fields and take the derivatives with respect to momenta of the two point function. We project onto the transversal mode to obtain the low energy contributions (this would correspond to the Goldstone modes in a continuous symmetry-breaking scenario). Explicitly,

$$Z_{\phi,k} = \frac{\partial}{\partial p^2}\int_q \frac{\delta}{\delta\Delta\Phi_2(-p)}\frac{\delta}{\delta\Delta\Phi_2(q)}\Gamma_k \tag{3.41}$$
$$Z_{\psi,k} = \frac{1}{Nd_\gamma D}\mathsf{Tr}\left[\gamma_\mu\frac{\partial}{\partial p_\mu}\int_q \frac{\delta}{\delta\bar{\Psi}(p)}\Gamma_k\frac{\delta}{\delta\Psi(q)}\right]\,, \tag{3.42}$$

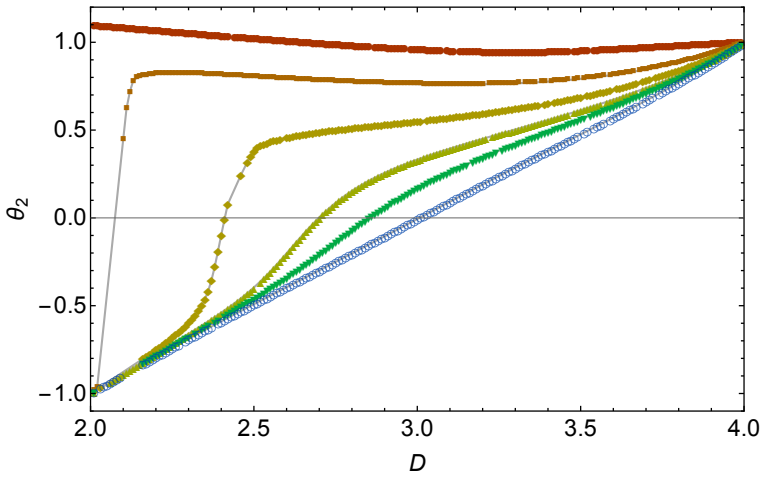

FIGURE 3.3: **Stability exponent** θ_2 for the $U(1)$ symmetric non-Gaußian fixed point of the $\mathbb{Z}_3$ GNY model. In the purely bosonic limit, this corresponds to the $O(2)$-symmetric Wilson-Fisher FP. We show different small numbers of fermion flavors N_f as function of the dimension. From top to bottom, we show $N_f \in \{0, \frac{1}{4}, \frac{1}{2}, \frac{3}{4}, 1, 2\}$. As soon as fermions are added, this FP becomes stable below some critical dimension. The results have been calculated in LPA8′.

from which one gets the flow equations

$$\eta_\psi = \frac{8v_D}{D} h^2 \left(m^{FB}_{(12)R_1} + m^{FB}_{(12)R_2} \right) , \tag{3.43}$$

$$\eta_\phi = \frac{4v_D}{D} \Big[m^B_{4R_2}(u_{222}, u_{221}) + m^B_{4R_1}(u_{211}, u_{221}) + 2m^B_{(22)R_1R_2}(u_{221}, u_{211}, u_{222}) + 2N_\mathrm{f} d_\gamma h^2 \left(m^F_4(\omega_\psi) + 2h^2 \kappa_\rho m^F_2(\omega_\psi) \right) \Big] , \tag{3.44}$$

where $v_D = (2^{D+1}\pi^{D/2}\Gamma(D/2))^{-1}$ is a geometric factor coming from the loop integrations. For a given truncation of the potential including powers of the field up to N_max, Eqs. (3.31) to (3.44) form a closed set of coupled differential equations, cf. Ref. [16].

3.2.3 Fixed point analysis

The FRG approach as set up in the previous section allows us to study the fixed-point properties of the system, as well as the RG flows in the symmetric and the symmetry-broken regime. In this section, we first extend previous investigations of the FIQCP by including spacetime dimensions $1+1 \leq D \leq 2+1$ which are accessible with the FRG [78–83]. Then, we present how the system flows from the Dirac semimetal regime to the ordered phase and we explain the different regimes of this flow in terms of the characteristic fixed point structure. Finally, we give estimates for the scaling exponent of the second length scale that emerges in the ordered phase.

Fermion-induced QCP below $D = 2 + 1$

The existence of the FIQCP above a critical $N_{\mathrm{f,c}} \approx 1.9$ in $D = 2 + 1$ was established in the work [16], where the FRG analysis of fixed points in the symmetric regime was carried out. there it was found that the FIQCP is characterized by an emergent $U(1)$ symmetry where all couplings that break the $U(1)$ down to $\mathbb{Z}_3$ vanish at the fixed point. Therefore, the FIQCP

coordinates and, more importantly, a subset of the critical exponents coincide with the ones from the chiral XY model which also exhibits a global $O(2) \cong U(1)$. An analysis of the fixed points for lower dimensions is the goal of this section.

Here, we show that this is also true for lower dimensions, cf. also Ref. [14]. We find that for any given non-zero number of Dirac fermions N_f, there is a critical dimension below which an $O(2)$ symmetric Gross-Neveu-Yukawa fixed point becomes stable so that a second order transition is induced realizing the FIQCP scenario. This can be seen in FIG. 3.3, where we plot the second largest critical exponent θ_2 of the $O(2)$-symmetric fixed point for different dimensions and N_f. If $\theta_2 < 0$, the fixed point is stable and describes a second order phase transition. We see how θ_2 of the $O(2)$-symmetric FP changes from the case without fermions $N_f = 0$ to the one with fermions and that it drops below zero at a critical dimensions $D_c > 2$ as soon as $N_\mathrm{f} \neq 0$. This critical dimension continuously connects to the value that was found before [16].

Interestingly, there is potentially another fixed point that can yield a second order transition for dimensions close to $D = 2$: in the system without fermions, this fixed point corresponds to the phase transition of the three-state Potts model [84–86], and disappears above a certain critical dimension in the vicinity of $D = 3$, see Sec. 3.4. We find, however, that as soon as the fermions are included, this Pott's fixed point always becomes unstable, so that the $O(2)$-symmetric FIQCP is the only possibility to obtain a second order transition. The reason for the destabilization of the Potts fixed point upon inclusion of fermions is that, even for small N_f, we introduce another RG direction represented by the Yukawa coupling h. At the Potts fixed point, the Yukawa coupling is $h^* = 0$, and below $D = 4$, this always introduces a relevant direction to the Potts fixed point making it unstable.

3.3 Flow from Dirac semimetal to Kekulé order

Turning back to the physical case of $D = 2+1$, we now study the renormalization group flow of the model, which exhibits a rich structure. In the phase diagram of the considered Gross-Neveu-Yukawa model, the FIQCP separates the symmetric or Dirac-semimetal (DSM) from the symmetry-broken regime. To see the scaling behavior as induced by the FIQCP, a fine-tuning of the RG-relevant parameter is required. Eventually, in the deep infrared, when almost all momentum-modes have been integrated out, the system ends up either in the DSM phase or in the symmetry-broken phase. To understand the semimetal-to-Kekulé-VBS transition in terms of the renormalization group flow, we have to consider the fixed point structure beyond the FIQCP. Generally, the renormalization group flow to the symmetry-broken phase in the vicinity of the fermion-induced QCP proceeds as follows [14]:

(1) At microscopic scales, the RG flow of the system is initialized in the symmetric regime and a fine-tuning of the mass parameter m^2 has to be performed to drive the system close to the FIQCP.

(2) The system still remains in the symmetric regime on intermediate scales where it approaches the FIQCP which then dominates the scaling behavior. In this regime the cubic coupling, $\lambda_{0,1} =: g$, is attracted to its fixed-point value $g^* = 0$ and therefore becomes small.

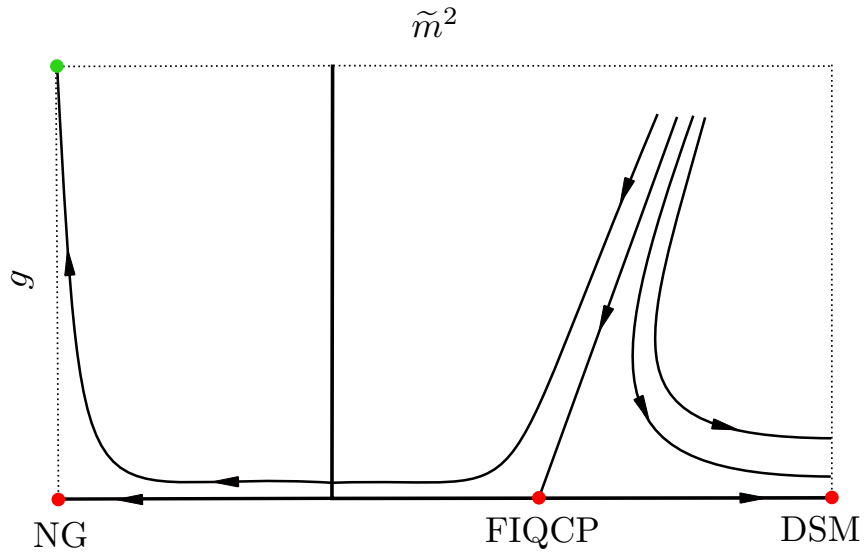

FIGURE 3.4: **Schematic flow of the cubic coupling** as a function of a tuning parameter $\widetilde{m}^2$. $\widetilde{m}^2 > 0$ indicates the system is in the symmetric regime and $\widetilde{m}^2 < 0$ that it is in the symmetry broken regime. Vertical dotted lines are $\widetilde{m}^2 = \pm\infty$. We show four trajectories for identical initial g and different values of $\widetilde{m}^2$.

(3) After some RG-time close to the FIQCP, the flow departs from it and goes towards the fixed point that characterizes the symmetry-broken phase of the $O(2)$ model - the Nambu-Goldstone (NG) fixed point. We note that due to the small but finite cubic coupling, the transversal mode already acquires a small mass.

(4) Finally, as the cubic coupling is relevant at the NG fixed point and $g \neq 0$ the flow will be driven away from the NG fixed point and the mass of the pseudo-Goldstone mode becomes more pronounced which is related to the appearance of the second length scale ξ'.

When the initial system is not fine-tuned, the flow will stay in the symmetric regime, dominated by a fixed point that we call DSM fixed point in the following. This behavior is schematically shown in FIG. 3.4. In the following, we describe the different fixed point regimes characterizing the symmetric and ordered phase in detail. Furthermore, we show representative RG flow trajectories of the quartic coupling in FIG. 3.5 running through all the described regimes explicitly. Thereby the different fixed point regimes are revealed as plateaus where the flow of the quartic coupling hardly changes. However, if there is a relevant direction, the flow is eventually driven away from the corresponding fixed point value.

Dirac semimetal regime.

When the system is in the DSM phase it is eventually dominated by the symmetric DSM fixed point which can be analytically found in the symmetric FRG flow equations upon taking the limit $\lambda_{1,0} =: m^2 \to \infty$. In this limit, we obtain the following β functions for e.g. the Yukawa coupling (h^2), the cubic (g) and the quartic scalar coupling ($\lambda := \lambda_{2,0}$)

$$\beta_{h^2} = h^2 \left(D - 4 + 2c_D N_\mathrm{f} h^2 \frac{3D-4}{D(D-2)} \right) , \tag{3.45}$$

$$\beta_g = \frac{g}{2} \left(D - 6 + 6c_D N_\mathrm{f} h^2 \frac{3D-4}{D(D-2)} \right) , \tag{3.46}$$

$$\beta_\lambda = \lambda(D-4) - \frac{4c_D N_\mathrm{f} h^2}{D}\left(8h^2 + \lambda\frac{4-3D}{(D-2)}\right), \tag{3.47}$$

where $c_D = d_\gamma v_D$. These admit a nontrivial fixed-point solution

$$h^{2,*}_{\mathrm{DSM}} = \frac{D}{2c_D N_\mathrm{f}}\frac{(4-D)(D-2)}{(3D-4)}, \tag{3.48}$$

$$g^*_{\mathrm{DSM}} = 0, \tag{3.49}$$

$$\lambda^*_{\mathrm{DSM}} = \frac{8D}{c_D N_\mathrm{f}}\frac{(4-D)(D-2)^2}{(3D-4)^2}. \tag{3.50}$$

We note that these β functions are not restricted to a finite expansion in the LPA′, but are valid to any order, i.e. in particular for LPAn' with $n \to \infty$. In fact, one can characterise the Dirac semimetallic phase by precisely these fixed point values and moreover, the values of the couplings at the DSM fixed point depend only on the dimension D and the fermion number N_f. As we mentioned before, they are independent of the order of truncation within the LPA′ and the fixed point solution can be generalized to arbitrary $\lambda_{r,s}$.

$$\lambda^{*\mathrm{DSM}}_{r,s} = \left(\frac{(4-D)(2-D)D}{c_D N_\mathrm{f}(3D-4)}\right)^r \frac{4c_D N_\mathrm{f} r!}{D(2r-D)}\delta_{s,0}, \tag{3.51}$$

for all $s \in \mathbb{N}_0$, $r \geq 2$. Further, the anomalous dimensions for the order parameter fluctuations and the Dirac fermions characterizing the DSM are

$$\eta^*_\phi = 4 - D, \tag{3.52}$$

$$\eta^*_\psi = 0. \tag{3.53}$$

An evaluation of the stability matrix at the DSM fixed point gives three leading eigenvalues

$$\theta_{1,\mathrm{DSM}} = D-3, \quad \theta_{2,\mathrm{DSM}} = \theta_{3,\mathrm{DSM}} = D-4. \tag{3.54}$$

Therefore, disregarding the flow of the mass term $\sim m^2$, there is no relevant direction at the DSM fixed point as $\theta_i \leq 0$. Only the direction corresponding to the cubic coupling turns out to be marginal. This implies that, while all other couplings flow to their respective DSM-fixed-point values, the cubic coupling freezes at different infrared values, depending on the initial conditions.

Symmetry-broken regime

After departing from the FIQCP in the symmetry-broken regime, the RG flow exhibits a window of scales where the couplings are dominated by the fermionic generalization of the Nambu-Goldstone fixed point, which is well-known from the purely bosonic $O(N)$ models. Therefore, it is characterized by the vanishing of all the $U(1)$ breaking couplings $\Lambda_{i,j} = 0$ for $j > 0$ and $h^2 = 0$. Furthermore, we can define it formally in terms of the limit $\kappa_\rho \to \infty$, which allows us to simplify the β functions in the symmetry-broken regime. The lowest order couplings have the β functions

$$\beta_{\Lambda_{2,0}} = \Lambda_{2,0}\left(\frac{8v_D\Lambda_{2,0}}{D} + (D-4)\right), \tag{3.55}$$

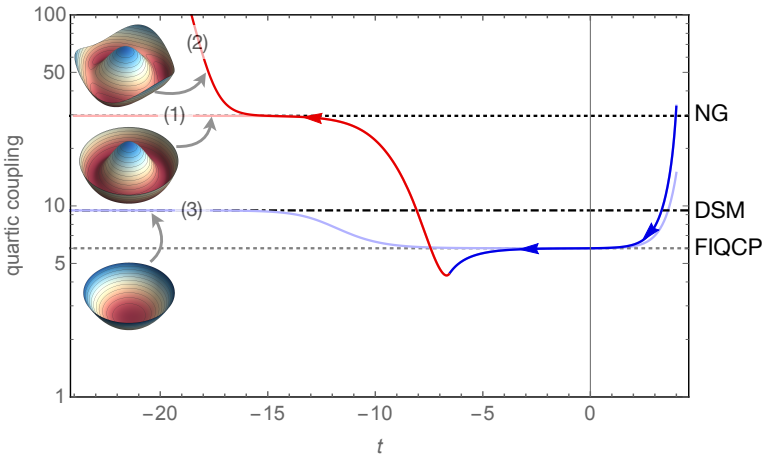

FIGURE 3.5: **Flow of the quartic coupling** into the different regimes: (1) for $g \equiv 0$ the flow generically starts in the symmetric regime in the ultraviolet and can be fine-tuned to approach the FIQCP. Later, it may enter the SSB regime (as indicated by the change of color from blue to red) and flows to the NG fixed point, where it remains (light red line). (2) For small $g \neq 0$ the flow trajectory is almost identical during the entire flow. Only in the deep IR it departs from the NG fixed point due to the dangerously irrelevant direction corresponding to the cubic operator. (3) There can also be flows which remain completely in the symmetric regime and no symmetry breaking occurs. In this case the flow approaches the DSM fixed point in the deep IR as indicated by the light blue line. In the insets, we schematically show the shape of the effective potential in the different regimes.

$$\beta_{\Lambda_{3,0}} = (2D-6)\Lambda_{3,0} + \frac{24 v_D \Lambda_{2,0}}{D}\left(\Lambda_{3,0} - \Lambda_{2,0}^2\right) \ . \tag{3.56}$$

These β functions admit a non-trivial fixed point solution for the scalar couplings, which we refer to as the Nambu-Goldstone (NG) fixed point, reading

$$\Lambda_{2,0}^{*\mathrm{NG}} = \frac{D(4-D)}{8 v_D}, \ \Lambda_{3,0}^{*\mathrm{NG}} = 3\left(\frac{D}{8 v_D}\right)^2 \frac{(4-D)^3}{6-D} \ . \tag{3.57}$$

Just as in the case of the DSM fixed points, the β functions Eq. (3.56), and therefore the fixed point values of the couplings, Eq. (3.57), are independent of the order of the truncation and are valid for any LPAn'. This can be traced back to the fact that for $h^2 \to 0$ and $\kappa_\rho \to \infty$, the β functions for any given coupling of order r depend only on the couplings of degrees less than r, i.e. there is some function depending on r, f_r, such that

$$\beta_{\Lambda_{r,0}} = f_r(\{\Lambda_{j,0}\}), \quad j \leq r \ . \tag{3.58}$$

Moreover, it can be seen that the NG fixed point solution is independent of N_f. The Yukawa coupling and the $U(1)$ breaking coupling are both relevant directions at the NG fixed point. Without them, i.e. in case of the $O(2)$ model, the NG fixed point is fully attractive and completely dominates the infrared behavior of the model in the symmetry-broken phase. The evaluation of the full stability matrix at the NG fixed point, taking into account perturbations in the direction induced by h^2 and $U(1)$-breaking couplings $\Lambda_{i,j}^{*\mathrm{NG}} = 0$ for $j > 0$, shows that the cubic coupling not only is relevant at the NG fixed point, but it is the most relevant

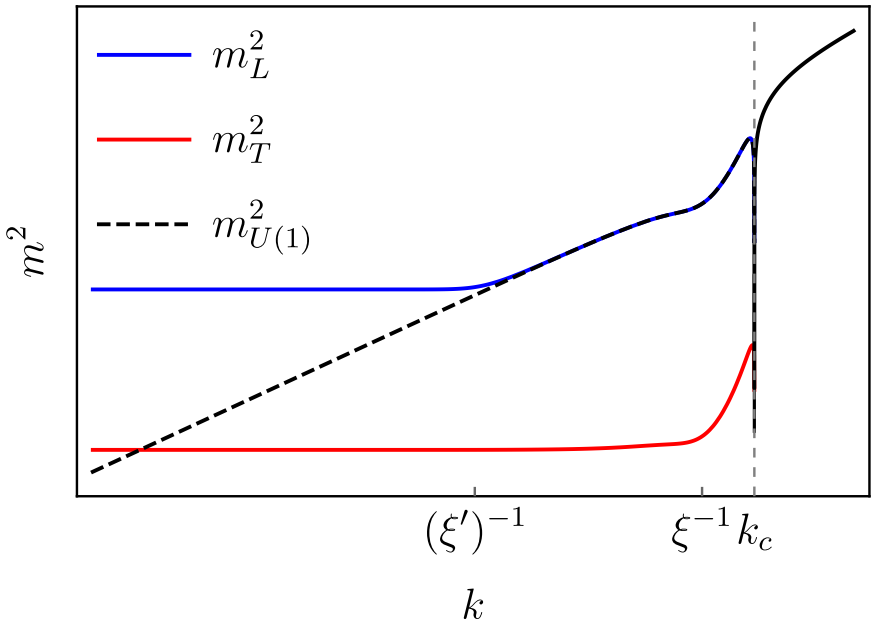

FIGURE 3.6: **Flow of the dimensionful masses** $m^2_{L,T}$, cf. Eqs. (3.29) and (3.30), in the symmetry broken regime. The red and blue curves correspond to the masses of one of the trajectories that escape the NG fixed point (i.e., when $g \neq 0$) and the black dashed curve corresponds to the flow of the purely $U(1)$ symmetric system with otherwise identical initial conditions. At the beginning of the flow all masses are identical and they eventually split when approaching the IR. In the IR both masses flow to non-zero values $m^2_L(k=0) \neq 0$, $m^2_T(k=0) \neq 0$.

coupling in $D = 3$, as

$$[g]_{\mathrm{NG}} = \frac{6-D}{2} \ , \ [h^2]_{\mathrm{NG}} = 4 - D \ , \ [\kappa_\rho]_{\mathrm{NG}} = 2 - D \ . \tag{3.59}$$

3.3.1 Second correlation length exponent

Having established the global RG flow of the model, we turn again to its implication for critical properties. The fact that the cubic coupling changes from being irrelevant at the FIQCP to relevant at the NG fixed point implies that eventually, in the deep infrared, the flow is driven away from the NG fixed point when the cubic coupling does not exactly vanish. This means that g will start to grow. As a result the transversal mass, which is zero for $g = 0$, also increases and thus provides a second mass scale besides the longitudinal mass (cf. Eq. (3.29)). We show the evolution of the dimensionful longitudinal and transversal masses in FIG. 3.6.

The two length scales ξ and ξ' can de defined from the values of k for which the flow departs from the FIQCP and the NG fixed point, respectively [87]. For $k > k_c$, the longitudinal and transversal mass are identical and both flow to zero at the transition to the Kekulé phase. On the symmetry-broken side of the transition $k < k_c$, they split and, after an initial increase, fluctuations lead to a decrease of the masses towards the infrared. The transversal inverse susceptibility (i.e. the mass) stops running beyond the scale given by $k\xi \lesssim 1$ while the longitudinal susceptibility does so at the scale $k\xi' \lesssim 1$. This means that the respective

dimensionless quantities flow according to their canonical dimension, i.e. for $k < \xi^{-1}$

$$m_T^2 \sim \sqrt{\kappa_\rho(k)}g(k) \sim \sqrt{\kappa_\rho(\xi^{-1})}(k\xi)^{(2-D)/2}g(\xi^{-1})(k\xi)^{(D-6)/2} \sim \sqrt{\kappa_\rho^*}g^* k^{-2}\xi^{-|\theta_2|-2} \\ =: k^{-2}\delta t^{\nu(2+|\theta_2|)} , \tag{3.60}$$

where, $\nu = \theta_1^{-1}$ corresponds to the inverse correlation length exponent of the $\mathbb{Z}_3$ order, θ_2 is the scaling exponent related of the cubic coupling at the FIQCP and δt the distance to the critical point. Since the second length scale marks where the (dimensionless) transversal mass escapes the NG, this happens when $m_T^2(k = \xi'^{-1}) \approx 1$, so by definition

$$m_T^2 \sim (k\xi')^{-2} =: k^{-2}\delta t^{2\nu'} . \tag{3.61}$$

Eqs. (3.60),(3.61) thus lead to

$$\frac{\nu'}{\nu} = 1 - \frac{\theta_2}{2} . \tag{3.62}$$

Despite the exclusive appearance of the second length scale in the symmetry-broken regime, the ratio of their correlation length exponents ν'/ν is uniquely determined by a scaling law employing properties of the FIQCP alone [14, 87]. This can be understood in terms of the dangerously irrelevant coupling g. Only if g is non-zero, the transversal mass, which is responsible for the second scale, will be finite away from the critical point. Therefore the scaling of m_T^2 must be related to scaling of g at the critical point. This scaling, in turn, is given by θ_2.

In Tab. 3.1, we show the two largest critical exponents for several choices of N_f and list our estimates for ν', whenever we find that the FIQCP is stable in $D = 2 + 1$. ν' shows only very small deviations from ν due to the smallness of $|\theta_2| \ll 1$ which we deem unlikely to be observed either in an experimental setup or in lattice Quantum Monte Carlo (QMC) simulations. Instead, as stated in earlier works [16], one can expect that large corrections to scaling will have to be considered in corresponding lattice QMC simulations.

TABLE 3.1: **Correlation length exponents:** Numerical values for the largest two critical exponents and the second correlation length exponent for different N_f in $D = 2 + 1$ in LPA$12'$. The exponents are given by $\nu = \theta_1^{-1}$ and $\nu' = \nu(1 - \theta_2/2)$. The exponent deciding over stability θ_2 is shown in boldface.

N_f	ν	θ_2	ν'
1	1.195	**+0.167**	-
2	1.157	**-0.0031**	1.159
3	1.109	**-0.0235**	1.122
4	1.082	**-0.0263**	1.096
5	1.066	**-0.0255**	1.080
∞	1	**0**	1

3.4 A sanity check: remark on the Potts model

Due to the fact that the FRG approach does not rely on any parameters being small, it is useful to find some form of benchmarking of our results other than the convergence described in Section 2.2.2. Some aspects of the Kekulé transition in $D = 3$ have been explored

with QMC simulations in [17], and the results there are in relatively good agreement with the corresponding FRG calculations of critical exponents in [16]. For $2 \leq D < 3$, to the best of our knowledge, there are no analogous numerical results.

For one particular case, however, there is something better: an exact result. Indeed, for $N_{\mathrm{f}} = 0$ and $D = 2$, the effective action reduces to the bosonic part only, i.e. Eq. (3.14) and this is the field theory of a three-state Potts model, for which the exact solution is known [85]. In particular, it is known that there are two critical points: a critical Potts and a tricritical fixed point (TCP) with three relevant directions. The Potts FP comes with correlation length exponent and anomalous dimension[85]

$$\mathrm{Potts}: \nu_{2,\mathrm{ex}} = \frac{5}{6} \approx 0.83\,, \;\; \eta_{2,\mathrm{ex}} = \frac{4}{15} \approx 0.27\,. \tag{3.63}$$

The critical and tricritical fixed points can be continued above two dimensions where they change their coordinates. It is expected [85] that these two collide and disappear to the complex plane for some $d_c > 2$. In that case no stable fixed point exists in the system and the transition from the symmetric to the $\mathbb{Z}_3$ ordered phase is discontinuous. Numerical results in $d = 3$ for the three-state Potts model suggest that $d_c < 3$.

Here, we explore a simple approach to the two-dimensional case by a finite expansion in the LPA′ and note that this can only provide qualitative results on the Potts fixed point. As has been shown in earlier work for scalar [78–81, 83] and scalar-fermion models [82], the FRG can also be used to describe critical behavior below three dimensions. For a quantitive estimate, it will be required to work with higher expansions or use methods beyond a finite expansion, as towards two dimensions more and more couplings become canonically relevant.

Employing an LPA8′ expansion in the symmetric regime, we can give first estimates on the limit of the purely bosonic Potts model. In fact, we find both the critical Potts fixed point and one tricritial fixed point, as expected. In $d = 2$ the Potts fixed has the critical exponents

$$\mathrm{Potts}: \nu_{2,\mathrm{LPA8'}} \approx 0.82\,, \quad \eta_{2,\mathrm{LPA8'}} \approx 0.22\,, \tag{3.64}$$

which already compares well to the exact results. Also, we can continue the fixed point search in higher dimensions towards $d = 3$ and beyond to exhibit the fixed-point collision. Within LPA8′, we find that the Potts FP and the tricritical FP indeed collide at a critical dimension of $d_{c,\mathrm{LPA8'}} \approx 3.2$ which seems too large in comparison with numerical results. We observe that higher orders in the LPA′ seem to push the critical dimension below three. However, we note that, in contrast to the FIQCP, going to higher orders in the LPA′ still leads to corrections and we do not yet see convergence. Therefore, to settle the convergence of the critical exponents and the critical dimension for the Pott's fixed point with the fRG, a more thorough study will be required, which is beyond the scope of this work. As one alternative, we suggest the pseudo-spectral methods as developed in Refs. [83, 88, 89] for FRG applications.

3.5 Conclusion

In this chapter, we have provided a thorough study of the renormalization group flow near the fluctuation-induced quantum phase transition to the Kekulé VBS state in Dirac semimetals as it appears for fermions on the two-dimensional honeycomb lattice. This transition is characterized by the condensation of the Kekulé order parameter which reduces the chiral $U(1)$ symmetry of the Dirac system to a discrete $\mathbb{Z}_3$ symmetry, resulting in a series of unconventional properties at and close to the quantum transition. Firstly, the fact that the transition is continuous and not discontinuous is an effect driven by strong (fermion) fluctuations. Secondly, there is an emergent $U(1)$ symmetry at the quantum critical point and, thirdly, a second length scale appears in the symmetry broken phase due to the breaking of the discrete symmetry. We noted that these properties are shared with the scenario of the deconfined QCPs.

We have investigated the semimetal-to-Kekulé quantum transition in terms of an appropriate Gross-Neveu-Yukawa model with the help of the non-perturbative functional renormalization group. While building on our previous work, we have extended it in various directions. First, we have established the FIQCP scenario for the full range of dimensions between $1+1 \leq D \leq 2+1$ for small numbers of fermion flavors $N_{\mathrm{f}} \leq 2$.

We have found that for every $N_{\mathrm{f}} > 0$, there is a critical dimension $2 < D < 4$ above which the fermion-enhanced $O(2)$ fixed point becomes stable, giving rise to a second order transition. This is in stark contrast to the model where $N_{\mathrm{f}} = 0$, corresponding to the field-theoretical formulation of the three-state Potts model, where only close to $D = 1+1$ does a stable $O(2)$-breaking fixed point appear. Our findings fit nicely to the observation that fermions in Dirac systems tend to support symmetry enhancement [26, 51, 90–92].

Furthermore, we have discussed that, due to the discrete symmetry breaking, there are no Goldstone modes. Instead, in the symmetry-broken regime, two finite masses appear - the longitudinal and transversal mass. Importantly, the scaling of the transversal mass depends on the scaling of the cubic term and defines a second length scale, which diverges at the QCP.

We provided a comprehensive analysis of the fixed-point structure in the symmetric as well as in the symmetry broken regime. By solving the flow equations in both regimes, we studied the complete behavior of the RG flow beyond a pure fixed point analysis. While the Dirac semimetal fixed point dominates the long-range behavior of the system in the semimetallic phase, the symmetry-broken regime shows a more subtle behavior: here, the Nambu-Goldstone fixed point dominates the system on intermediate length scales. Eventually, when the cubic coupling is finite, the RG flow leaves the NG regime giving rise to a sizable transversal mass and the concomitant second length scale.

We also calculated improved estimates for the correlation length exponent of the second length scale and show that it is very close to the order parameter correlation length exponent. We therefore expect that it will be very challenging to observe this behavior in numerical simulations.

In summary, we provided a unified picture of the system close to the fermion-induced QCP in the symmetric as well as in the symmetry-broken phases.

Chapter 4

Order-to-order transitions of Dirac fermions with compatible orders

As mentioned briefly in the introduction 1, a prominent example of a transition that cannot be described within Landau-Ginzburg theory, is a Deconfined Quantum Critical Point (DQCP) in spin-$\frac{1}{2}$ antiferromagnets on a square lattice. This is a critical point describing a continuous transition between a Néel ordered phase (which breaks $O(3)$ symmetry) and a valence bond solid (VBS) phase (which breaks $O(2)$ symmetry), where an emergent gauge field couples to spinons which are confined in both of the ordered phases [20–22]. Numerical analysis of several models expected to exhibit such a transition [23–25], moreover reveal that there is an enlarged $O(N)$ symmetry at the critical point.

Quantum critical points with emergent $O(N)$ symmetry are not entirely new, and indeed have been argued to exist in different unrelated contexts, e.g. [93, 94]; nevertheless, the emergent symmetry has been mostly seen as a secondary feature and considered independently from the nature of the transition. There is, however, at least one case where the non-Landau nature of the transition and the emergent symmetry coexist: the Landau-forbidden phase transition describing a semimetallic to Kekulé VBS phase of graphene studied in the previous chapter shows an enlarged $O(2)$ symmetry at the critical point [14, 16, 17, 55]. Because in that case the continuity of the transition can be seen as a consequence of fluctuations of the massless fermions, it is natural to ask if the two phenomena are related, namely, what is the relation - if any - between fermionic-induced criticality and Landau-forbidden transitions (like the one found at a DQCP).

An interesting development from recent QMC simulations[19] suggests that the connection could be more than circumstantial and might indeed play a role for the kind of non-Landau transition expected in DQCPs, namely the existence of a direct order-to-order transition which is possible not only at a multicritical point where the phases meet, but also away from it. Moreover, the findings in [19] seem to indicate that there is a line separating the two phases (with broken $O(3)$ and $\mathbb{Z}_2$ symmetry, respectively) with an emergent $O(4)$ symmetry (see Fig. 4.1).

It is worth to emphasize that evidence for some of the features expected to be present in non-Landau transitions comes mostly from numerical simulations of various models, and it is desirable to have complementary analytical methods to better understand this phenomena. Progress in this direction has been achieved already and indeed, the emergent $O(5)$ symmetry observed in Quantum Monte Carlo simulations [23] can be argued for within the

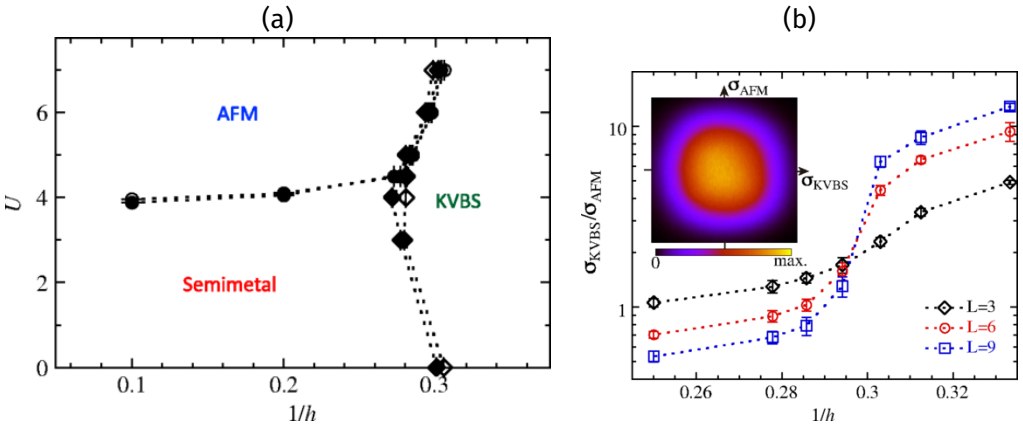

FIGURE 4.1: (a) **Expected phase diagram from Quantum Monte Carlo simulations** of a system of hopping electrons on the Honeycomb lattice with on site Hubbard repulsion U and Ising-like bond interactions h. The Antiferromagnetic phase is characterised by broken $O(3)$ symmetry and the KVBS ohase breaks $\mathbb{Z}_2$ symmetry by allowing only one of the possible patterns described in Chapter 3. (b) **Emergent $O(4)$ symmetry** across the putative line of continuous transitions. Pictures taken from [19].

recently proposed web of dualities of $D = 2 + 1$ field theories [34, 95], while the expected existence of a second length scale at the continuous transition proposed in [96] and supported by QMC simulations therein can, for example, be understood to be a general feature of a continuum field theory with a dangerously irrelevant parameter in the flow of the theory [87]. In the case of itinerant quasirelativistic massless fermions interacting with two families of order parameters, the first efforts to understand analytically the emergent symmetry at the critical point were made by means of a first-order ϵ-expansion [26, 27].

For this reason, in this chapter we concern ourselves with the investigation of the quantum phase and the multicritical behavior of Dirac fermions with two compatible orders in the vicinity of a multicritical point where the two ordered phases meet with the semimetallic phase. Our goal is a better understanding of the recent numerical studies that found evidence for non-Landau transitions and emergent symmetry between the two ordered states arguing in favor for deconfined quantum criticality in 2+1d Dirac materials. Here, we provide a field-theoretical analysis of this transition in a generalized model based on nonperturbative functional renormalization group equations. Our findings support the emergence of enhanced symmetry at the multicritical point and further suggest that the transition between the two ordered phases away from the multicritical point takes place as a sequence of two continuous transitions with an intermediate region of coexistence with approximate $O(N)$ symmetry. We compare to the numerical Quantum Monte Carlo simulations for the case in which the order parameters correspond to phases with broken $O(3)$ and $\mathbb{Z}_2$ symmetry.

The main result of this chapter is the phase diagram presented in FIG. 4.11. Our main result thus consists of different key results, the first being the confirmation of the existence and stability of an Isotropic Fixed Point (IFP) for all consistent values of N_{f} and N (see the definition of 'consistent' below). We show that some of the features observed in simulations (emergent symmetry away from the IFP and increase of the one particle gap across the transition and phase boundaries composed of continuous transitions) are consistent with the scenario described above.

This chapter is organized as follows: in section 4.1 we describe the general features of the model we consider, set up some of the notation to be used, and make a short recap of the results obtained in [26, 27] by ϵ-expansion methods. Section 4.2 presents our main results including a detailed description of the properties of each of the phases. Finally we discuss our results and their relevance to QMC simulations in section 4.3. The contents of this chapter are currently being prepared for submission [97].

4.1 Compatible orders in Dirac systems

In a system of gapless Dirac fermions, several ordered states can take place. If one characterizes the ordering tendencies by the symmetry they break, one can moreover study the interplay of different interactions in terms of the relations between the operators that generate said symmetries. If the generators anticommute with each other we say that they are *compatible*. If they, moreover, anticommute with the kinetic terms of the free Hamiltonian in d spatial dimensions, they are said to be compatible *masses*. This is because if $\mathcal{H}_0$ is the free Dirac hamiltonian, built out of gamma matrices γ_j ($j = 1, \cdots, d$) and the two generators of the compatible symmetries are members of the Clifford algebra $\beta_\alpha \in Cl(d)$ for $\alpha = 1, 2$ satisfying

$$\{\beta\alpha, \gamma_j\} = \{\beta_1, \beta_2\} = 0 \,, \tag{4.1}$$

then adding terms of the form $\Delta\mathcal{H} = m_1\beta_1 + m_2\beta_2$ to $\mathcal{H}_0$ opens a gap in the spectrum as

$$E(\vec{p}) = |\vec{p}| \longrightarrow \sqrt{\vec{p}^2 + m_1^2 + m_2^2} \,. \tag{4.2}$$

The generalization to two families of compatible masses, with N_1 and N_2 generators respectively thus generate a $O(N_1) \oplus O(N_2)$ symmetry under which the mass operators $\beta_i m_i$ transform as vectors. Depending on the kind of interactions, the order parameters involved can take several forms.

For example, and as discussed at length in the previous chapter, a 2 component OP with a global $\mathbb{Z}_3$ symmetry - i.e. a Kekulé texture - is one candidate for such a mass. Another mass-like OP is the one induced when the lattice system possesses some on-site spin dependent repulsive interactions. In that case an antiferromagnetic order can take place. If this interaction acts identically on both chiral sectors, the orders are compatible. For spinless fermions on the honeycomb lattice one can moreover define another mass compatible with the Kekulé texture that takes the form of a staggered chemical potential [66].

To construct an effective theory of the onset of any of these kind of orders, one needs to take into account the gaplessness of the fermions, since they cannot be described by mere LG theory alone and, instead, the effective low energy theory takes the form of a Gross Neveu Yukawa (GNY) model [59, 62]. Concretely, this means the critical properties of the system are described by the microscopic euclidean lagrangean [1]

$$\mathscr{L} = \sum_{\alpha=1}^{N_\mathrm{f}} \overline{\psi}_\alpha \left(-i\partial\!\!\!/ + g_1 \sum_{a=1}^{N_1} \gamma_\phi^a \phi_a + g_2 \sum_{b=1}^{N_2} \gamma_\chi^b \chi_b \right) \psi_\alpha$$

[1] Note that, as in the previous chapter, we assume from the outset that the system has Lorentz invariance at the critical point.

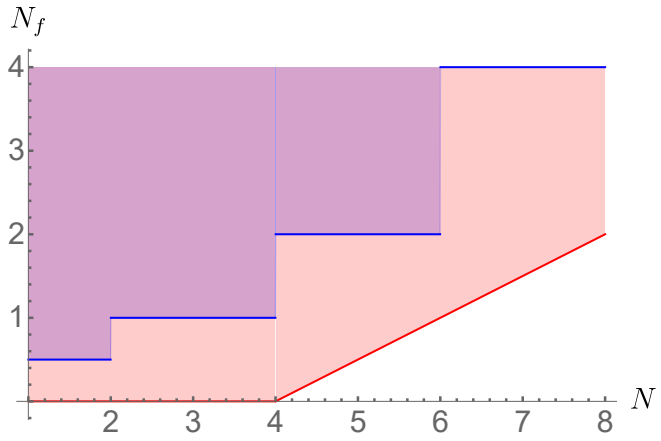

FIGURE 4.2: **Domain of consistency** of the model of Eq. 4.3 as a function of fermion flavour number N_f and OP components $N := N_1 + N_2$ is depicted as the blue shaded region and the region of stability of the IFP (according to the ϵ-expansion) as the red shaded region.

$$+\frac{1}{2}\sum_{a=1}^{N_1}\phi_a\left(-\partial^2+m_1^2\right)\phi_a+\frac{1}{2}\sum_{b=1}^{N_2}\chi_b\left(-\partial^2+m_2^2\right)\chi_b$$
$$+\frac{u_1}{8}\left(\sum_{a=1}^{N_1}\phi_a^2\right)^2+\frac{u_2}{8}\left(\sum_{b=1}^{N_2}\chi_b^2\right)^2+\frac{u_3}{4}\sum_{a,b}\phi_a^2\chi_b^2\,, \tag{4.3}$$

where the *real* order parameters (OPs) $\phi = (\phi_1, ..., \phi_{N_1})$ and $\chi = (\chi_1, ..., \chi_{N_2})$ couple to the N_f flavours of fermions via the Yukawa couplings $g_{1/2}$ and the $N_1 + N_2$ matrices $\gamma_\phi^a, \gamma_\chi^b$ anticommute with each other as well as with the ones coming from the kinetic terms of the fermions.

Letting $N := N_1 + N_2$ it becomes clear that the model of Eq. (4.3) requires $d + N$ anticommuting matrices, where d is the spatial dimension. Since the dimension d_γ of the irreducible representations of $Cl(m)$ - the Clifford algebra generated by m elements [98] - is

$$d_\gamma = 2^{\lfloor \frac{m}{2} \rfloor}\,, \tag{4.4}$$

a minimal requirement for the model to be consistent is thus that the number of flavours of 4-component fermions satisfies $4N_\mathrm{f} \geq d_\gamma$ (see FIG. 4.2). For graphene ($N_\mathrm{f} = 2$ and $d = 2$), for example, this implies $N \leq 5$.

The first-order ϵ-expansion analysis is sufficient to confirm the existence of an RG fixed point with an enlarged $O(N)$ symmetry, from now on to be referred to as the isotropic fixed point (IFP), which is stable for all consistent combinations of N_f and N. However, it is known from studies of purely bosonic $O(N_1) \oplus O(N_2)$ theories [99, 100] that the perturbative analysis not only grossly overestimates the stability of fixed points, but can "find" features of the system which do not exist beyond the first order expansion. Additionally, in the bosonic $O(N_1)\oplus O(N_2)$ theory it is known that the stability of all fixed points depends heavily on the particular value of N and, for example, in $d = 2+1$ the IFP is unstable for $N \geq 3$. Moreover, because the nature of a multicritical point (e.g. bicritical vs tetracritical) is usually described in terms of the sign of

$$\widetilde{\delta} := u_1 u_2 - u_3^2 \tag{4.5}$$

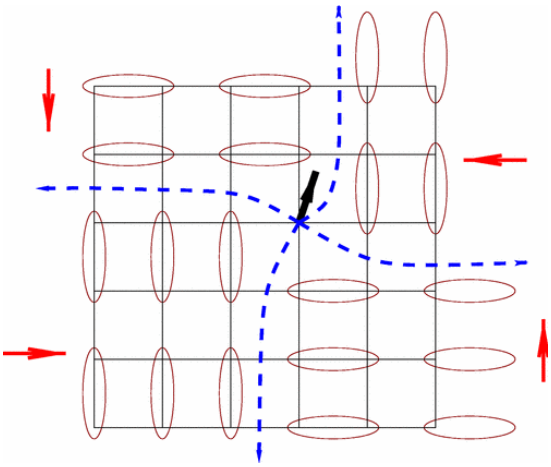

FIGURE 4.3: **Topological defect** in a system of spin-$\frac{1}{2}$ particles on a square lattice. At a point where 4 domain walls corresponding to the different ground states meet, there is an unpaired spin $\frac{1}{2}$. The defect thus carries a spin quantum number. Figure taken from [101].

at the fixed RG point, there are no general statements that can be said about the transition between the ordered phases when, like in our case, the fixed point has $\widetilde{\delta} = 0$.

What could be missing in this picture?

For order parameters transforming as vectors under $O(N)$, one can in principle associate certain "topological defects". These can be thought of as singular configurations of the OP fields that carry some nontrivial quantum numbers, and whose conserved current can be encoded as the flux of a gauge field. The most physically transparent example of this is that of the Valence Bond State (VBS) of a system of spin-$\frac{1}{2}$ particles on a square lattice [101]. In that case there are four degenerate ground states that correspond to the four different dimerization patterns and the system is said to be in a VBS if it is in any of these ground states. A topological defect of the VBS is just a domain wall between two different dimer patterns as seen in FIG 4.3.

The effect of the vortices in the system can be understood easily: when they proliferate, the VBS order is destroyed. An effective description of the transition between a VBS-ordered and a vortex-condensed phase takes the form of a field theory of a 2-component spinon z with a $\mathbb{Z}_4$ anisotropy and minimally coupled to a $U(1)$ gauge field, i.e. a theory whose low energy description is given by the lagrangean

$$\mathscr{L} = \frac{1}{2}\sum_{a=1}^{2} |\left(\partial_\mu - iea_\mu\right) z_a|^2 + \frac{r}{2}\left(\sum_{a=1}^{2} z_a^2\right) + \frac{u_1}{8}\left(\sum_{a=1}^{2} z_a^2\right)^2 + \frac{u_2}{8}\sum_{a=1}^{2} z_a^4 + \frac{1}{4} f_{\mu\nu} f^{\mu\nu} \,, \tag{4.6}$$

with $f_{\mu\nu} = \partial_\mu a_\nu - \partial_\nu a_\mu$, the field strength tensor. Because of the spinful nature of the vortices, the destruction of VBS order comes with the onset of $SU(2) = SO(3)$ spin symmetry breaking. The field theory of Eq.(4.6) should thus describe a second order phase transition (upon tuning r) between two ordered phases: one breaking $O(2)$-symmetry (the VBS state) and one breaking $O(3)$ symmetry (in this case, it can be identified with an antiferromagnetic Néel ordered state).

Such a description in terms of the topological defects becomes relevant (in the standard, non-RG sense of the word) if *both* ordered adjacent phases can be described in terms of the proliferation of their corresponding topological defects. The take-home message is that the inclusion of topological defects through a gauge field becomes pertinent, if not necessary, in this case. This in turn, provides an answer to the question raised in the title of this section. Indeed, Eq. (4.3) includes several cases where there is no description in terms of topological defects, namely, whenever $N_1 = 1$ or $N_2 = 1$. In these cases, Eq. (4.3) can still describe the vicinity of the transition between a phase with broken $O(1) = \mathbb{Z}_2$ and a phase with broken $O(N)$ symmetry, and the presence of topological defects of the $O(N)$ order parameter (if allowed) should play no significant role in the nature of the transition. We adopt this point of view also in the case where both OPs can have topological defects in the following, and discuss briefly the general case in Sec.4.3.

4.2 FRG analysis

For our renormalization group analysis we can immediately postulate the form of the LPA' ansatz for Γ_k based on the original form of the microscopic action in Eq. (4.3), namely

$$\begin{aligned}\Gamma_k = \int d^D x \Big\{ & \overline{\psi}_\nu \left(-i Z_{\psi,k} \not{\partial} + \bar{g}_{1,k} M_\phi + \bar{g}_{2,k} M_\chi \right) \psi_\nu \\ & - \frac{1}{2} Z_{\phi,k} \phi_a \partial^2 \phi_a - \frac{1}{2} Z_{\chi,k} \chi_b \partial^2 \chi_b + V_k(\phi_a, \chi_b) \Big\} \, . \end{aligned} \tag{4.7}$$

where we use the summation convention on repeated indices. In the following we denote with a bar dimensionful quantities. The scale dependence of the Yukawa couplings $\bar{g}_{1,k}$ and $\bar{g}_{2,k}$ as well as the wavefunction renormalizations $Z_{\Phi,k}$ have been made explicit and the mass terms in the previous equation M_ϕ, M_χ are given by

$$M_\phi = \gamma^a_\phi \phi_a, \qquad M_\chi = \gamma^b_\chi \chi_b \, . \tag{4.8}$$

Furthermore the bosonic potential $V_k(\phi, \chi)$ is an analytic function of the $O(N_1)$ and $O(N_2)$ invariant quantities

$$\rho_\phi := \frac{\phi_a \phi_a}{2}, \qquad \rho_\chi := \frac{\chi_b \chi_b}{2} \, , \tag{4.9}$$

and it can be expanded around a (running) minimum, denoted by $\kappa_{\phi/\chi} := \rho_{\phi/\chi,\min}$. The nature of the minimum corresponds to three different scenarios:

(i) Both OPs remain in their symmetric phases - $\kappa_{\phi/\chi} = 0$.

(ii) One of the OPs acquires an expectation value, while the other one remains in its symmetric phase.

(iii) Both OPs acquire an expectation value - $\kappa_{\phi/\chi} \neq 0$.

The beta functions for the dimensionless Yukawa couplings $g_{i,k}$, defined as

$$g_1^2 = \frac{\bar{g}_i^2}{Z_\phi Z_\psi^2 k^{4-D}} \, , \qquad g_2^2 = \frac{\bar{g}_2^2}{Z_\chi Z_\psi^2 k^{4-D}} \, , \tag{4.10}$$

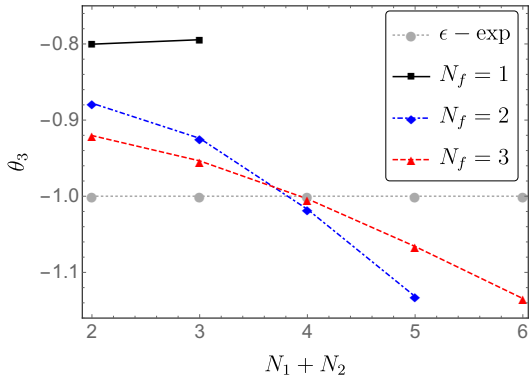

FIGURE 4.4: **Stability exponent.** The third exponent of the stability matrix at the IFP (θ_3), as a function of $N := N_1 + N_2$ for fixed N_f. determines if the MCP is stable. The lines include only consistent values of N_f and N. All values except for the gray line correspond to FRG results within LPA'12.

as well as for the anomalous dimensions $\partial_t Z_{\psi/\phi/\chi}$ are obtained by taking the corresponding derivatives of the Ansatz Eq. (4.7). The details of the regulators used as well as the choice of projections can be found in the appendix A.

4.2.1 Fixed points and criticality from FRG

Denoting the set of flowing couplings by $\mathbf{x}$ and the coordinates of the fixed point by $\mathbf{x}^*$, the fixed point will be stable if θ_3, the third largest eigenvalue of the stability matrix,

$$\mathbb{M}_{ij} := -\frac{\partial \beta_i}{\partial x_j}\Big|_{\mathbf{x}^*} , \tag{4.11}$$

is negative. We find that all values of N_f, N which are consistent are also such that the IFP is stable. Unlike in the perturbative result, where $\theta_3 = -1$ for all combinations of N_f, N, we see that for fixed N_f, the IFP becomes more stable with increasing N. This is depicted in FIG. 4.4.

4.2.2 Constructing the phase diagram

The IFP can be found from a truncation in which both OPs have vanishing expectations values, that is, when we use the expansion

$$u(\rho_\phi, \rho_\chi) = m_1^2 \rho_\phi + m_2^2 \rho_\chi + \sum_{m+n=2}^{M/2} \frac{\lambda_{mn}}{m!n!} \rho_\phi^m \rho_\chi^n \, . \tag{4.12}$$

for the dimensionless bosonic potential. Note that in this notation the quartic couplings correspond to $\lambda_{2,0}, \lambda_{0,2}$ and $\lambda_{1,1}$. A first guess about the phase structure of the system can be obtained from the RG flow diagram in the relevant sector, corresponding to the bosonic masses (m_1^2, m_2^2), by setting all other couplings to ther fixed point values. This is depicted in FIG. 4.5 for $N_\mathrm{f} = 2$ and $N = 2, 3, 4, 5$ within LPA'4, but the situation is qualitatively the same for different consistent values of N_f.

Taking into account that negative values of m_i^2 correspond to a phase where the symmetry $O(N_i)$ is broken, one can infer that at the IFP with coordinates (m_c^2, m_c^2), the phases where

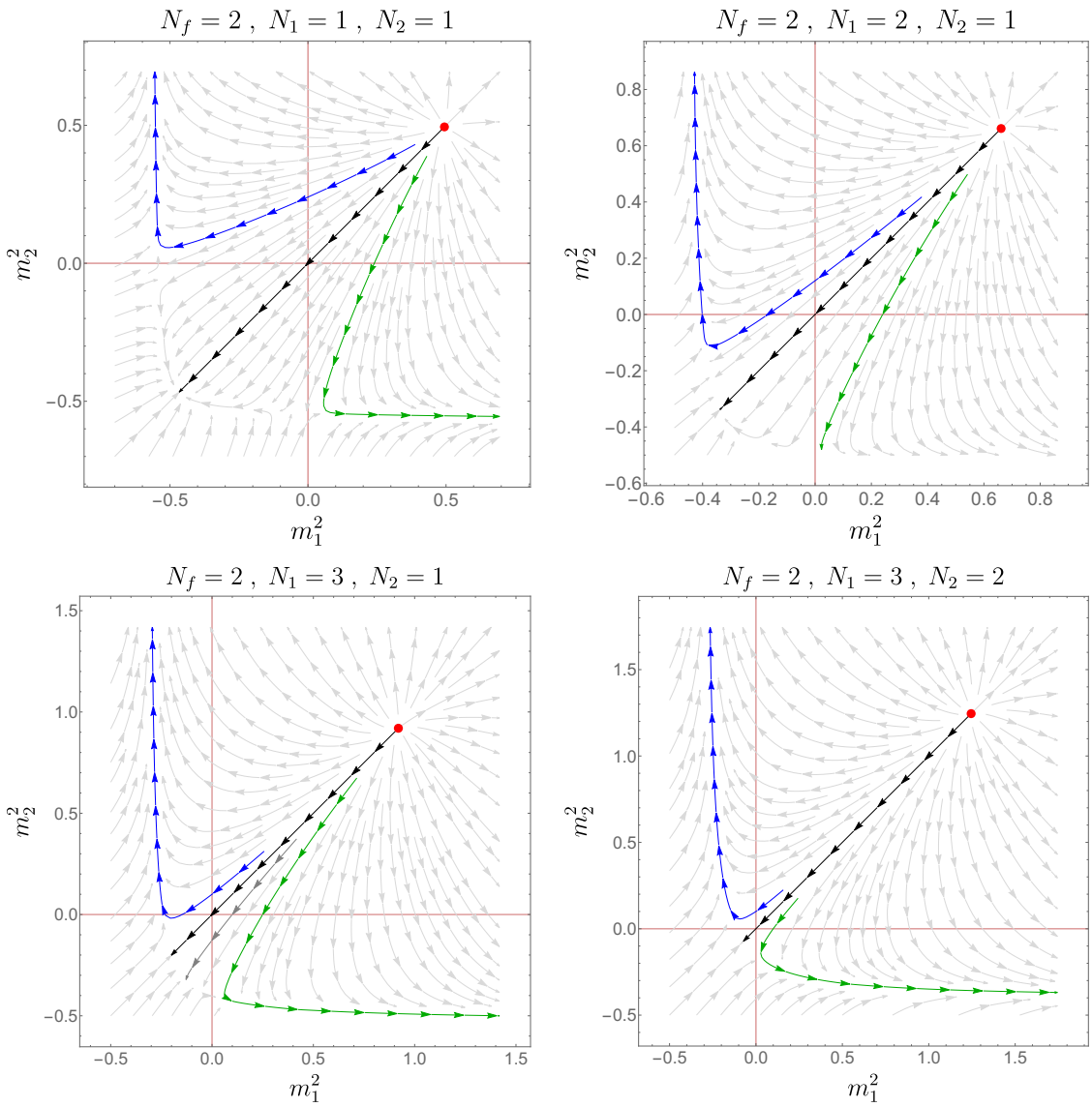

FIGURE 4.5: **Flow diagram** in the (RG-) relevant submanifold spanned by (m_1^2, m_2^2) for $N_\mathrm{f} = 2$ when all other couplings are set to their IFP values. The red dot corresponds to the IFP, and the black stream line to a flow within the enlarged-symmetry subspace. Stream lines that cross the vertical (horizontal) red line correspond to flows where the $O(N_1)$ ($O(N_2)$) symmetry breaks. Note that most flows crossing one of the red lines are ultimately directed *away* from the red line perpendicular to it.

only one of the symmetries is broken meet with the semimetallic one, and that the phases with one of the symmetries broken are generically characterised by the other symmetry being always present i.e. flows where $m_1^2 < 0$ stay in the $m_2^2 > 0$ region and viceversa. This is portrayed as the blue and green stream lines in FIG. 4.5. However the diagram seems to suggest that for all combinations of $N_{1/2}$ there are flows that remain in the region $m_1^2, m_2^2 < 0$ so that a coexistence of phases seems possible in a fan around the line where $m_1^2 = m_2^2$ - i.e. the line with exact $O(N)$ symmetry - and whose thickness depends on the particular combinations of N_i. This is displayed as the dark gray line in the bottom left panel of FIG. 4.5.

This preliminary analysis is incomplete for several reasons. First and foremost is the fact that the flows for $m_{i,k}^2 < 0$ need to take into account that the minimum of the bosonic potential

lies away from the origin in field space, a fact which is neglected in Eq. (4.12). Additionally, these streams can be misleading in the sense that there appears to be a saddle point for $m_1^2 = m_2^2 < 0$ which upon closer examination is, in fact, not a fixed point of the whole set of flow equations.

Additionally, whenever there are two relevant directions (like at the IFP), the presence of κ_i can lead, e.g. to the full $O(N_i)$ symmetry getting restored, i.e. the blue, green and gray flow lines in FIG. 4.5 can return to the $m_i^2 > 0$ region along the $k \to 0$ flow. In fact, examples of flows where a nonzero minimum of the potential develops only at intermediate scales are known from renormalization group studies of ultra cold atoms and QC$_2$D [102, 103]. Consequently, to determine what phases are allowed in the system, one needs to follow how the expectation values of the OPs flow towards the infrarred, i.e., to compute

$$\lim_{k\to 0} \overline{\kappa}_{\phi,k} \ , \text{ and } \lim_{k\to 0} \overline{\kappa}_{\chi,k} \ . \tag{4.13}$$

We do this by solving the initial value problem for the whole set of beta functions where the initial conditions are drawn from paths in the plane of (RG-) relevant couplings in the vicinity of the IFP and computing the quantities of Eq. (4.13) from the solutions obtained. The (dimensionful) expectation values of the OPs in units of the scale Λ along a curve enclosing the IFP take the form depicted in FIG. 4.6.

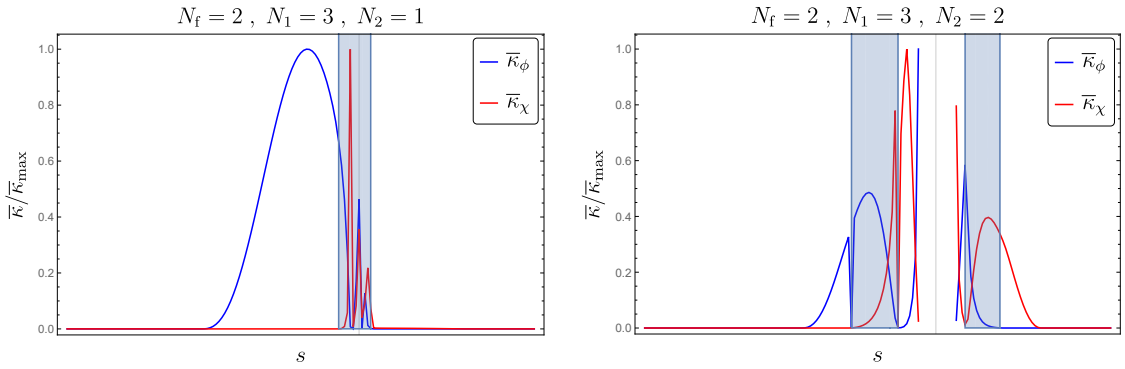

FIGURE 4.6: **Dimensionful expectation values of the order parameters** along a circular path on the relevant plane centered at the IFP and parameterised by the angle $s \in \{0, 2\pi\}$ (in units of the maximum value obtained along the trajectory). The path has a radius of $r = m_c^2/300$. the gray vertical line corresponds to the point where the trajectory crosses the direction along the line $m_1^2 = m_2^2$. For these parameters there seems to be some regions of coexistence within the blue shaded area, with widths of at least $9\pi/80$ (top) and $3\pi/20$ (bottom). The lack of points in the region closest to the line of exact $O(N)$ symmetry is caused by numerical instability of the integrated flow, which serves as an indirect evidence of the preservation of $O(N)$ symmetry in the coexistence regions - see main text for details.

From this we can already confirm our earlier suspicion and infer that a system described by the low energy effective theory of Eq. (4.7) indeed realizes all three possibilities mentioned at the beginning of Sec. 4.2, which means that there is a semimetallic phase, two ordered phases with broken $O(N_i)$ symmetry *and* at least one region of coexistence of both orders. The one different case is when both OPs are of Ising type ($N_1 = N_2 = 1$). Then, there is no coexistence region at all, and the transition between both phases appears to be of first order, we discuss this particular case in Sec. 4.2.3

From the global plots in FIG. 4.6 it is not evident that there is some extra structure within the coexistence region for $N_1 = 3, N_2 = 1$. To see exactly what happens in this region, we can zoom in on the same trajectory, and find the behaviour observed in FIG. 4.7, where it can be seen that there is a thin strip within the in which one of the symmetries gets restored, and that this symmetry gets broken again on approaching the line of $O(N)$ symmetry, which is inside the region where the integrated equations remain unstable - depicted as the white region in that figure.

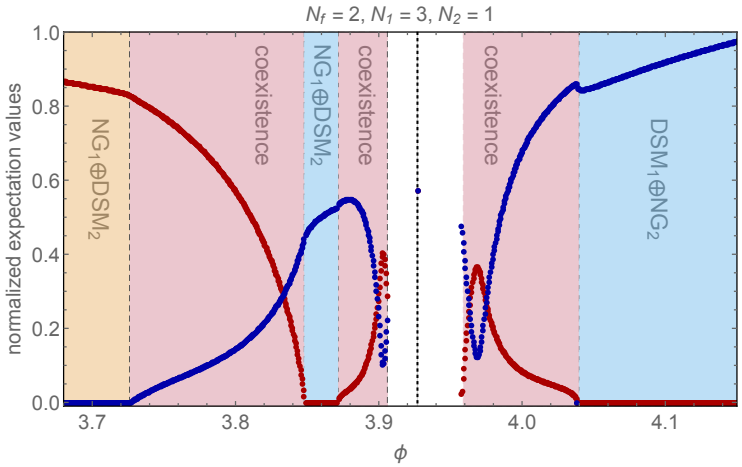

FIGURE 4.7: **Expectation values of the order parameters** in units of the UV cutoff Λ along the same circular path described in FIG.4.6. $\phi_c = 5\pi/4 \approx 3.927$ marks the line emerging from the IFP where $\tilde{m}_1^2 = \tilde{m}_2^2$. Color code is identical to FIG. 4.11.

A direct and continuous transition between the ordered phases thus seems possible, but not *generically*. By this we mean that such a transition is possible only within a finely tuned trajectory that passes *exactly* through the IFP. From FIG. 4.7, it appears that all transitions involved are continuous, so that the multicritical point in question is closer to a tetracritical point than to a bicritical one [99]. There is also a hidden hint in FIG. 4.6 about the existence of an enlarged $O(N)$ symmetry away from the IFP and in the coexistence region.

The lack of data points in this region is caused by a numerical instability of the integrated beta functions, which we interpret as a consequence of the fact that the expectation values of the OPs flow according to (see the exact expression in the Appendix A)

$$\partial_t \kappa_i \propto \frac{1}{\delta_k} , \tag{4.14}$$

where

$$\delta_k := \lambda_{2,0}\lambda_{0,2} - \lambda_{1,1}^2 \tag{4.15}$$

is the scale dependent version of the quantity defined in Eq. (4.5). In the region closest to the line of exact $O(N)$ symmetry, where all couplings are identical, we have $\lim_{k\to 0} \delta_k \approx 0$, which causes said numerical instability. We now describe in more detail each of the phases.

DSM$_{1+2}$ phase

The phase where $\lim_{k\to 0}\kappa_{\phi,k} = \lim_{k\to 0}\kappa_{\chi,k} = 0$, i.e. where both symmetries are left unbroken, is connected to the Dirac semimetallic one and, as expected [26], is trivially $O(N_1+N_2)$-symmetric. We denote it as DSM_{1+2}. Moreover, this phase is characterised in LPA'∞ by nonvanishing universal fixed point values for all running couplings [55]. This means, in particular, that the Yukawa and quartic couplings satisfy $g_1^2 = g_2^2 =: g^2/v_D$ and $\lambda_{2,0} = \lambda_{1,1} = \lambda_{0,2} =: \lambda/v_D$, and they flow to the universal values

$$g^2_{\mathrm{DSM},*} = \frac{D(4-D)(D-2)}{8(3D-4)N_\mathrm{f}}\,, \tag{4.16}$$

$$\lambda_{\mathrm{DSM},*} = \frac{2D(4-D)(D-2)^2}{(3D-4)^2 N_\mathrm{f}}\,, \tag{4.17}$$

as can be seen in FIG. 4.8.

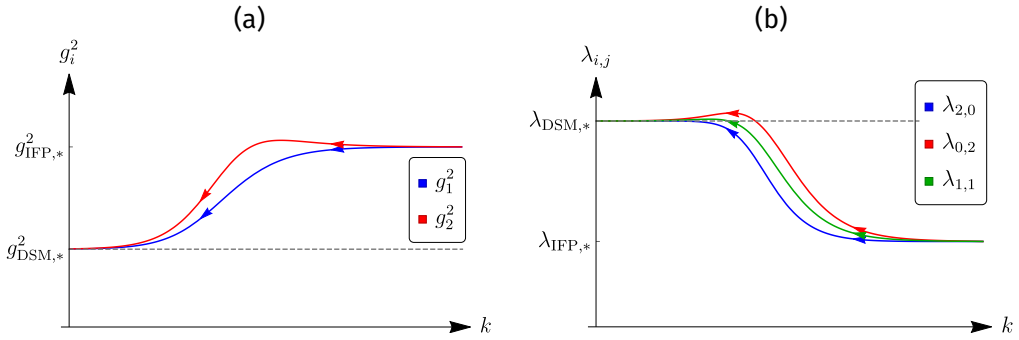

FIGURE 4.8: **Flow of dimensionless couplings** (a) Yukawa couplings and (b) quartic couplings, for initial conditions such that the system remains in the disordered phase. The initial conditions for both sets of couplings here depicted are identical and coincide with the values at the fixed point. Note that, unlike in a purely bosonic theory [99], the system leaves the higher symmetry subspace at intermediate scales $0 < k < \Lambda$ and returns to it at the end of the flow.

We note here that this just implies that the dimensionful quantities flow according to their canonical scaling, and the physically relevant quantity controlling the strength of interactions flows to zero in the infrarred [104],

$$\frac{\bar{g}_i^2}{\bar{m}_i^2} \to 0\,. \tag{4.18}$$

NG$_i\oplus$DSM$_j$ phases

For a range of initial conditions, only one of the OPs acquires a finite expectation value. In the following discussion we fix the OP with the broken symmetry to be that corresponding to N_1, i.e. ϕ, so that our statement can be rephrased as

$$\lim_{k\to 0}\bar{\kappa}_{\phi,k} \neq 0\,, \text{ and } \lim_{k\to 0}\bar{\kappa}_{\chi,k} = 0\,.$$

This OP can thus be described as flowing to a Nambu-Goldstone infrared fixed point (of that symmetry) where the dimensionless expectation value satisfies

$$\lim_{k\to 0} \kappa_{\phi,k} = \infty \ , \tag{4.19}$$

while the other OP approximately decouples and flows to a semimetallic-like fixed point (of the other symmetry), i.e, one where Eq. (4.18) holds. We denote such a phase as $\mathrm{NG}_i \oplus \mathrm{DSM}_j$.

Order-to-order transitions with $O(N)$ symmetry

The most interesting part of the phase diagram is, arguably, where the two phases meet. As mentioned in the previous section , crossing from an $O(N_1)$-broken phase into an $O(N_2)$-broken phase takes place as a continuous two-step process in which both symmetries are broken after the first step. This is clearly in FIG. 4.7 is the definition of a coexistence region. One consequence of this is that the one particle gap at the Dirac points does not close during the whole process, unless one fine tunes the system to go exactly through the IFP. Denoting the single particle gap by

$$\Delta_{\mathrm{sp}} := 2g_1^2\kappa_\phi + 2g_2^2\kappa_\chi \ , \tag{4.20}$$

the previous statement can be seen in FIG. 4.9.

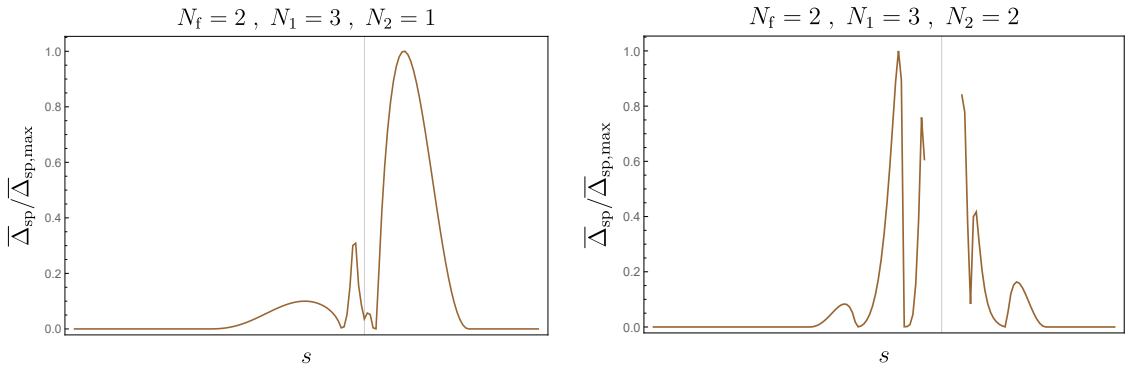

FIGURE 4.9: **Single particle gap at the Dirac point** along the same kind of circular path described in 4.6, and normalized to the maximum attained along this trajectory, $\bar{\Delta}_{\mathrm{sp,max}}$. As before, the vertical line corresponds to the direction of exact $O(N)$ symmetry.

Unsurprisingly thus, the two symmetries do not decouple inside the coexistence regions. Keeping up with the previous conventions this means that the fan is *not* a $\mathrm{NG}_1 \oplus \mathrm{NG}_2$ phase, i.e. the infrarred behaviour of the couplings differs from that of two decoupled bosonic theories in their respective symmetry-broken regimes. Instead, the phase is closer to what we could denote a NG_{1+2}-phase, i.e., to a phase where all bosonic couplings flow together to an infrarred fixed point of broken $O(N)$ symmetry. The approximate conservation of the enlarged symmetry was already adressed in the discussion of FIG. 4.6 and we now provide a more direct evidence.

To this end we consider different initial conditions corresponding to points within the coexistence regions in FIG. 4.6, and to the left and right of the line of exact $O(N)$ symmetry.

We choose initial conditions such that

$$0 \neq \lim_{k\to 0} \kappa_{\phi,k} \neq \lim_{k\to 0} \kappa_{\chi,k} \neq 0 \,. \tag{4.21}$$

Exact $O(N)$ symmetry would imply

$$f(\phi_a, \chi_b) := \lim_{k\to 0} V_k(\phi, \chi) = f(\phi_a^2 + \chi_b^2) \,, \tag{4.22}$$

$$\lim_{k\to 0} \delta_k = 0 \,, \tag{4.23}$$

where V_k is the running bosonic potential and δ_k is defined in Eq. (4.15). This, in turn, implies that lines of constant f, i.e. contour lines, are *circles* as a function of ϕ_a, χ_b. FIG. 4.10 shows the contour lines for the two points mentioned, where it is clear that to a very good approximation these contours are indeed circular close to the center ($\phi_a = \chi_b = 0$) although they are both characterised by $\lim_{k\to 0} \delta_k \neq 0$.

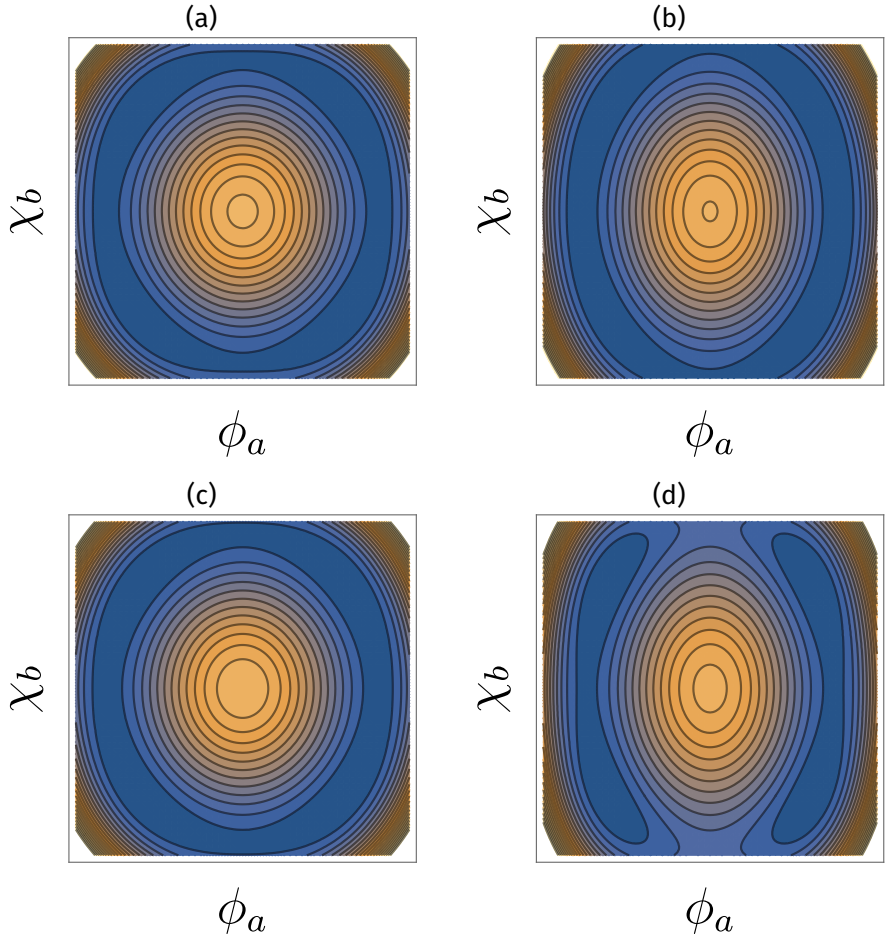

FIGURE 4.10: **Contour plots of the bosonic potential** close to the line of exact $O(N)$ for different points on the path described in 4.6 in arbitrary units. For $N_1 = 3$, $N_2 = 1$ (figures (a) and (b)), the initial conditions correspond to $|s - 5\pi/4| =$ (a) $11\pi/800$ (b) $7\pi/400$, while for $N_1 = 3$, $N_2 = 2$ (figures (c) and (d)) they correspond to $|s - 5\pi/4| =$(c) $\frac{\pi}{80}$ and (d) $\frac{\pi}{40}$.

Phase diagram

A summary of the considerations exposed in the previous sections is given by the phase diagram in FIG. 4.11. As a final remark, we note that the continuous transitions that make up the border of the coexistence region - i.e. away from the IFP - have critical behaviour in the universality class corresponding to the OP that develops a nonzero expectation value. By this we mean that for the first transition observed when crossing from a $O(N_1)-$ to a $O(N_2)-$broken phase, the critical exponents should be that of the chiral $O(N_2)$ universality class, while the second transition belongs to the chiral $O(N_1)$ universality class. This is in contrast to the expected chiral $O(N_1+N_2)$ criticality that would be observed crossing exactly through the IFP.

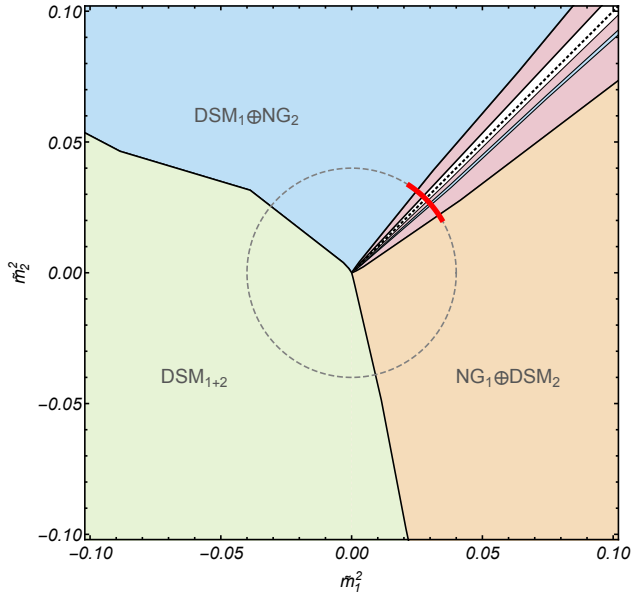

FIGURE 4.11: **Phase diagram close to the IFP** for $N_1 = 3, N_2 = 1, N_\mathrm{f} = 2$. The tuning parameters required to reach the IFP are $\tilde{m}_i^2$ and the phases with broken $O(N_i)$ and unbroken $O(N_j)$ symmetry are denoted NG$_i$⊕DSM$_j$. The evolution of the expectation values is along the red path marked in the figure and described in FIG. 4.6. For the case with $N_1 = 3, N_2 = 2, N_\mathrm{f} = 2$, the phase diagram looks very similar, but the very narrow region of DSM$_1$⊕NG$_2$ within the coexistence region is missing.

4.2.3 The case $N_1 = N_2 = 1$

The case where both OPs are of Ising type is different from the ones discussed thus far. As can be seen in FIG. 4.12, there are no regions where both OPs have nonzero expectation value, which means there is no coexistence of phases in this case. This is further confirmation that, unlike what the top left panel in FIG. 4.5 suggests, the flow of the couplings in the symmetry-broken regime can differ dramatically from the phase diagram expected from an analysis based solely on the symmetric expansion.

From FIG. 4.12 it moreover appears that the transition is of first order, since the values of the expectations values of both OPs seem to jump abruptly to zero along the line of $O(2)$ symmetry. The phase diagram for this case thus looks like that of a bicritical MCP, i.e. the

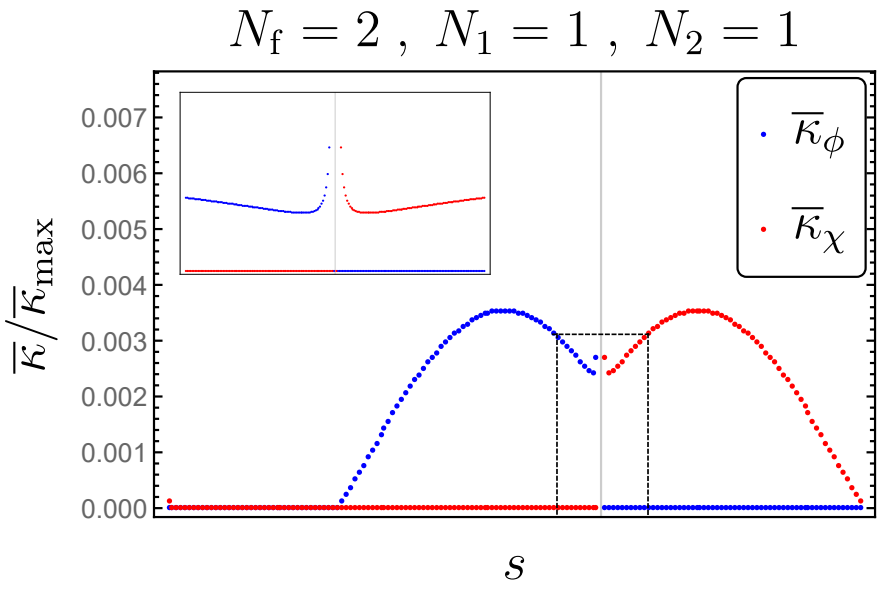

FIGURE 4.12: **Dimensionful expectation values of the order parameters** along the whole path described in FIG. 4.6 for $N_1 = N_2 = 1$. The closeup (inset) suggests no evidence of a coexistence region or numerical instability of the integrated flow.

left panel of FIG. 1.2. The one particle gap also remains open in this case, as can be seen in FIG. 4.13.

4.3 Conclusion

We investigated a system of massless $D = 2 + 1$ dimensional Dirac fermions interacting with two families of compatible order parameters with $O(N_1)$ and $O(N_2)$ symmetry and found that, contrary to earlier field theoretical [27] and numerical expectations [19], this system does not seem exhibit a line of direct continuous order-to-order transitions. For the particular case $N_1 = N_2 = 1$, it does seem to support a line of *discontinuous* transitions.

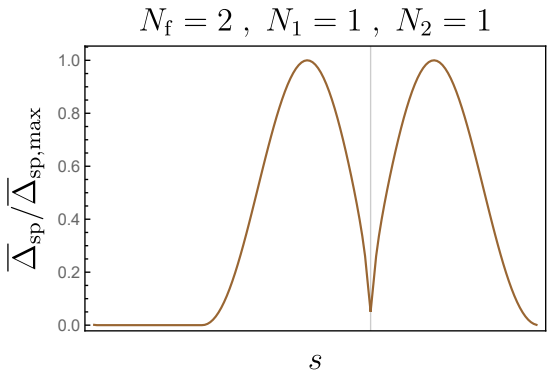

FIGURE 4.13: **Single particle gap at the Dirac point** along the same kind of circular path described in 4.6, and normalized to the maximum attained along this trajectory, $\bar{\Delta}_{\mathrm{sp,max}}$. The gap diminishes at the line of exact $O(2)$ symmetry but remains nonzero across the (discontinuous) transition.

The previously established emergent $O(N_1 + N_2)$ symmetry [26] is exact only at the multicritical point, but the enlarged symmetry survives to a good approximation within a finite portion of the phase diagram of the system as long as both OPs are not of Ising type. These results, in particular the phase diagram, depend solely on the properties of the effective action when $k \to 0$, and are thus robust to all orders of the local potential approximation [55]. Our results explain the two seemingly incompatible findings of recent Quantum Monte Carlo simulations [19], namely the continuity of the transition and the nonvanishing of the single particle gap at the Dirac points *away* from the multicritical point. Indeed, note that a direct order-to-order transition in a system where the order parameters are masses and no other mechanism is at play, can only be made continuous by closing the gap. Conversely, a direct transition where the gap does not close cannot be continuous. We observed this latter scenario for the case where both of the involved symmetries are $\mathbb{Z}_2$. Then, the transition is discontinuous while the gap remains open, and the fact that no topological defects can be defined in this case suggests that there is no other mechanism that can change the nature of the transition.

As we found, the key ingredient to bridge these two situations is the fact that the transition is not *direct* but takes place as a sequence of two transitions. The width of the coexistence region could, in principle, be made to vanish by the inclusion of topological defects of the involved order parameters [101], as long as they are irrelevant at the fixed point. Note, however, that our findings are qualitatively the same for all values of consistent N_f and N and in particular for all systems where one of the order parameters does not support such a topological defect, e.g., where $N_1 \neq 1 = N_2$. It would be an interesting problem to see, for example with the help of dualities [95], what happens to the topological defects of the $O(N_1)$ order parameter in this case.

Chapter 5

Conformal symmetry of QED$_3$ at $N_{\rm F} = 1$ and its dual description

The previous two chapters dealt with quantum phase transitions described by massless Dirac fermions that can acquire a mass by the fluctuations induced from interactions. In contrast, this chapter deals with Dirac fermions that do not get gapped by interactions. Our system of interest is QED$_3$, i.e. Dirac fermions interacting with a $U(1)$ gauge field. Different incarnations of this quantum field theory have been proposed as an effective description of several physical situations of relevance in condensed matter systems. These include algebraic spin liquids [31], high temperature superconductors [32] and, more recently, as a theory for the surface states of interacting topological insulators [29, 30] and of the half-filled Landau level [33]. The latter two proposals are peculiar in that they involve a single two-component Dirac fermion ($N_{\rm F} = 1$) coupled to an emergent $U(1)$ gauge field, and it is this particular version of the theory that has been proposed to be a fermionic analogue of particle-vortex duality in two spatial dimensions [34, 35].

Because the physics of the problems dealt with in the previous chapters led naturally to this choice, we kept the convention of high-energy physics, where Dirac fermions are collected in a 4D-representation of the fermion spinor algebra. We will keep the notation used so far (namely, $N_{\rm f}$) to refer to the 4D representation, and use in this chapter $N_{\rm F}$ to refer to the 2D representation. The case of interest in this chapter can therefore be referred to as "$N_{\rm f} = 1/2$". It has only recently received attention due to its association to topological condensed matter systems.

QED$_3$ at $N_{\rm F} = 1$ poses two interesting questions. The first is related to the fact that according to many studies (e.g. [28, 105]), chiral symmetry is expected to be spontaneously broken below a certain fermion number. That is, for $N_{\rm f} < N_{\rm f,cr}^{\chi} \sim 4$, the fermions are expected to acquire a mass dynamically in the $\bar{\psi}\psi$ channel (cf. FIG. 1.3). Since the $N_{\rm f} = 1/2$ case does not have the full chiral symmetry to begin with, as it may be viewed to operate within one chiral sector, this expectation may not hold. One can thus ask, what symmetries can be broken in this case? The second is related to the aforementioned proposals, where the strongly interacting field theory at hand appears to be dual to a free Dirac fermion. The question that can naturally arise is: assuming such a duality, what can we learn about QED$_3$? That is, can we obtain nontrivial results for observables of a strongly interacting theory (QED$_3$) based on exact knowledge of the properties of a noninteracting one?

Using the functional renormalization group, we explore the first of these two questions. We find that the interplay of gauge fluctuations with generated interactions in the four-fermi sector stabilizes an interacting conformal field theory (CFT) with finite four-fermi coupling in the infrared. The number of symmetries that can be broken is now reduced and there remains essentially only one independent four-fermi coupling (λ) of the associated Fierz algebra, as explained in detail in Sec. 5.2). With this, we find that gauge fluctuations never destabilize the four-fermi sector toward symmetry-breaking sufficiently strongly; instead, the flow is *always* attracted toward an infrared stable fixed-point for the four-fermi coupling, which preserves the scaling/conformal symmetry of the gauge sector. Surprisingly, this is due to the absence of a λ^2 term in the β-function for the four-fermi coupling: the flavor trace carries a $\sim (N_\mathrm{F}-1)\lambda^2$. This is what stabilizes the CFT at $N_\mathrm{F} = 1$. Related cancellations of β-functions in the single-flavor case also appear in the Gross-Neveu model; in particular these also hold at higher loop orders [106–108]. To answer the second question we explore some of the consequences of the proposed particle-vortex duality between a free Dirac cone and QED$_3$. We do this by studying the constraints imposed by the duality on the strongly interacting theory and compute the universal constants of the topological current correlator of the latter.

This chapter is organized as follows: in Sec. 5.1, we recapitulate how related runaway flows of different physical origin have been detected in Ref. [28]. Then, the Fierz-complete action of N_f 4-component Dirac fermions from which we project out the β-functions for a single two-component fermion, $N_\mathrm{F} = 1$ is presented in Sec. 5.2. Details of a direct derivation of the β-function for the four-fermi coupling λ are relegated to appendix B. In Sec. 5.3, we explore consequences of a fermionic particle-vortex duality. We determine *exactly* the universal constant of the topological current correlator of QED$_3$, an interacting theory, by relating it to the electromagnetic response of a free Dirac cone. Finally, in Subsec. 5.3.2 we point out the need to include the generated four-fermi coupling (and possibly other ingredients) in order to establish exponent identities for operator dimensions in compliance with the duality.

Disclaimer The contents of this chapter have been published in [109]. All figures coincide with the published manuscript, and several parts of the texts are reproduced almost identically and with only minor changes. Several portions of the text have been rewritten for clarity and a recap subsection 5.3.1 has been included to provide context. Some references have been updated to include recent results.

5.1 Conformal scaling and its breakdown for QED$_3$ at low N_f

In Ref. [28], β-functions for QED$_3$ with four-fermion couplings were calculated using a 4D-reducible representation of the fermionic spinor fields. The main scope of that work was an investigation of the symmetry breaking patterns of QED$_3$, including chiral channels, by detection of runaway flows for fermionic couplings caused by fixed point annihilation. To set the stage for QED$_3$ with a 2D-irreducible representation of the fermionic spinor fields, we now recapitulate the key elements of this analysis.

5.1.1 Fierz-complete action

Based on the bare action of a Maxwell term for the photons coupled to a set of N_f flavors of 4-component Dirac fermions (flavor index implicit)

$$S = \int \mathrm{d}^3x \left\{ \bar{\psi} \left(i\partial\!\!\!/ + \bar{e}A\!\!\!/ \right) \psi + \frac{1}{4} F_{\mu\nu} F^{\mu\nu} \right\}, \tag{5.1}$$

the following Fierz-complete LPA ansatz for the euclidean, scale (k-) dependent effective action is sufficient to study symmetry-breaking into the complete set of all possible fermionic channels

$$\begin{aligned} \Gamma_k[\bar{\psi}, \psi, a] = \int \mathrm{d}^3x \Big\{ & \bar{\psi} \left(i Z_\psi \partial\!\!\!/ + \bar{e}A\!\!\!/ \right) \psi + \frac{Z_a}{4} F_{\mu\nu} F_{\mu\nu} + \frac{Z_a}{2\xi} (\partial_\mu a_\mu)^2 \\ & + \frac{\tilde{\bar{g}}}{2N_\mathrm{f}} (\bar{\psi}\gamma_{45}\psi)^2 + \frac{\bar{g}}{2N_\mathrm{f}} (\bar{\psi}\gamma_\mu\psi)^2 \Big\} \ . \end{aligned} \tag{5.2}$$

Here we used the Feynman "slash-convention", where $\gamma^\mu x_\mu = x\!\!\!/$. For later convenience, we introduce an explicit representation of the gamma matrices, namely, for $\mu = 1, 2, 3$,

$$\gamma_\mu = \sigma_2 \otimes \sigma_\mu \ , \tag{5.3a}$$

$$\gamma_4 = \sigma_1 \otimes \mathbb{1} \ , \tag{5.3b}$$

$$\gamma_5 = \gamma_1\gamma_2\gamma_3\gamma_4 = \sigma_3 \otimes \mathbb{1} \ , \tag{5.3c}$$

$$\gamma_{45} = i\gamma_4\gamma_5 = \sigma_2 \otimes \mathbb{1} \ . \tag{5.3d}$$

In the ansatz Eq. (5.2), the last two terms $\tilde{\bar{g}}$, $\bar{g}$ are two four-fermi couplings from which all possible interaction channels, which can lead to condensation of fermion bilinears, can be constructed. ξ is a gauge fixing parameter which will be set to $\xi = 0$ in the following (Landau gauge). In total, Eq. (5.2) has 5 running couplings (Z_ψ, Z_a, $\bar{e}$, $\tilde{\bar{g}}$ and $\bar{g}$), which depend on the cutoff scale k. We will be interested in their flow as $k \to 0$.

5.1.2 β-functions

The quantities discussed so far are dimensionful quantities (denoted with a bar). Since we are not only interested in their evolution in the infrared, but also in the fixed point properties, we define the associated dimensionless quantities (without the bar) as

$$e^2 = \frac{\bar{e}^2}{Z_a Z_\psi^2 k} \ , \tag{5.4a}$$

$$g = \frac{k\bar{g}}{Z_\psi^2} \ , \tag{5.4b}$$

$$\tilde{g} = \frac{k\tilde{\bar{g}}}{Z_\psi^2} \ . \tag{5.4c}$$

In the simplest, point-like truncation for the couplings, projected onto the most singular point in frequency- and momentum space (the origin at $q = 0$), the leading order β-functions

for the gauge coupling e^2 and the two four-fermi couplings $\tilde{g}$, g of Eq. (5.2) are:

$$\partial_t e^2 = (\eta_a - 1)e^2 \,, \tag{5.5a}$$

$$\partial_t g = g(1 + 2\eta_\psi) + l^1_\psi \left(\frac{1}{N_{\mathrm{f}}} \tilde{g} g + \frac{2N_{\mathrm{f}} + 1}{3N_{\mathrm{f}}} g^2 \right) - \frac{l^{1,1}_{a,\psi}}{3} \left(4\tilde{g}e^2 - 2ge^2 \right) \,, \tag{5.5b}$$

$$\begin{aligned} \partial_t \tilde{g} =& \tilde{g}(1 + 2\eta_\psi) - l^1_\psi \left(\frac{2N_{\mathrm{f}} - 1}{N_{\mathrm{f}}} \tilde{g}^2 - \frac{3}{N_{\mathrm{f}}} \tilde{g} g - \frac{2}{N_{\mathrm{f}}} g^2 \right) \\ & - l^{1,1}_{a,\psi} \left(2\tilde{g}e^2 + 4ge^2 \right) + l^{2,1}_{a,\psi} 2N_{\mathrm{f}} e^4 \,. \end{aligned} \tag{5.5c}$$

Here, as per our convention, we have abbreviated the scale-derivative $\partial_t = k\,\partial_k$. The set of β-functions Eq. (5.5) is closed by two anomalous dimensions making it 5 equations and 5 couplings to solve. The anomalous dimension of fermions η_ψ is given by

$$\eta_\psi = \frac{2e^2}{3} \left[m^{2,1}_{a,\psi} - \tilde{m}^{1,1}_{a,\psi} \right] \,, \tag{5.6}$$

where the threshold functions take the form

$$\begin{aligned} \tilde{m}^{1,1}_{a,\psi} &= \frac{3}{2} - \frac{1}{6}\eta_\psi - \frac{1}{4}\eta_a \\ m^{2,1}_{a,\psi} &= 1 - \frac{1}{4}\eta_a \,. \end{aligned} \tag{5.7a}$$

The photon anomalous dimension η_a is physically caused by decay and recombination into fermion-antifermion pairs. In general, the gauge sector of QED$_3$ requires a delicate treatment due to its complicated momentum structure in the infrared regime, as detailed in [28]. For our purposes, it will be enough to make use of the analysis developed there, that delivers the following form for η_a:

$$\eta_a = N_{\mathrm{f}} e^2 \mathcal{L}^{(F)}_1(\eta_\psi) \,. \tag{5.8}$$

The threshold function appearing in Eq. (5.8) is listed in the appendix A.3 and those in Eq. (5.5) are (for the linear Litim regulator)

$$l^1_\psi = \frac{2}{3} - \frac{1}{6}\eta_\psi \tag{5.9}$$

$$l^{1,1}_{a,\psi} = \frac{4}{3} - \frac{1}{6}\eta_\psi - \frac{2}{15}\eta_a \tag{5.10}$$

$$l^{2,1}_{a,\psi} = 2 - \frac{1}{6}\eta_\psi - \frac{4}{15}\eta_a \tag{5.11}$$

and are positive in the regimes of interest, that is, the "RG-corrections" by the anomalous dimensions are subdominant when compared to the leading term.

The 5 β-functions Eq. (5.5) and Eqs. (5.6,5.8) have nontrivial (i.e where not all couplings are zero) scale-invariant, real-valued solutions for large enough $N_{\mathrm{f}} > N_{\mathrm{f,c}}$; these signify a conformal phase. We now first describe the nature of these conformal fixed-points and subsequently explain how the scaling breaks down at $N_{\mathrm{f}} = N_{\mathrm{f,c}}$.

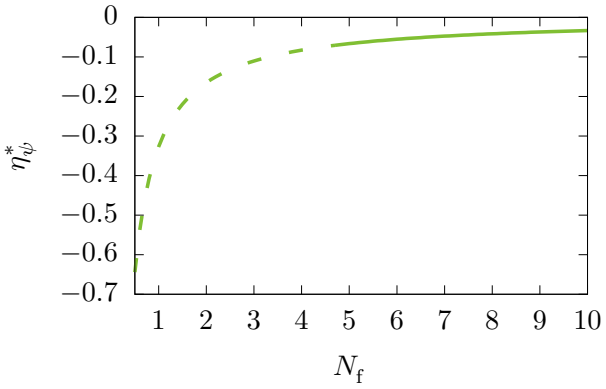

N_f	η^*_ψ	e^2_*
5	-0.066	0.195
6	-0.055	0.163
7	-0.048	0.140
8	-0.042	0.123
9	-0.037	0.109
10	-0.033	0.099

FIGURE 5.1: **Fermion anomalous dimension and value of the gauge coupling** in the conformal phase as a function of the flavor number N_f. The dashed line indicates the regime below $N_{\mathrm{f,c}}$, where the conformal fixed point becomes unstable and likely spontaneous symmetry breaking sets in.

5.1.3 Interacting conformal fixed point for $N_\mathrm{f} > N_{\mathrm{f,c}}$

Due to charge conservation, the photon anomalous dimension is exactly equal to one for any value of $N_\mathrm{f} > N_{\mathrm{f,c}}$:

$$\eta^*_a = 1\ , \tag{5.12}$$

that is, along the line of interacting conformal fixed points corresponding to the conformal phase. This follows from Eq. (5.5a). Since η^*_a depends on e^2_* itself, this fixes the numerical value of the gauge coupling, given in FIG. 5.1, as a function of N_f. The values of η^*_ψ depend on the number of fermion flavors. This follows from a solution of the coupled equations for the anomalous dimensions Eqs. (5.6),(5.8). Its values are given in FIG. 5.1 for the linear regulator.Alternative techniques to access the conformal phase and its exponents and operator dimensions are the $1/N_\mathrm{f}$ expansion, which offers perturbative control for sufficiently large N_f (e.g.: [31, 110–116]), and the ϵ-expansion around $d = 4$ in the limit $\epsilon \to 1$ (e.g.: [116–118]).

It is a feature of the β-functions that the flow of the gauge coupling Eq. (5.5a) and consequently the universal fixed-point values $e^2_*(N_\mathrm{f})$ shown in FIG. 5.1 do not depend on $\tilde{g}$ or g. At the level of the perturbative Ward identity, this is diagrammatically due to Furry's theorem, i.e., the vanishing of graphs with an odd number of external gauge field insertions. This decoupling of the gauge flow from the fermion sector permits a simplified analysis of symmetry breaking patterns. e^2 may be viewed as an external parameter for the fermionic flow Eqs. (5.5c) and (5.5b). Here we have taken the fermionic couplings to be not fundamental in the UV, $\tilde{g}_{k=\Lambda} = g_{k=\Lambda} = 0$. They first need to be generated by gauge field fluctuations. We now recapitulate how to detect symmetry breaking from the flows of Eqs. (5.5,5.6,5.8).

5.1.4 Breakdown criterion of conformal scaling at $N_{\mathrm{f,c}}$

For sufficiently large $N_\mathrm{f} > N_{\mathrm{f,c}}$, the initial values, $g_{k=\Lambda} = \tilde{g}_{k=\Lambda} = 0$ lie in the basin of attraction of a conformal fixed point. Note that in general there are four fixed point solutions, only one of which is infrared attractive. This is the conformal fixed-point at finite $e^2_{k\to 0} = e^2_*$. This point will be labeled as $\mathcal{O}$.

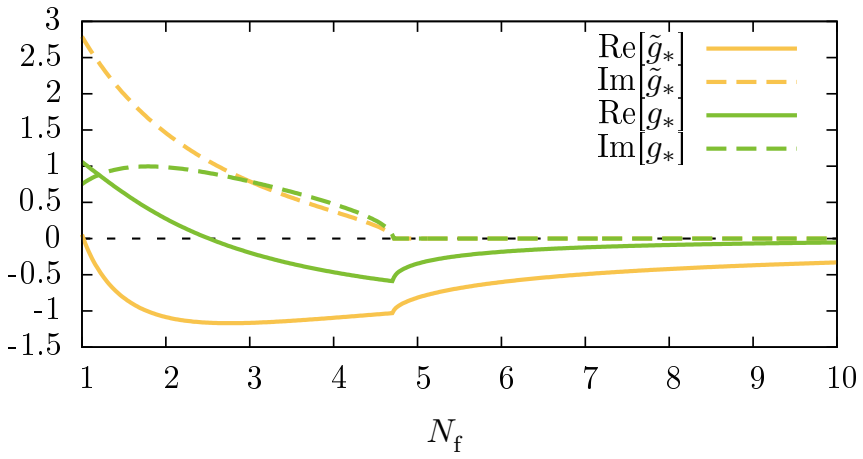

FIGURE 5.2: **Fixed point values of the fermionic couplings** $\tilde{g}$ and g at the scale-invariant/conformal fixed point $\mathcal{O}$ for a range of $N_\mathrm{f} > N_{\mathrm{f,c}}$. The gauge coupling is set to the respective fixed point value $e^2_*(N_\mathrm{f})$. Finite imaginary parts indicate spontaneous symmetry-breaking. Here this happens below $N_{\mathrm{f,c}} = 4.7$.

For $N_\mathrm{f} \leq N_{\mathrm{f,c}}$, however, the four-fermi couplings at $\mathcal{O}$ start developing imaginary parts, which is indicative of spontaneous symmetry breaking and the phase boundary between the conformal phase and a phase with spontaneously broken symmetry.

In FIG. 5.2, we plot the fixed-point values of g and $\tilde{g}$ in the complex plane for varying N_f. We observe that at $N_\mathrm{f} \leq N_{\mathrm{f,c}} \approx 4.7$ the couplings develop imaginary parts. This estimate is coincidentally close to a recent computation from the F-theorem and a resummed ϵ-expansion $N_{\mathrm{f,c}} \approx 4.4$ [117] as well as to another recent estimate from the ϵ-expansion at $N_{\mathrm{f,c}} \approx 4.5$ [118].

An explicit solution of the 5 coupled flow equations as a function of k confirms this picture: for $N_\mathrm{f} \leq 4.7$, the four-fermi couplings diverge at some finite scale k_sb. These runaway flows indicate that fluctuations in one, or several, fermion bilinear channels become so strong that one, or a combination, of bilinears are likely to condense and spontaneously break the conformal symmetry.

5.2 QED$_3$ with $N_\mathrm{F} = 1$

We now adapt the analysis of the previous section to the novel case of $N_\mathrm{F} = 1$ and delay the discussion of the physical realizations of this system to the next subsection. The 2D irreducible representation of the Clifford algebra can be obtained by a procedure described in Ref. [28] and that we now reproduce for completeness.

Defining the projectors

$$P_{\mathrm{L,R}} := \frac{1}{2}(\mathbb{1}_4 \pm \gamma_{45}) \,, \tag{5.13}$$

one can define 2D-spinors by the prescriptions (with $a = 1, ..., N_\mathrm{f}$ a flavor index),

$$P_\mathrm{L}\psi^a =: \frac{1}{\sqrt{2}}\chi^a \otimes \begin{pmatrix} 1 \\ i \end{pmatrix} \,, \quad \bar{\psi}^a P_\mathrm{L} =: \frac{1}{\sqrt{2}}\bar{\chi}^a \otimes \begin{pmatrix} 1 & -i \end{pmatrix} \,, \tag{5.14}$$

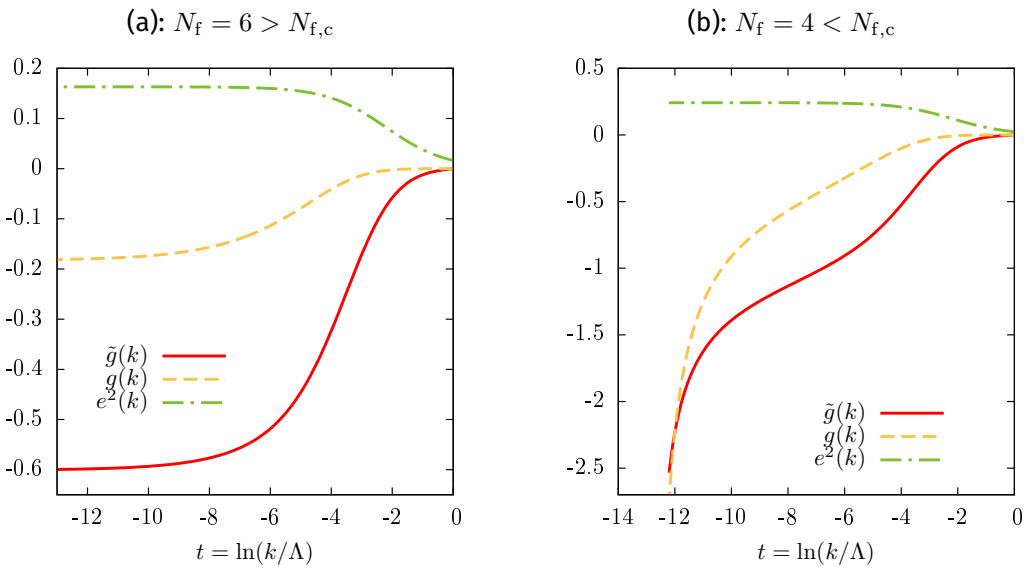

FIGURE 5.3: **Explicit solutions of the flow equations** in the conformal phase (a) and in the phase with putatively broken symmetry (b). In the second case, the fermionic flow diverges at $t_{sb} = -12.9$.

$$P_R \psi^a =: \frac{1}{\sqrt{2}} \chi^{a+N_f} \otimes \begin{pmatrix} 1 \\ -i \end{pmatrix} , \qquad \bar{\psi}^a P_R =: -\frac{1}{\sqrt{2}} \chi^{a+N_f} \otimes \begin{pmatrix} 1 & i \end{pmatrix} . \tag{5.15}$$

The four fermi interactions then become

$$\left(\bar{\psi}^a \gamma_{45} \psi^a\right)^2_{a=1\ldots N_f} \to \left(\bar{\chi}^i \chi^i\right)^2_{i=1\ldots N_F} , \tag{5.16a}$$

$$\left(\bar{\psi}^a \gamma_\mu \psi^a\right)^2_{a=1\ldots N_f} \to \left(\bar{\chi}^i \sigma_\mu \chi^i\right)^2_{i=1\ldots N_F} , \tag{5.16b}$$

which implies, for $N_F = 1$,

$$-3(\bar{\chi}\chi)^2 = (\bar{\chi}\sigma_\mu\chi)^2 , \tag{5.17}$$

which in turn means there is only one independent fermionic interaction term left. The LPA ansatz for the effective action Eq. (5.2) then reduces to

$$\Gamma_k[\bar{\psi}, \psi, a] = \int \mathrm{d}^3x \left\{ \bar{\chi} \left(i Z_\psi \partial\!\!\!/ + \bar{e} a\!\!\!/ \right) \chi + \frac{Z_a}{4} F_{\mu\nu} F_{\mu\nu} + \frac{Z_a}{2\xi} (\partial_\mu a_\mu)^2 + \bar{\lambda} (\bar{\chi}\chi)^2 \right\} \tag{5.18}$$

with $\bar{\lambda} = \tilde{\bar{g}}_k - 3\bar{g}_k$. Making use of the flow Eqs. (5.5), the β-function for $\bar{\lambda}$ can be obtained from $\partial_t \bar{\lambda} = \partial_t \tilde{\bar{g}}_k - 3\partial_t \bar{g}_k$. Consequently, the flow equation for the dimensionless renormalized coupling $\lambda = \bar{\lambda} k Z_\psi^{-2}$ is given by

$$\partial_t \lambda = \lambda(1 + 2\eta_\psi) + 2 l^{1,1}_{a,\psi} \lambda e^2 + l^{2,1}_{a,\psi} e^4 . \tag{5.19}$$

The key feature of this equation is the absence of a λ^2 term. This is due to cancellations in the β-function special to the $N_F = 1$ case as we explain in Appendix B.2. This structural specialty is already visible upon setting $N_f = 1/2$ in Eq. (5.5c); then the $\tilde{g}^2$ in that equation disappears and the fixed-point structure qualitatively changes. Further implementing the symmetry Eq. (5.17), then yields Eq. (5.19) for a single four-fermi coupling. Of course, this β-function Eq. (5.19) may also be derived directly from applying the Polchinski-Wetterich

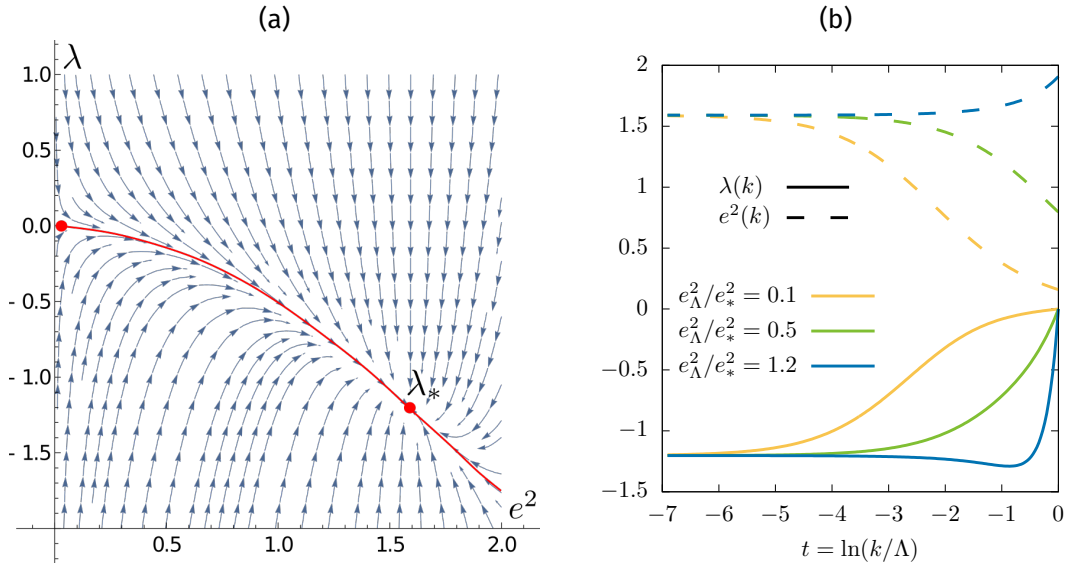

FIGURE 5.4: (a): **Universal location of the interacting conformal fixed point** in the plane of interaction couplings for $N_\mathrm{F} = 1$. Arrows point towards the infrared. (b): **Explicit numerical solutions** for a range of initial values e^2_Λ showing convergence of both, the gauge coupling e^2 and the four-fermi coupling λ, toward fixed-point plateaus in the infrared as $k \to 0$.

equation [46, 119] to the ansatz Eq. (5.18). This is performed explicitly in Appendix B.

5.2.1 Interacting conformal fixed point

We can now perform the symmetry-breaking analysis along the lines explained above but with the reduced number of equations, by feeding the gauge sector and anomalous dimensions into Eq. (5.19). Given the IR fixed point of the gauge sector ($e^2 = e^2_* = 1.59$, $\eta^*_a = 1$, $\eta^*_\psi = -0.64$) as an input, and because $\partial_t\lambda$ is linear in λ, there can be only one fixed point solution to Eq. (5.19):

$$\lambda_* = -\frac{l^{2,1}_{A,\psi} e^4_*}{1 + 2\eta_\psi + 2l^{1,1}_{A,\psi} e^2_*} = -1.20, \qquad \left.\frac{\partial(\partial_t\lambda)}{\partial\lambda}\right|_{(\lambda_*)} = 1 + 2\eta_\psi + l^{1,1}_{A,\psi} e^2_* = 3.87 \tag{5.20}$$

The numerical values are provided for the linear regulator and in Landau gauge as before. Given the positive slope of $\partial_t\lambda$, the fixed point λ_* is found to be infrared attractive. Therefore, no runaway flow occurs for arbitrary initial values $e^2_{k=\Lambda}$ and the fixed-point structure and explicit flows (see FIG. 5.4) preserve scaling/conformal invariance as $k \to 0$.

5.2.2 Discussion

In principle, by virtue of Eqs. (5.16b,5.17) a runaway flow in the four-fermi sector with gauge-invariant regularization can lead to quadratic mass terms $\sim m\bar\chi\chi$ and spontaneous background currents $\sim \langle j^\mu\rangle\bar\chi\sigma^\mu\chi$ thereby breaking time-reversal and space-reflection symmetry. In fact, this parity anomaly appears generically if the entire set of large gauge transformations is allowed, such that Chern-Simons terms of all levels are induced [120–123].

This seems to not be the case in the physical systems where Eq. (5.1) is supposed to be a good effective description. Indeed, as a theory for the surface states of topological insulators, QED$_3$ with $N_{\mathrm{F}} = 1$ is a good description provided that 4π units of flux of a_μ are identified with the creation operator of one electron (this will be discussed in some more detail below). As such, a single Chern-Simons term (corresponding to a 2π-flux of a_μ) breaks charge conservation and is therefore not allowed in the effective theory [29].

5.3 Fermionic particle-vortex duality: an application

In this section we first discuss the general idea of a field theory duality and the particular form that we will be interested in latter parts of the chapter. The discussion in section 5.3.1 is based primarily on [124, 125]. The recap on bosonic particle-vortex duality consists of widely known facts and can, accordingly, be found in standard textbooks, e.g. [37, 126]. The version of fermionic duality that we describe here is adapted from [34, 35].

5.3.1 The general idea and the bosonic version

Two physical systems are said to be dual to each other if they are equivalent. In the simplest form, this just means that one system is a "rewriting" of the other. To illustrate this point, consider systems described by hamiltonians H, H' depending on some degrees of freedom (DOF) ϕ, ϕ', and coupling constants g, g', respectively. If it is possible to find a transformation of the DOFs, $\phi = T(\phi')$, as well as of the couplings, $g = \tilde{T}(g')$, such that

$$H(\phi(\phi'); g(g')) = H'(\phi'; g') \ , \tag{5.21}$$

then the systems are clearly equivalent to each other, and there is a direct way to obtain all information of one of the systems from knowledge of the corresponding information of the other. Exactly this kind of dualities were the first ones to be discovered in the context of statistical physics, where, e.g. a rewriting of variables of the Ising model on a square lattice leads to a self duality relating strong to weak couplings [43].

This seemingly trivial kind of duality can be seen to be at the heart of the celebrated bosonization procedure in 1+1 dimensional field theories [127, 128]. Concretely, the fact that the field theories S_{f} and S_{b} given by

$$S_{\mathrm{f}} = \int \mathrm{d}^2 x \left(i\bar{\psi}\gamma^\mu \partial_\mu \psi - m\bar{\psi}\psi - \frac{g}{2}\bar{\psi}\gamma^\mu\psi\bar{\psi}\gamma_\mu\psi \right) \ , \tag{5.22a}$$

$$S_{\mathrm{f}} = \int \mathrm{d}^2 x \left(-\frac{1}{2}\partial^\mu\phi\partial_\mu\phi + m\cos(\beta\phi) \right) \ , \tag{5.22b}$$

produce the same amplitudes (i.e. all n-point correlators) upon the identifications

$$\frac{\beta^2}{4\pi} = \frac{\pi}{\pi + g} \ , \tag{5.23a}$$

$$\bar{\psi}\gamma^\mu\psi \longleftrightarrow \frac{\beta}{2\pi}\epsilon^{\mu\nu}\partial_\nu\phi \ , \tag{5.23b}$$

$$\bar{\psi}\psi \longleftrightarrow \cos(\beta\phi) \ , \tag{5.23c}$$

can be seen to be a consequence of the possibility of constructing bosonic operators out of the fermionic ones and viceversa. Incidentally, this fact is hidden in the dictionary between theories Eq. (5.23), as only pairs of fermionic fields there are mapped to bosonic ones. If one is not interested in an exact rewriting of individual operators, but only in comparing correlators, the dictionary translating fermionic into bosonic theories can be roughly[1] summarized as

$$\psi(x) = \frac{1}{\sqrt{2\pi a}} \exp\left(i\sqrt{4\pi}\phi(x)\right) \ , \tag{5.24}$$

with a a cutoff regularizing the short distance $x \to 0$ limit in correlators. In these terms, the theories are dual if *the same cutoff* is chosen to regularize both the fermionic and the bosonic theory.

As written, both theories in Eq. (5.23) are strongly interacting, so the usefulness of the duality is not all too evident. However, for $m = 0$, the bosonic side of the duality is noninteracting and thus exactly solvable while the fermionic side remains interacting. Although care is needed when translating the results obtained from the bosonic system into the fermionic one, the duality provides a full solution of a strongly interacting theory. Of course, for any given interacting theory we cannot expect to find a dual free theory describing it, but if *some* dual description is available, we can still gain some clear physical picture from it. This is illustrated with a further example in the next section.

The duality just described is an example of a 'weak duality' in the language of [125]. It is weak in the sense that the equivalence holds when both field theories are exactly as written. In contrast, a 'strong' duality is a statement about RG flows and fixed points of the two related theories, as we will see in the next section.

Bosonic particle-vortex duality in $2d$

To define what a strong duality means, we start with an example, namely the the bosonic version of particle vortex duality. To this end, consider a complex order parameter field ϕ living in 2+1d and described by the action (in Minkowski signature)

$$S_{\rm p} = \int {\rm d}^3 x \left(|\partial_\mu \phi|^2 - r|\phi|^2 - u|\phi|^4\right) \ . \tag{5.25}$$

This field theory is dual [129] to a gauged version of itself, namely

$$S_{\rm v} = \int {\rm d}^3 x \left(|(\partial_\mu - i\tilde{e}a_\mu)\varphi|^2 - \tilde{r}|\varphi|^2 - \tilde{u}|\varphi|^4 + \frac{1}{2\tilde{e}^2} f_{\mu\nu} f^{\mu\nu}\right) \ , \tag{5.26}$$

with $f_{\mu\nu} = \partial_\mu a_\nu - \partial_\nu a_\mu$ the srength tensor of the $U(1)$ gauge field a_μ. The dictionary relating the two theories is given by

$$\phi^* \partial^\mu \phi - (\partial^\mu \phi^*)\phi \longleftrightarrow \frac{1}{2\pi} \epsilon^{\mu\nu\rho} \partial_\nu a_\rho \ , \tag{5.27}$$

[1] The standard treatment starts with *two* bosonic fields $\phi_\pm$ out of which left/right-handed fermions are defined according to $\psi_{L/R} \sim \exp(\pm i\sqrt{4\pi}\phi_\pm)$

i.e. the particle current of ϕ corresponds to a flux of the gauge field a, so that the particle number operator for ϕ translates to an operator destroying a monopole (or magnetic flux vortex) of a. This is precisely where the name of the duality comes from.

The last fact can be easily encoded to produce a statement about path integrals with the help of a *background gauge field* A_μ and a coupling constant e. This is done by minimal coupling in the theory of Eq. (5.25), $\partial_\mu \to \partial_\mu - ieA_\mu$, and by adding a so called BF-term to the lagrangean density of Eq. (5.26),

$$S_{\mathrm{v}} \longrightarrow S_{\mathrm{v}} + \int \mathrm{d}^3\, x \frac{e\tilde{e}}{2\pi} \epsilon^{\mu\nu\rho} A_\mu \partial_\nu a_\rho \; ; \tag{5.28}$$

in this way $S_{\mathrm{p/v}} \to S_{\mathrm{p/v}}[A]$ and the duality can be expressed as

$$Z_{\mathrm{p}}[A] = Z_{\mathrm{v}}[A] \; , \tag{5.29}$$

with

$$Z_{\mathrm{p}}[A] := \int \mathscr{D}\phi \exp(iS_{\mathrm{p}}[A]) \; , \tag{5.30}$$

$$Z_{\mathrm{v}}[A] := \int \mathscr{D}\varphi \mathscr{D} a_\mu \exp(iS_{\mathrm{v}}[A]) \; . \tag{5.31}$$

A concrete physical model where the action of Eq. (5.25) is of relevance is that of an effective theory for the Mott insulating to superfluid transition in a bosonic Hubbard model at filling one. Then ϕ is an order parameter for the superfluid density, and tuning the parameter r through zero in Eq. (5.25) leads to a conformal field theory describing the transition between these two phases. In the "particle" formulation, the disordered phase with $\langle\phi\rangle = 0$ corresponds to the Mott insulator, while in the "vortex" picture, it is a condensate of the vortices of the gauge field a, and corresponds to the Higgs phase of Eq. (5.26), with $\langle\varphi\rangle \neq 0$.

Note that, although the duality gives information about the phases of the system, for the partition functions in Eq. (5.29) to be gauge invariant with respect to the background field A, the scalar fields on both sides of the duality must remain massless [35]. Thus, the extra step of rewriting the duality as an equality of partition functions gives a statement about the *conformal* phases of both theories: the phase transition described by Eq. (5.26) obtained by tuning the parameter $\tilde{r}$ to zero describes the same transition as Eq. (5.25) when the parameter r is tuned to zero.

The new formulation of the phase transition is not only conceptually rich, but carries more information than it may at first appear. Indeed, by identifying the CFTs of *both* field theories we have made a statement about the equality of the scaling dimensions of all operators involved, and therefore, about the involved universality classes. This means, in particular, that complete families of field theories that differ from each other by irrelevant operators get identified by this duality. It is in this sense that this equivalence is referred to as a "strong" duality in the literature [125]. From the equivalence of the CFTs, the equality of e.g. the following scaling dimensions can be deduced

$$[|\phi|^2] = [|\varphi|^2] \; , \tag{5.32a}$$

$$[\phi^* \partial^\mu \phi] = [\epsilon^{\mu\nu\rho} \partial_\nu a_\rho] \; . \tag{5.32b}$$

5.3.2 The fermionic duality

Starting with the works [29, 30, 33], it was suggested that QED$_3$ at $N_{\mathrm{F}} = 1$ is dual to a much simpler theory, namely a free Dirac cone[2]. In terms of the path integrals involved, the duality is

$$Z_{\psi}[A] = Z_{\Psi}[A] \, , \tag{5.33}$$

where

$$S_{\psi}[A] = \int \mathrm{d}^3 \, x \left(\bar{\psi} \left[i\gamma^{\mu} (\partial_{\mu} - ieA_{\mu}) \right] \psi \right) \, , \tag{5.34}$$

and

$$S_{\Psi} = \int \mathrm{d}^3 \, x \left(\overline{\Psi} \left[i\gamma^{\mu} (\partial_{\mu} - i\tilde{e}a_{\mu}) \right] \Psi + \frac{1}{2\tilde{e}^2} f_{\mu\nu} f^{\mu\nu} + \frac{\tilde{e}e}{4\pi} \epsilon^{\mu\nu\rho} A_{\mu} \partial_{\nu} a_{\rho} \right) \, . \tag{5.35}$$

and both fermionic fields ψ, Ψ are two-component spinors. The form of the two actions involved makes already evident why we refer to this duality as the fermionic version of particle-vortex duality. In the following we will also refer to the theory Eq. (5.34) as the Dirac cone and to the theory Eq. (5.35) as the composite fermion. Moreover, the dictionary relating the two theories can be read off the previous two equations and is explicitly given by

$$\bar{\psi} \gamma^{\mu} \psi \longleftrightarrow \frac{1}{4\pi} \epsilon^{\mu\nu\rho} \partial_{\nu} a_{\rho} \, , \tag{5.36}$$

i.e., the density of the ψ-fermions corresponds to *two* (in units of 2π) fluxes of the gauge field a.

A good argument for the veracity of the duality has been made in [130], and we will content ourselves with taking the arguments there as a proof, i.e. we assume that the strong form of the duality holds. In this section, and based on the considerations from the previous subsection, we thus want to make *universal* statements regarding the CFTs of both sides of the duality, similar to those in Eq.(5.32), which are independent of energy scales and, in particular, of the fixed point value of the couplings involved. We can therefore set the couplings $e, \tilde{e}$ to their fixed point values $e_*, \tilde{e}_*$ and redefine the gauge fields, i.e. $a \to a/\tilde{e}_*$ and $A \to A/e_*$. This sets the stage for our program: constraining the topological current correlator in Subsec. 5.3.2 and the mass dimension in Subsec. 5.3.2.

Constraining the topological current correlator

The current-current correlator on the Dirac cone side of the duality Eq. (5.34) can be computed explicitly

$$\langle j_{\mu}(-p) j_{\nu}(p) \rangle = -N_{\mathrm{F}} C_j^{\psi} |p| \left(\delta_{\mu\nu} - \frac{p_{\mu} p_{\nu}}{p^2} \right) \tag{5.37}$$

[2]There are several technicalities involved in defining this duality rigorously which, however, add nothing to the present discussion. The interested reader can find all the details in [34]

where $j_\mu = \bar{\psi}\gamma_\mu\psi$ is the ψ-fermion current, $N_{\rm F} = 1$ is the number of ψ-fermions and

$$C_j^\psi = \frac{1}{16} \, . \tag{5.38}$$

This equation is exact because the CFT in the Dirac cone side Eq. (5.34) is that of a quadratic, free theory. On the composite fermion side, the ψ current gets mapped to the topological current

$$J_\mu^{\rm top} = \frac{1}{4\pi}\epsilon_\mu^{\nu\kappa}\partial_\nu a_\kappa \, , \tag{5.39}$$

and we should have

$$\langle j_\mu(-p) j_\nu(p)\rangle = \langle J_\mu^{\rm top}(-p) J_\nu^{\rm top}(p)\rangle \, , \tag{5.40}$$

where it is understood that the expectation values on each side of (5.40) are taken with respect to their respective actions. Now, for zero doping and in a conformal phase (characterized by $\eta_a^* = 1$) with conserved topological current $\partial_\mu J_\mu^{\rm top} = 0$, the correlator must also have the form of Eq. (5.37) with an independent universal constant

$$\langle J_\mu^{\rm top}(-p) J_\nu^{\rm top}(p)\rangle = -N_{\rm F,cf} C_J^{\rm top}|p| \left(\delta_{\mu\nu} - \frac{p_\mu p_\nu}{p^2}\right) \tag{5.41}$$

with $N_{\rm F,cf} = 1$ the number of composite fermions Ψ. The number $C_J^{\rm top}$ is, however, not known, since the composite fermion theory is interacting. We can now use Eq. (5.40) to determine $C_J^{\rm top}$ *exactly* thus constraining perturbative computations for $C_J^{\rm top}$. The best estimate for $C_J^{\rm top}$ has been obtained by large-N diagrammatic methods [3]. Denoting the number of fermionic components as $N_{\rm G}$, the result reported in Ref. [116] (Eq. (4.3.)) then reads:

$$C_J^{\rm top} = \left[\frac{2}{\pi^2 N_{\rm G}}\left(1 + \frac{1}{N_{\rm G}}\left(8 - \frac{736}{9\pi^2}\right)\right) + \Delta X^{\rm top}(N_{\rm G})\right] \tag{5.42}$$

where we have gathered the unknown interaction corrections to all orders in $1/N_{\rm G}$ into the variable $\Delta X^{\rm top}(N_{\rm G})$ and already adjusted the conventions defining the current correlator, i.e. $J_\mu^{\rm top} \to J_\mu^{\rm top}/2$. Recalling that our spinors are two-dimensional,

$$N_{\rm G} = 4N_{\rm f} = 2N_{\rm F} \, , \tag{5.43}$$

and invoking Eqs. (5.38,5.40), we obtain for $N_{\rm F} = 1$

$$C_J^{\rm top} = \left[0.347365 + \Delta X^{\rm top}(N_{\rm G} = 2)\right] \, , \tag{5.44}$$

$$\Delta X^{\rm top}(N_{\rm G} = 2) = -0.0973652 \, . \tag{5.45}$$

Knowledge of the exact value for this and other universal constants may help to constrain perturbative computations of thermodynamics, entanglement, and response functions of QED$_3$ and possibly extensions thereof.

[3] By this we mean that a counting of diagrams is performed to order $1/N$, but no assumptions are made about the size of N.

Scaling dimension of mass operator at one-loop

Our analysis of QED$_3$ in Sec. 5.2 was based on an Ansatz with massless fermions, so it does not allow us to obtain directly an estimate of the scaling dimension of the fermion mass operator. As advertised before, the duality allows one to obtain such scaling dimensions. In particular, in addition to the matching of particle current and gauge field flux, the strong form of a duality implies that the mass scaling dimensions coincide [130]. The analogue of Eq. (5.32) is then

$$[\bar{\psi}\psi] = [\overline{\Psi}\Psi] \ . \tag{5.46}$$

The left hand side of Eq. (5.46) is exactly zero, as are the anomalous dimensions of any free theory. To obtain the right hand side, we use a more pedestrian approach, namely a one-loop calculation. That is, we compute the singular corrections to the scaling dimension of the mass operator $\overline{\Psi}\Psi$ for the fermion fields at the fixed-point of Subsec. 5.2.1:

$$\int \mathrm{d}^3\, x\, \tilde{m}\, Z_{\tilde{m}} Z_\Psi\, \overline{\Psi}\Psi \tag{5.47}$$

Defining the anomalous exponents (Λ is the running cutoff scale),

$$\eta_\Psi = -\frac{\partial \log Z_\Psi}{\partial \log \Lambda} \ , \tag{5.48a}$$

$$\eta_{\tilde{m}} = -\frac{\partial \log Z_{\tilde{m}}}{\partial \log \Lambda} \ , \tag{5.48b}$$

the total correction to the scaling dimension of the mass operator is then

$$\eta_{\rm mass} = \eta_{\tilde{m}} + \eta_\Psi \ . \tag{5.49}$$

We first compute the fermionic field renormalization Z_Ψ and η_Ψ from the one-loop self-energy shown in FIG. 5.5. The photon anomalous dimension is $\eta_a^* = 1$ so we can use the overdamped one-loop form for the propagator of the gauge field, i.e., for $N_{\rm F}=1$:

$$D_{\mu\nu}(q) = \frac{16}{\tilde{e}_*^2|q|}\left(\eta_{\mu\nu} - (1-\xi)\frac{q_\mu q_\nu}{q^2}\right) \ , \tag{5.50}$$

where, as before, $\tilde{e}$ is the charge of the Ψ fermion with respect to the gauge field a, as denoted in Eq. (5.35). For simplicity, we use the Feynman gauge $\xi = 1$ in what follows.

FIGURE 5.5: **One-loop fermion self energy** for Z_Ψ and the corresponding anomalous dimension η_Ψ.

With this, the singular fermion self-energy correction is:

$$\delta\Sigma_\Psi(q) = \tilde{e}_*^2 \int \frac{\mathrm{d}^3\, p}{(2\pi)^3}(-\gamma^\mu) G_\psi(q+p)(-\gamma^\nu) D_{\mu\nu}(p)$$

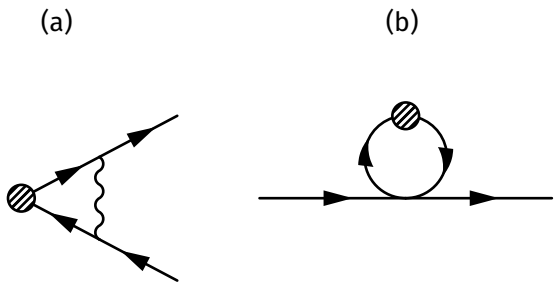

FIGURE 5.6: **One-loop graphs for insertions of the mass operator** $\tilde{m} = \overline{\Psi}\Psi$. (a) is computed in the text and (b) arises from the four-fermi coupling λ and does not produce singular corrections, when approximating λ as momentum-independent. Upon keeping the momentum-dependence of the four-fermi coupling, for example via σ-meson exchange [131], (b) can also generate singular corrections to operator dimensions.

$$= -\frac{8}{3\pi^2} \not{q} \log\left(\frac{\Lambda}{|q|}\right) , \tag{5.51}$$

and the anomalous dimension for the fermions is

$$\eta_\Psi = -\Lambda \frac{\partial}{\partial \Lambda} \operatorname{tr}\left(\gamma^\mu \frac{\partial}{\partial q^\mu} \delta\Sigma_\Psi(q)\right)\Big|_{q=0} = \frac{8}{3\pi^2} , \tag{5.52}$$

in agreement with a previous calculation upon setting their N to $1/2$ and gauge fixing $\xi = 1$ [32].

The one-loop graphs for the correction to the mass operator $\delta m(k)$ are shown in FIG. 5.6. Graph (a) is non-vanishing and yields the divergent correction

$$\begin{aligned} \delta\tilde{m}(k) &= \mathbb{1} \frac{24}{\pi^2} \log\left(\frac{\Lambda}{|k|}\right) \\ \eta_{\tilde{m}} &= -\frac{24}{\pi^2} . \end{aligned} \tag{5.53}$$

Adding the exponents as per Eq. (5.49) we get the final result

$$\eta_{\text{mass}} = -\frac{64}{3\pi^2} , \tag{5.54}$$

which agrees with the leading term in a computation of the same quantity by Gracey upon setting his $N_f = 1/2$ [132]. This differs by a lot from the expected result from the duality. However, one must bear in mind that the computation just presented is based on a one-loop computation, which is not the best estimate for low fermion numbers. Implementing the momentum-dependent four-fermi coupling via σ-meson exchange [131] will produce corrections to Eq. (5.54), as may other additional terms to the truncation Eq. (5.18). It is an interesting project to establish explicitly the exponent identities conjectured by the duality.

For the insertion of the (conserved) current operator, the cancellation can be seen already at the level of our approximation. That is, for

$$\int dd^3x \, j_\mu \, Z_{j_\mu} Z_\Psi \, \overline{\Psi}\gamma^\mu\Psi , \tag{5.55}$$

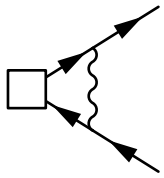

FIGURE 5.7: **One-loop correction** to insertions of the current operator $j_\mu = \overline{\Psi}\gamma_\mu\Psi$.

with $j_\mu = \overline{\Psi}\gamma_\mu\Psi$, the current anomalous dimension is

$$\eta_{\mathrm{current}} = \eta_{j_\mu} + \eta_\Psi = -\frac{8}{3\pi^2} + \frac{8}{3\pi^2} = 0 \,, \tag{5.56}$$

which follows from evaluating the diagram of FIG. 5.7:

$$\delta j^\mu(q) = \frac{8}{3\pi^2}\left(\gamma^\mu \log\left(\frac{\Lambda}{|q|}\right) - \frac{q^\mu}{q^2}\not{q}\right), \tag{5.57}$$

5.4 Conclusion

This chapter explored aspects of a particle-vortex duality for Dirac fermions in two space dimensions. We raised the question whether a single two-component Dirac fermion coupled to $U(1)$ gauge field can have a conformally invariant ground state and found indications that this may the case, at least for the initially only weakly coupled model. The CFT we found is not free but has non-trivial anomalous dimensions and finite four-fermi couplings. It would desirable to have a (non-perturbative) proof of the absence of spontaneous symmetry-breaking in the ground state of Eq. (5.2) by generalizing the Vafa-Witten theorem to smaller flavor numbers down to $N_{\mathrm{F}} = 1$.

The strong form of the duality between QED$_3$ and a free Dirac cone constrains operator dimensions and, as we tried to show, also universal constants of electromagnetic response functions. Admitting the presence of Chern-Simons terms would in principle open up the possibility to investigate a number of other possible dualities [34, 35]. Coupling the dynamical gauge field a_μ to a dynamic field b_μ via $\frac{1}{2\pi}\int \mathrm{d}^3x\epsilon^{\mu\nu\rho}a_\mu\partial_\nu b_\rho$, for instance, a duality to the Wilson-Fisher fixed-point of φ^4 theory has been conjectured recently [34, 35]. In the future, it will be interesting to investigate this scenario within the present RG framework by adding the corresponding terms to the ansatz for the scale dependent effective action Eq. (5.2). The computation of the respective flow equations, however, may not be straightforward. As discussed in [28] in detail, the gauge sector of QED$_3$ requires a delicate treatment due to its complicated momentum structure in the infrared regime. While the computation in [28] on which the present work relies was specifically tailored to account for this subtlety, it is not clear whether the modification due to a Chern-Simons term can be incorporated directly. We leave this more generalized problem for future work.

It would also be interesting to establish exponent identities and possibly emergent conservation laws of dual QED$_3$ more completely and to higher loop order. To strengthen the link to

a specific condensed matter situation, a further topic of interest are the “non-universalities" of dual QED_3 such as the kinematics, velocities, additional interactions, and energy scales below which the continuum field theories for the effective degrees of freedoms emerge.

Chapter 6

Summary and outlook

In this work, we have presented a functional renormalization group study of quantum phase transitions and phases of Dirac materials, with a focus on spacetime dimension $D = 3$ and with an eye on transitions that might present behaviour outside the expected scope of a naïve Landau description. In Chapters 3 and 4 we showed the important role that gapless fermions play in the dynamics of the order parameters and how they provide a simple mechanism to observe transitions that would otherwise not be allowed within the Landau-Ginzburg paradigm.

Our results moreover illustrate the versatility of the FRG method. Indeed, many of the relevant features of the transitions studied in this work can be best observed when analyzing the critical points by approaching them from the ordered phases, a task which is much more easily achieved within our nonperturbative treatment when compared to usual perturbative approaches. In chapter 2 we moreover provided an original example of this versatility by showing how all quantum critical points that involve mass-like order parameters in Dirac systems approach a Lorentz invariant form in the low energy limit, regardless of the dimensionality of the system, the number of fermions involved or the particular details of the bosonic self-interactions, but provided that these are isotropic in the spatial dimensions. A potentially interesting extension of our arguments to e.g. interactions mediated by emergent gauge fields could lead to novel fixed points or phases where no Lorentz symmetry is achieved [52].

The treatment of compatible orderings presented in Chapter 4 certainly allows room for improvement. As mentioned in detail there, although it is reasonable to consider the transition as mediated just by fluctuations of the local order parameters and of the fermions, it is of course not unthinkable that monopole operators for the order parameters play an important role. To what extent they effect the symmetry enhancement properties of the gapless fermions is not at all clear and could lead to a better understanding of not only the phases of Dirac materials, but also of spin models in which deconfined quantum critical points are presumed to exist.

Additionally, we showed in Chapter 5 how the condensed matter realizations of well known theories like Quantum Electrodynamics can present unexpected behaviours differing from their high energy counterparts. In Chapter 5 we moreover explored a dual description of QED_3 that allowed us to obtain nontrivial information of this strongly interacting theory. This latter fact opens the door to study similar systems. The duality that we considered is

perhaps the simplest of a recently proposed web of dualities that seems to provide unexpected and far reaching connections between many field theories, yielding complementary descriptions of several condensed matter systems.

One need not even consider other "threads" of the web, as the exact same duality that we have analyzed in Chapter 5 offers a rich variety of phenomena that can be theoretically challenging and experimentally accessible [133]. The connection that this duality provides to the physics of the half-filled Landau level promises to provide several interesting options that remain to be explored [134, 135].

Appendix A

Threshold functions

This appendix lists all the threshold functions not written explicitly in the main text.

A.1 Threshold functions - Kekulé Valence Bond Solid

Here we present the threshold functions that appear in the flow equations and the anomalous dimensions of chapter 3. In the following we restrict to a choice of cutoff $R_{\Phi,k}(q)$ that allows explicit analytic evaluation of the integrals involved and has favorable convergence properties [47, 136–139]:

$$R_{\phi,k}(q) = Z_{\phi,k}(k^2 - q^2)\theta(k^2 - q^2)\,, \tag{A.1}$$

$$qR_{\psi,k}(q) = iZ_{\psi,k}\not{q}(k - q)\theta(k^2 - q^2)\,. \tag{A.2}$$

The threshold functions in the effective potential read

$$l_B(\omega) = \frac{2v_D}{D}\left(1 - \frac{\eta_\phi}{D+2}\right)\frac{1}{1+\omega}\,, \tag{A.3}$$

$$l_F(\omega) = \frac{2v_D}{D}\left(1 - \frac{\eta_\psi}{D+1}\right)\frac{1}{1+\omega}\,. \tag{A.4}$$

In the anomalous dimensions the threshold functions are

$$m_2^F = \frac{1}{(1+\omega_\psi)^4}\,, \tag{A.5}$$

$$m_4^F = \frac{1}{(1+\omega_\psi)^4} + \frac{1-\eta_\psi}{D-2}\frac{1}{(1+\omega_\psi)^3} - \left(\frac{1-\eta_\psi}{2D-4} + \frac{1}{4}\right)\frac{1}{(1+\omega_\psi)^2}\,. \tag{A.6}$$

For any of the three equivalent minima of the order parameter potential, the remaining threshold functions are somewhat more involved and read

$$\begin{aligned} m^B_{(4)R_{1/2}}(v_1, v_2) = v_D \Bigg(&(1 + u_{22/11})\frac{(1 + u_{22/11})v_1 - u_{12}v_2}{((1 + u_{11})(1 + u_{22}) - u_{12}^2)^2} - \\ &u_{12}\frac{(1 + u_{11/22})v_2 - u_{12}v_1}{((1 + u_{11})(1 + u_{22}) - u_{12}^2)^2}\Bigg)^2\,, \end{aligned} \tag{A.7}$$

$$m^B_{(22)R_1R_2}(v_1, v_2, v_3) = v_D \left((1 + u_{11})(1 + u_{22})\frac{((1 + u_{11})v_1 - u_{12}v_2)((1 + u_{22})v_1 - u_{12}v_3)}{((1 + u_{11})(1 + u_{22}) - u_{12}^2)^4}\right.$$

$$
\begin{aligned}
&+ u_{12}^2 \frac{((1+u_{22})v_2 - u_{12}v_1)((1+u_{11})v_3 - u_{12}v_1)}{((1+u_{11})(1+u_{22}) - u_{12}^2)^4} \\
&- u_{12}(1+u_{22}) \frac{((1+u_{22})v_2 - u_{12}v_1)((1+u_{22})v_1 - u_{12}v_3)}{((1+u_{11})(1+u_{22}) - u_{12}^2)^4} \\
&- u_{12}(1+u_{11}) \frac{((1+u_{11})v_1 - u_{12}v_2)((1+u_{11})v_3 - u_{12}v_1)}{((1+u_{11})(1+u_{22}) - u_{12}^2)^4} \Big) \,, \qquad \text{(A.8)}
\end{aligned}
$$

$$
m^{FB}_{(12)R_{1/2}} = \left(1 - \frac{\eta_\phi}{D+1}\right) \frac{(1+u_{22/11})^2 + u_{12}^2}{\Big((1+u_{11})(1+u_{22}) - u_{12}^2\Big)^2 (1+\omega_\psi)} \,, \qquad \text{(A.9)}
$$

$$
\begin{aligned}
l^{FR_{1/2}}_{nm} =& \frac{2v_D}{D} \left[m \left(1 - \frac{\eta_\phi}{D+2}\right) \frac{(1+u_{22/11})^2 + u_{12}^2}{\Big((1+u_{11})(1+u_{22}) - u_{12}^2\Big)(1+u_{22/11})} \right. \\
&\left. + n \left(1 - \frac{\eta_\psi}{D+1}\right) \frac{1}{1+\omega_\psi} \right] \times \frac{(1+u_{22/11})^m}{\Big((1+u_{11})(1+u_{22}) - u_{12}^2\Big)^m (1+\omega_\psi)^n} \,, \qquad \text{(A.10)} \\
l^{FR_1R_2}_{111} =& \frac{2v_D}{D} \left[\left(1 - \frac{\eta_\phi}{D+2}\right)(2 + u_{11} + u_{22}) \frac{(1+u_{11})(1+u_{22}) + u_{12}^2}{(1+u_{11})(1+u_{22}) - u_{12}^2} \right. \\
&\left. + \left(1 - \frac{\eta_\psi}{D+1}\right) \frac{(1+u_{11})(1+u_{22})}{1+\omega_\psi} \right] \times \frac{1}{\Big((1+u_{11})(1+u_{22}) - u_{12}^2\Big)^2 (1+\omega_\psi)} \,. \qquad \text{(A.11)}
\end{aligned}
$$

Let us note that these threshold functions simplify for our choice of the minimum as $u_{12} = 0$ in this case.

A.2 Threshold functions for compatible orders

A.2.1 FRG equations

Anticipating the splitting of the bosonic degrees of freedom into longitudinal and transversal, we denote the combined independent fields as $\Phi := \{\phi_L, \phi_T, \chi_L, \chi_T\}$. We moreover make use of the standard linear regulators for bosons and fermions, $R_\Phi(p) = Z_\Phi p^2 r_B(p^2)$ and $R_\psi(p) = -Z_\psi \not{p} r_F(p^2)$, and feed the Ansatz of Eq. (3.19) into the Wetterich equation. The respective projections are described below.

Masses and bosonic potential

The different masses appearing in the threshold equations are obtained from the Hessian of the dimensionless potential $u(\rho_\phi, \rho_\chi)$. Denoting derivatives with respect to Φ with subscripts and derivatives with respect to ρ_ϕ, ρ_χ with superscripts, (i.e. $u^{(m,n)} := \frac{\partial^{m+n} u}{\partial \rho_\phi^m \partial \rho_\chi^n}$), the nonzero entries are given by

$$
\begin{aligned}
u_{11} &= u^{(1,0)} + 2\rho_\phi u^{(2,0)} \,, \qquad u_{22} = u^{(1,0)} \,, \qquad \text{(A.12)} \\
u_{33} &= u^{(0,1)} + 2\rho_\chi u^{(0,2)} \,, \qquad u_{44} = u^{(0,1)} \,, \\
u_{13} = u_{31} &= 2\sqrt{\rho_\phi \rho_\chi} u^{(1,1)} \,, \qquad \omega_\psi = 2(g_1^2 \rho_\phi + g_2^2 \rho_\chi) \,,
\end{aligned}
$$

from which we define the entries of the bosonic propagator matrix as

$$d_{1/2,L} := \frac{1+u_{33/11}}{(1+u_{11})(1+u_{33})-u_{13}^2} , \tag{A.13}$$

$$d_{iT} := \frac{1}{1+u_{2i2i}} , \tag{A.14}$$

$$d_{\phi\chi} := \frac{u_{13}}{u_{13}^2-(1+u_{11})(1+u_{33})} . \tag{A.15}$$

The flow equation for the potential therefore takes the form

$$\begin{aligned}\partial_t u = &-Du + (D-2+\eta_\phi)\rho_\phi u^{(1,0)} + (D-2+\eta_\chi)\rho_\chi u^{(0,1)} \\ &+ \ell_{1L}^B + (N_1-1)\ell_{1T}^B + \ell_{2L}^B + (N_2-1)\ell_{2T}^B - d_\gamma \ell^F ,\end{aligned} \tag{A.16}$$

with threshold functions

$$\ell_{i\alpha}^B := \frac{4v_D}{D}\left(1-\frac{\eta_i}{D+2}\right) d_{i\alpha} , \tag{A.17}$$

$$\ell^F := \frac{4v_D}{D}\left(1-\frac{\eta_\psi}{D+1}\right)\frac{1}{1+\omega_\psi} . \tag{A.18}$$

Yukawa couplings

In order not to introduce a bias between order parameters with and without goldstone modes (i.e. when one of the OPs is of Ising type), we take a projection along the longitudinal directions of the OPs. The coordinates are chosen such that ϕ_1 and χ_1 are the massive directions, this means

$$\partial_t g_i = \frac{1}{d_\gamma}\,\mathrm{tr}\left(\gamma_\Phi^1 \frac{\delta}{\delta\Phi_{2i-1}(q)}\frac{\overrightarrow{\delta}}{\delta\bar{\psi}(q)}\partial_t\Gamma_k\frac{\overleftarrow{\delta}}{\delta\psi(q)}\right)\Bigg|_{\Phi=\bar{\psi}=\psi=0,q=0} . \tag{A.19}$$

The full flow equations thus obtained are

$$\begin{aligned}\partial_t g_1^2 = &(D-4+\eta_1+2\eta_\psi)g_1^2 - 2g_1^2\Big[g_1^2\Big((N_1-1)L_{110,1T}^{FB} - L_{111,1L}^{FB}\Big) \\ &+ g_2^2\Big((N_2-1)L_{110,2T}^{FB} + L_{111,2L}^{FB}\Big)\Big] - 16g_1^4 g_2^2\sqrt{\rho_\phi\rho_\chi}L_{21}^{BB} \\ &+ 2g_1^2\Big[u_{221}(N_1-1)\sqrt{2\rho_\phi}g_1^2 L_{120,1T}^{FB} + u_{441}(N_2-1)\sqrt{2\rho_\chi}g_2^2 L_{120,2T}^{FB}\Big] \\ &- 2g_1^2 u_{111}\Big[\sqrt{2\rho_\phi}\Big(g_1^2 L_{122,1L}^{FB} - g_2^2 L_{12}^{BB}\Big) + 2g_2^2\sqrt{2\rho_\chi}L_{12,1}^{FR}\Big] \\ &- 2g_1^2 u_{331}\Big[\sqrt{2\rho_\phi}\Big(g_1^2 L_{12}^{BB} - g_2^2 L_{122,2L}^{FB}\Big) + 2g_2^2\sqrt{2\rho_\chi}L_{12,2}^{FR}\Big] \\ &- 2g_1^2(u_{131}+u_{311})\Big[\sqrt{2\rho_\phi}\Big(g_1^2 L_{12,1}^{FR} - g_2^2 L_{12,2}^{FR}\Big) + g_2^2\sqrt{2\rho_\chi}(L_{11}^{BR}+L_{02}^{BR})\Big] \\ &- 8g_1^4\rho_\phi\Big[g_1^2(L_{211,1L}^{FB} - (N_1-1)L_{210,1T}^{FB}) - g_2^2((N_2-1)L_{210,2T}^{FB} + L_{211,2L}^{FB})\Big] ,\end{aligned}$$

and

$$
\begin{aligned}
\partial_t g_2^2 = (D-4+\eta_2+2\eta_\psi)g_2^2 &- 2g_2^2\Big[g_2^2\Big((N_2-1)L^{FB}_{110,2T}-L^{FB}_{111,2L}\Big)\\
&+ g_1^2\Big((N_1-1)L^{FB}_{110,1T}+L^{FB}_{111,1L}\Big)\Big] - 16g_2^4 g_1^2\sqrt{\rho_\phi\rho_\chi}L^{BB}_{21}\\
&+ 2g_2^2\Big[u_{443}(N_2-1)\sqrt{2\rho_\chi}g_2^2L^{FB}_{120,2T}+u_{223}(N_1-1)\sqrt{2\rho_\phi}g_1^2L^{FB}_{120,1T}\Big]\\
&- 2g_2^2u_{333}\Big[\sqrt{2\rho_\chi}\Big(g_2^2L^{FB}_{122,2L}-g_1^2L^{BB}_{12}\Big)+2g_1^2\sqrt{2\rho_\phi}L^{FR}_{12,2}\Big]\\
&- 2g_2^2u_{113}\Big[\sqrt{2\rho_\chi}\Big(g_2^2L^{BB}_{12}-g_1^2L^{FB}_{122,1L}\Big)+2g_1^2\sqrt{2\rho_\phi}L^{FR}_{12,1}\Big]\\
&- 2g_2^2(u_{313}+u_{133})\Big[\sqrt{2\rho_\chi}\Big(g_2^2L^{FR}_{12,2}-g_1^2L^{FR}_{12,1}\Big)+g_1^2\sqrt{2\rho_\phi}(L^{BR}_{11}+L^{BR}_{02})\Big]\\
&- 8g_2^4\rho_\chi\Big[g_2^2(L^{FB}_{211,2L}-(N_2-1)L^{FB}_{210,2T})-g_1^2((N_1-1)L^{FB}_{210,1T}+L^{FB}_{211,1L})\Big]\,,
\end{aligned}
$$

with threshold functions given by

$$
\begin{aligned}
L^{FB}_{mnr,i\alpha} :=& \frac{8v_D}{D}\left[\left(1-\frac{\eta_\psi}{D+1}\right)\frac{md_{i\alpha}}{1+\omega_\psi}+\left(1-\frac{\eta_i}{D+2}\right)nd_{i\alpha}^2\right.\\
&\left.+\left(1-\frac{\eta_j}{D+2}\right)r|\epsilon_{ij}|d_{\phi\chi}^2\right]\frac{d_{i\alpha}^{n-1}}{(1+\omega_\psi)^m}\,, \qquad \text{(A.20)}\\
L^{FR}_{mn,i} :=& \frac{8v_D}{D}\left[\left(1-\frac{\eta_\psi}{D+1}\right)\frac{md_{iL}}{1+\omega_\psi}+\left(1-\frac{\eta_i}{D+2}\right)nd_{iL}^2\right.\\
&\left.+\left(1-\frac{\eta_j}{D+2}\right)|\epsilon_{ij}|(d_{\phi\chi}^2+d_{1L}d_{2L})\right]\frac{d_{\phi\chi}}{(1+\omega_\psi)^m}\,, \qquad \text{(A.21)}\\
L^{BB}_{mn} :=& \frac{8v_D}{D}\left[\left(1-\frac{\eta_\psi}{D+1}\right)\frac{m}{1+\omega_\psi}\right.\\
&\left.+n\left(\left(1-\frac{\eta_1}{D+2}\right)d_{1L}+\left(1-\frac{\eta_2}{D+2}\right)d_{2L}\right)\right]\frac{d_{\phi\chi}^n}{(1+\omega_\psi)^m}\,, \qquad \text{(A.22)}\\
L^{BR}_{mn} :=& \frac{8v_D}{D}\left[\left(1-\frac{\eta_\psi}{D+1}\right)\frac{m}{1+\omega_\psi}\right.\\
&\left.+n\left(\left(1-\frac{\eta_1}{D+2}\right)d_{1L}+\left(1-\frac{\eta_2}{D+2}\right)d_{2L}\right)\right]\frac{d_{\phi\chi}^2+md_{1L}d_{2L}}{1+\omega_\psi}\,, \qquad \text{(A.23)}
\end{aligned}
$$

where the index $i,j\in\{1,2\}$, which refers to the two distinct Yukawa couplings, is summed over when repeated and $\alpha\in\{L,T\}$ refers to the longitudinal or transverse components, respectively.

Anomalous dimensions

Finally, the set of equations is closed by considering the anomalous dimensions.

$$
\partial_t Z_i = \lim_{q\to 0}\frac{\partial}{\partial q^2}\frac{\overrightarrow{\delta}}{\delta\Phi_{2i-1}(q)}\partial_t\Gamma_k\frac{\overleftarrow{\delta}}{\delta\Phi_{2i-1}(-q)}\bigg|_{\Phi=\bar\psi=\psi=0}\,, \qquad \text{(A.24)}
$$

$$
\partial_t Z_\psi = -\lim_{q\to 0}\frac{1}{d_\gamma D}\,\mathrm{tr}\left(\gamma^\mu\frac{\partial}{\partial q^\mu}\frac{\overrightarrow{\delta}}{\delta\bar\psi(q)}\partial_t\Gamma_k\frac{\overleftarrow{\delta}}{\delta\psi(q)}\right)\bigg|_{\Phi=\bar\psi=\psi=0}\,, \qquad \text{(A.25)}
$$

from which one gets

$$\eta_i = \frac{4v_D}{D}\left[m_i^B + N_f d_\gamma g_i^2 m^F\right] , \tag{A.26}$$

$$\eta_\psi = \frac{8v_D}{D}\left(g_1^2\left(m_{11,1L}^{FB} + (N_1-1)m_{10,1T}^{FB}\right) + g_2^2\left(m_{11,2L}^{FB} + (N_2-1)m_{10,2T}^{FB}\right)\right) , \tag{A.27}$$

with

$$m^F := \left(\frac{1-\eta_\psi}{D-2}+1\right)\frac{2}{(1+\omega_\psi)^3} - \left(\frac{1-\eta_\psi}{D-2}+\frac{1}{2}\right)\frac{1}{(1+\omega_\psi)^2} , \tag{A.28}$$

$$m_1^B := d_{1T}^2\left((u_{122}d_{1L}+u_{322}d_{\phi\chi})^2 + (u_{322}d_{2L}+u_{122}d_{\phi\chi})^2\right) , \tag{A.29}$$

$$m_2^B := d_{2T}^2\left((u_{344}d_{2L}+u_{144}d_{\phi\chi})^2 + (u_{144}d_{1L}+u_{344}d_{\phi\chi})^2\right) , \tag{A.30}$$

$$m_{mn,i\alpha}^{FB} := \left(m\left(1-\frac{\eta_i}{D+1}\right)d_{i\alpha}^2 + n\left(1-\frac{\eta_j}{D+1}\right)|\epsilon_{ij}|d_{\phi\chi}^2\right)\frac{1}{1+\omega_\psi} . \tag{A.31}$$

A.3 Threshold function for the gauge field anomalous dimension

To compute the photon anomalous dimension it is necessary to take into account the momentum dependence of the wavefunction renormalization factor. Because we expect the polarization to go as $\sim 1/p$, the naive zero momentum limit might be ill-defined. To have control over the calculation, one instead defines the anomalous dimension as dependent on a control parameter ζ by defining

$$\eta_a := -\partial_t \ln Z_a(p^2 = \zeta^2 k^2) , \tag{A.32}$$

where k is the running scale. The pointlike limit that we used for all other couplings is thus achieved by setting $\zeta \to 0$ if the limit is well defined. This produces, upon inserting the projection into the Wetterich equation the following threshold function

$$\begin{aligned}\mathcal{L}_1^{(F)}(\eta_\psi) := \lim_{\zeta\to 0}\frac{8v_3}{\zeta^2}\int_0^\infty \mathrm{d}y\Bigg\{&\frac{2}{3}\frac{\partial_t r_\psi(y)-\eta_\psi r_\psi(y)}{\sqrt{y}\left[1+r_\psi(y)\right]^3} - \frac{1}{2}\int_{-1}^{1}\mathrm{d}x\frac{\sqrt{y}x^2-\zeta x}{y-2\zeta x\sqrt{y}+\zeta^2}\\ &\left[\frac{[\partial_t r_\psi](y)-\eta_\psi r_\psi(y)}{[1+r_\psi(y)]^2[1+r_\psi(y-2\zeta x\sqrt{y}+\zeta^2)]}\right.\\ &\left.+\frac{[\partial_t r_\psi](y-2\zeta x\sqrt{y}+\zeta^2)-\eta_\psi r_\psi(y-2\zeta x\sqrt{y}+\zeta^2)}{[1+r_\psi(y)][1+r_\psi(y-2\zeta x\sqrt{y}+\zeta^2)]^2}\right]\Bigg\}.\end{aligned} \tag{A.33}$$

For the Litim linear regulator shape function $r_\psi(x) = (\sqrt{x}^{-1}-1)\Theta(1-x)$, the limit $\zeta \to 0$ is finite.

Appendix B

Direct derivations of β-functions of four-fermi couplings

B.1 Derivation of β-function $\partial_t\lambda$ for four-fermi coupling λ

The beta function for the single fermionic coupling λ can be derived without making reference to the flow equations (5.5) by applying the ansatz to the Wetterich equation 2.26

$$\partial_t\Gamma_k = \frac{1}{2}\mathrm{STr}\left[\frac{\partial_t R_k}{\Gamma_k^{(2)}+R_k}\right] = \frac{1}{2}\mathrm{STr}\left[\tilde{\partial}_t\mathcal{P}_k\right] + \frac{1}{2}\mathrm{STr}\left[\tilde{\partial}_t\sum_{n=1}^{\infty}\frac{(-1)^{n-1}}{n}(\mathcal{P}_k^{-1}\mathcal{F}_k)^n\right] \tag{B.1}$$

to extract $\partial_t\lambda$ from the ansatz (5.18). The expansion of this equation on terms of propagator and fluctuation matrices $\Gamma_k^{(2)}+R_k = \mathcal{P}_k^{-1}+\mathcal{F}_k$ facilitates a projection onto the respective operator structures. The propagator matrix is given by

$$\mathcal{P}_k^{-1} = \delta^{(3)}(p-q)\begin{pmatrix} P_a^{\mu\nu} & 0 & 0 \\ 0 & 0 & -P_\chi \\ 0 & -P_\chi^T & 0 \end{pmatrix}, \tag{B.2}$$

$$P_\chi = \not{q}\cdot[Z_\psi(1+r_\psi)]^{-1}, \tag{B.3}$$

$$P_a = [\delta_{\mu\nu}q^2 - q_\mu q_\nu]\cdot[Z_a q^2(1+r_a)]^{-1}. \tag{B.4}$$

Here, only terms $\sim(\bar{\chi}\chi)$ are of interest. Therefore, any explicit dependence of the fluctuation matrix on the gauge field a_μ can safely be dropped from the outset and we get

$$\mathcal{F}_k = \begin{pmatrix} 0 & \bar{e}\bar{\chi}_{q-p}\sigma_\mu & -\bar{e}\chi_{p-q}^T\sigma_\mu^T \\ -\bar{e}\sigma_\nu^T\bar{\chi}_{q-p}^T & -2\bar{\lambda}\int_{p_1}\bar{\chi}_{p_1}^T\bar{\chi}_{p-q+p_1} & 2\bar{\lambda}\int_{p_1}\left[\bar{\chi}_{p_1}^T\chi_{p-q+p_1}^T - (\bar{\chi}_{p_1}\chi_{p-q+p_1})\mathbb{1}\right] \\ \bar{e}\sigma_\nu\chi_{p-q} & 2\bar{\lambda}\int_{p_1}\left[(\bar{\chi}_{p_1}\chi_{p-q+p_1})\mathbb{1} + \chi_{p_1}\bar{\chi}_{p-q+p_1}\right] & -2\bar{\lambda}\int_{p_1}\chi_{p_1}\chi_{p-q-p_1}^T \end{pmatrix} \tag{B.5}$$

Projecting onto spatially constant fermion fields $\chi_p := \chi\delta^{(3)}(p)$, the basic building block of the expansion (B.1) can be expressed as

$$\left[\mathcal{P}_k^{-1}\mathcal{F}_k\right]_{\mu\nu} = \delta^{(3)}(p-q)\begin{pmatrix} 0 & P_a^{\mu\nu}\bar{e}\bar{\chi}\sigma_\nu & -P_a^{\mu\nu}\bar{e}\chi^T\sigma_\nu^T \\ -P_\chi\bar{e}\sigma_\mu\chi & -P_\chi 2\bar{\lambda}\left[(\bar{\chi}\chi)\mathbb{1}+\chi\bar{\chi}\right] & P_\chi 2\bar{\lambda}\chi\chi^T \\ P_\chi^T\bar{e}\sigma_\nu^T\bar{\chi}^T & P_\chi^T 2\bar{\lambda}\bar{\chi}^T\bar{\chi} & -P_\chi^T 2\bar{\lambda}\left[\bar{\chi}^T\chi^T - (\bar{\chi}\chi)\mathbb{1}\right] \end{pmatrix}. \tag{B.6}$$

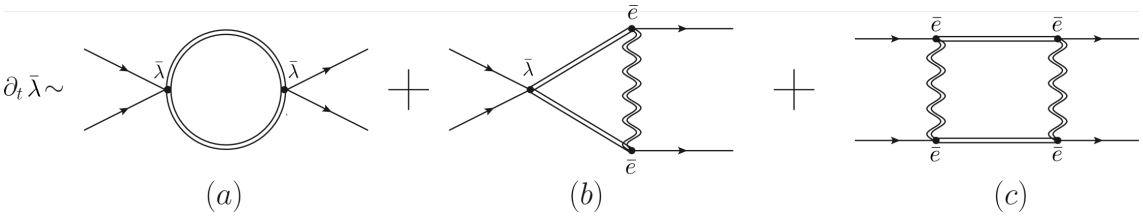

FIGURE B.1: Diagrammatic representation of the contributions to $\partial_t \bar{\lambda}$. It is a special feature here that diagram (a) vanishes after the trace.

There are three contributions to the flow of the bare coupling $\bar{\lambda}$ which can be depicted diagrammatically as in fig. B.1 below.

Here, double lines symbolize the (full) renormalized propagators in (B.2).

Fermionic self interaction This contribution does not involve the gauge vertex. Consequently, only the lower right submatrix of eq. (B.6) is needed. Projecting onto $(\bar{\chi}\chi)^2$ gives

$$\partial_t \bar{\lambda}|_{\bar{\lambda}^2} (\bar{\chi}\chi)^2 = \frac{1}{\Omega}\frac{1}{2}\frac{-1}{2}\mathrm{STr}\left[\left(\mathcal{P}_k^{-1}\mathcal{F}_k\right)^2_{\bar{\lambda}^2}\right] = 0 \tag{B.7}$$

where Ω is the three-dimensional spacetime volume. Thus, tracelessness of the quadratic term in the expansion enforces linearity of the β-function. This finding is crucial for QED$_3$ being conformal for $N_{\mathrm{f}}^{(2)} = 1$ and it only occurs for this flavor number. Some details of why this is the case are given in App. B.2 below.

Triangle diagram Both gauge and fermionic sectors are involved in the computation of this diagram. It is given by

$$\partial_t \bar{\lambda}|_{\bar{\lambda}\bar{e}^2} (\bar{\chi}\chi)^2 = \frac{1}{\Omega}\frac{1}{2}\frac{1}{3}\mathrm{STr}\left[\left(\mathcal{P}_k^{-1}\mathcal{F}_k\right)^3_{\bar{\lambda}\bar{e}^2}\right] = \frac{l^{1,1}_{a,\psi}}{\pi^2}\frac{2}{kZ_\psi^2 Z_a}(\bar{\chi}\chi)^2 \tag{B.8}$$

Here, the usual compact notation in terms of a threshold function has been introduced,

$$l^{n_a,n_\psi}_{a,\psi} = k^{2n_A-2n_\psi-3}\int \mathrm{d}qq^4\left[n_a\frac{\partial_t r_a - \eta_a r_a}{P_{r_a}} + 2n_\psi\frac{1+r_\psi}{P_{r_\psi}}(\partial_t r_\psi - \eta_\psi r_\psi)\right]P_{r_a}^{-n_a}P_{r_\psi}^{-n_\psi}, \tag{B.9}$$

with

$$P_{r_a} = q^2\left[1+r_a\right], \quad P_{r_\psi} = q^2[1+r_\psi]^2. \tag{B.10}$$

Box diagram The last diagram is particularly important as it is responsible to generate the fermionic interaction when starting from the QED$_3$ action in the UV, where $\bar{\lambda}_\Lambda = 0$. When computing its value, the lower right submatrix of Eq.(B.6) may be ignored as only the gauge vertex contributes.

$$\partial_t \bar{\lambda}|_{\bar{e}^4} (\bar{\chi}\chi)^2 = \frac{1}{\Omega}\frac{1}{2}\frac{-1}{4}\mathrm{STr}\left[\left(\mathcal{P}_k^{-1}\mathcal{F}_k\right)^4_{\bar{e}^4}\right] = \frac{l^{2,1}_{a,\psi}}{\pi^2}\frac{1}{k^3 Z_\psi^2 Z_a^2}\bar{e}^4(\bar{\chi}\chi)^2 \tag{B.11}$$

Renormalization and rescaling In a last step, a renormalization of the couplings as in eq. (5.4) and the fields as $\chi \to \chi/\sqrt{Z_\psi}$ as well as a rescaling of e^2 and λ with π^2 provides

the final result for the β-function:

$$\partial_t\lambda = \lambda(1+2\eta_\psi) + \frac{k}{Z_\psi^2}\partial_t\bar{\lambda} = \lambda(1+2\eta_\psi) + 2l^{1,1}_{A,\psi}\lambda e^2 + l^{2,1}_{A,\psi}e^4. \tag{B.12}$$

This reproduces Eq. (5.19) of the main text.

B.2 Cancellation of λ^2 term from flavor trace in $\partial_t\lambda$

In order to understand the origin of the cancellation enforcing linearity of the β-function (B.12) with respect to λ, it is necessary to revisit the corresponding contributions for general flavor number N_F. Although there are two independent quartic fermion terms for $N_\mathrm{F} > 1$ (see Eq. (5.16b)), it is sufficient to consider the generalized interaction

$$(\bar{\chi}\chi)^2 \;\to\; \left(\bar{\chi}^i\chi^i\right)^2_{i=1\ldots N_\mathrm{F}}. \tag{B.13}$$

The fermion sector of the analog to eq. (B.6) is then given by

$$\left[\mathcal{P}_k^{-1}\mathcal{F}_k\right]^{ij}_{\bar{\chi}\chi} = \delta^{(3)}(p-q)\frac{2\bar{\lambda}}{N_\mathrm{F}}\begin{pmatrix} -P_\chi\left[(\bar{\chi}\chi)\mathbb{1}\delta^{ij} + \chi^i\bar{\chi^j}\right] & P_\chi\chi^i\left(\chi^j\right)^T \\ P_\chi^T\left(\bar{\chi}^i\right)^T\bar{\chi}^j & -P_\chi^T\left[\left(\bar{\chi}^i\right)^T\left(\chi^j\right)^T - (\bar{\chi}\chi)\mathbb{1}\delta^{ij}\right]\end{pmatrix}, \tag{B.14}$$

where the flavor dependence of the fermion propagator has already been absorbed. It is then

$$\begin{aligned}\partial_t\bar{\lambda}|_{\bar{\lambda}^2}(\bar{\chi}^i\chi^i)^2 &= \frac{N_\mathrm{F}}{\Omega}\frac{1}{2}\left(\frac{-1}{2}\right)\mathrm{STr}\left[\left(\mathcal{P}_k^{-1}\mathcal{F}_k\right)^2_{\bar{\lambda}^2}\right] = 2\frac{l^1_\psi}{N_\mathrm{F}\pi^2}\mathrm{Tr}_\mathrm{f}\left[\left(\bar{\chi}^a\chi^a\right)\bar{\chi}^i\chi^j - \left(\bar{\chi}^a\chi^a\right)^2\delta^{ij}\right] \\ &= 2\frac{l^1_\psi}{N_\mathrm{F}\pi^2}\left(1-N_\mathrm{F}\right)\bar{\lambda}^2\left(\bar{\chi}^i\chi^i\right)^2\end{aligned} \tag{B.15}$$

where in the first line all traces but the flavor one have been performed and

$$l^n_\psi = 2nk^{2n-3}\int \mathsf{d}qq^4(\partial_t r_\psi - \eta_\psi r_\psi)\frac{1+r_\psi}{P^{n+1}_{r_\psi}}. \tag{B.16}$$

We emphasize the prefactor in this expression vanishes for the case of interest $N_\mathrm{F} = 1$ as announced in the main text. This is due to the absence of flavor off-diagonal terms in Eq. (B.15) for this case. For $N_\mathrm{F} = 1$, the flavor indices $a = i = j$ must fall onto each other and the bracket $[\ldots]$ in the first line of Eq. (B.15) vanishes. Related vanishing of β-functions in the single-flavor case also appears in the Gross-Neveu model and in particular also holds at higher loop orders [106–108]. Complete cancellations of individual contractions in a β-function for a four-fermion vertex also appear in Luttinger liquids [53], although these are specific to spatial dimension $D = 1$.

Bibliography

[1] K. S. Novoselov, A. K. Geim, S. V. Morozov, D. Jiang, Y. Zhang, S. V. Dubonos, I. V. Grigorieva, and A. A. Firsov, "Electric field effect in atomically thin carbon films", Science **306**, 666–669 (2004).

[2] D. P. DiVincenzo and E. J. Mele, "Self-consistent effective-mass theory for intralayer screening in graphite intercalation compounds", Phys. Rev. B **29**, 1685–1694 (1984).

[3] G. W. Semenoff, "Condensed-Matter Simulation of a Three-Dimensional Anomaly", Phys. Rev. Lett. **53**, 2449–2452 (1984).

[4] A. H. Castro Neto, F. Guinea, N. M. R. Peres, K. S. Novoselov, and A. K. Geim, "The electronic properties of graphene", Rev. Mod. Phys. **81**, 109–162 (2009).

[5] C. Poli, J. Arkinstall, and H. Schomerus, "Degeneracy doubling and sublattice polarization in strain-induced pseudo-landau levels", Phys. Rev. B **90**, 155418 (2014).

[6] S. Rachel, I. Göthel, D. P. Arovas, and M. Vojta, "Strain-induced landau levels in arbitrary dimensions with an exact spectrum", Phys. Rev. Lett. **117**, 266801 (2016).

[7] A. A. Zyuzin and A. A. Burkov, "Topological response in weyl semimetals and the chiral anomaly", Phys. Rev. B **86**, 115133 (2012).

[8] B. Rosenstein, M. Lewkowicz, and T. Maniv, "Chiral anomaly and strength of the electron-electron interaction in graphene", Phys. Rev. Lett. **110**, 066602 (2013).

[9] Y. Hatsugai, T. Kawarabayashi, and H. Aoki, "Survival of sharp $n = 0$ landau levels in massive tilted dirac fermions: role of the generalized chiral operator", Phys. Rev. B **91**, 085112 (2015).

[10] V. Cheianov, V. Fal'ko, O. Syljuåsen, and B. Altshuler, "Hidden kekulé ordering of adatoms on graphene", Solid State Communications **149**, 1499 –1501 (2009).

[11] V. V. Cheianov, O. Syljuåsen, B. L. Altshuler, and V. Fal'ko, "Ordered states of adatoms on graphene", Phys. Rev. B **80**, 233409 (2009).

[12] S. Kopylov, V. Cheianov, B. L. Altshuler, and V. I. Fal'ko, "Transport anomaly at the ordering transition for adatoms on graphene", Phys. Rev. B **83**, 201401 (2011).

[13] C. Gutiérrez, C.-J. Kim, L. Brown, T. Schiros, D. Nordlund, E. B. Lochocki, K. M. Shen, J. Park, and A. N. Pasupathy, "Imaging chiral symmetry breaking from Kekulé bond order in graphene", Nature Physics **12**, 950–958 (2016).

[14] S.-K. Jian and H. Yao, "Fermion-induced quantum critical points in two-dimensional Dirac semimetals", Phys. Rev. B **96**, 195162 (2017).

[15] M. M. Scherer and I. F. Herbut, "Gauge-field-assisted Kekulé quantum criticality", Phys. Rev. B **94**, 205136 (2016).

[16] L. Classen, I. F. Herbut, and M. M. Scherer, "Fluctuation-induced continuous transition and quantum criticality in Dirac semimetals", Phys. Rev. B **96**, 115132 (2017).

[17] Z.-X. Li, Y.-F. Jiang, S.-K. Jian, and H. Yao, "Fermion-induced quantum critical points", Nature Communications **8**, 314 (2017).

[18] L. D. Landau and E. M. Lifshitz, *Statistical Physics, Part 1*, Vol. 5, Course of Theoretical Physics (Butterworth-Heinemann, Oxford, 1980).

[19] T. Sato, M. Hohenadler, and F. F. Assaad, "Dirac fermions with competing orders: non-landau transition with emergent symmetry", Phys. Rev. Lett. **119**, 197203 (2017).

[20] T. Senthil, L. Balents, S. Sachdev, A. Vishwanath, and M. P. A. Fisher, "Quantum criticality beyond the Landau-Ginzburg-Wilson paradigm", Phys. Rev. B **70**, 144407 (2004).

[21] T. Senthil, A. Vishwanath, L. Balents, S. Sachdev, and M. P. A. Fisher, "Deconfined Quantum Critical Points", Science **303**, 1490–1494 (2004).

[22] T. Senthil, L. Balents, S. Sachdev, A. Vishwanath, and M. P. A. Fisher, "Deconfined Criticality Critically Defined", Journal of the Physical Society of Japan **74**, 1–9 (2005).

[23] A. Nahum, P. Serna, J. T. Chalker, M. Ortuño, and A. M. Somoza, "Emergent $SO(5)$ Symmetry at the Néel to Valence-Bond-Solid Transition", Phys. Rev. Lett. **115**, 267203 (2015).

[24] P. Serna and A. Nahum, "Emergence and spontaneous breaking of approximate $O(4)$ symmetry at a weakly first-order deconfined phase transition", (2018).

[25] Y. Q. Qin, Y.-Y. He, Y.-Z. You, Z.-Y. Lu, A. Sen, A. W. Sandvik, C. Xu, and Z. Y. Meng, "Duality between the deconfined quantum-critical point and the bosonic topological transition", Phys. Rev. X **7**, 031052 (2017).

[26] L. Janssen, I. F. Herbut, and M. M. Scherer, "Compatible orders and fermion-induced emergent symmetry in dirac systems", Phys. Rev. B **97**, 041117 (2018).

[27] B. Roy, P. Goswami, and V. Juričić, "Itinerant quantum multicriticality of two-dimensional dirac fermions", Phys. Rev. B **97**, 205117 (2018).

[28] J. Braun, H. Gies, L. Janssen, and D. Roscher, "Phase structure of many-flavor QED_3", Phys. Rev. D **90**, 036002 (2014).

[29] M. A. Metlitski and A. Vishwanath, "Particle-vortex duality of two-dimensional dirac fermion from electric-magnetic duality of three-dimensional topological insulators", Phys. Rev. B **93**, 245151 (2016).

[30] C. Wang and T. Senthil, "Dual dirac liquid on the surface of the electron topological insulator", Phys. Rev. X **5**, 041031 (2015).

[31] W. Rantner and X.-G. Wen, "Spin correlations in the algebraic spin liquid: Implications for high-T_c superconductors", Phys. Rev. B **66**, 144501 (2002).

[32] M. Franz, Z. Tešanović, and O. Vafek, "QED_3 theory of pairing pseudogap in cuprates: From d-wave superconductor to antiferromagnet via an algebraic Fermi liquid", Phys. Rev. B **66**, 054535 (2002).

[33] D. T. Son, "Is the composite fermion a dirac particle?", Phys. Rev. X **5**, 031027 (2015).

[34] N. Seiberg, T. Senthil, C. Wang, and E. Witten, "A duality web in 2+1 dimensions and condensed matter physics", Annals Phys. **374**, 395–433 (2016).

[35] A. Karch and D. Tong, "Particle-vortex duality from 3d bosonization", Phys. Rev. X **6**, 031043 (2016).

[36] S. Sachdev, *Quantum phase transitions*, 2nd ed. (Cambridge University Press, 2011).

[37] X. G. Wen, *Quantum field theory of many-body systems: From the origin of sound to an origin of light and electrons* (2004).

[38] P. Kopietz, L. Bartosch, and F. Schütz, *Introduction to the functional renormalization group*, Vol. 798 (2010), pp. 1–380.

[39] I. Herbut, *A modern approach to critical phenomena* (Cambridge University Press, 2007).

[40] L. Classen, I. F. Herbut, L. Janssen, and M. M. Scherer, "Competition of density waves and quantum multicritical behavior in Dirac materials from functional renormalization", Phys. Rev. B **93**, 125119 (2016).

[41] I. F. Herbut, V. Juričić, and O. Vafek, "Relativistic mott criticality in graphene", Phys. Rev. B **80**, 075432 (2009).

[42] J. Berges, N. Tetradis, and C. Wetterich, "Nonperturbative renormalization flow in quantum field theory and statistical physics", Phys. Rept. **363**, 223–386 (2002).

[43] M. Kardar, *Statistical physics of fields* (Cambridge University Press, 2007).

[44] A. Katok and B. Hasselblatt, *Introduction to the modern theory of dynamical systems*, Encyclopedia of Mathematics and its Applications (Cambridge University Press, 1995).

[45] S. Gukov, "Rg flows and bifurcations", Nuclear Physics B **919**, 583 –638 (2017).

[46] C. Wetterich, "Exact evolution equation for the effective potential", Phys. Lett. **B301**, 90–94 (1993).

[47] D. F. Litim, "Optimized renormalization group flows", Phys. Rev. **D64**, 105007 (2001).

[48] M. Hogervorst, S. Rychkov, and B. C. van Rees, "Unitarity violation at the Wilson-Fisher fixed point in $4-\epsilon$ dimensions", Phys. Rev. D **93**, 125025 (2016).

[49] B. Knorr, "Ising and Gross-Neveu model in next-to-leading order", Phys. Rev. **B94**, 245102 (2016).

[50] B. Knorr, "Critical (Chiral) Heisenberg Model with the Functional Renormalisation Group", Phys. Rev. B 97, 075129 (2018) (2017).

[51] B. Roy, V. Juričić, and I. F. Herbut, "Emergent Lorentz symmetry near fermionic quantum critical points in two and three dimensions", JHEP **04**, 018 (2016).

[52] O. Pozo, Y. Ferreiros, and M. A. H. Vozmediano, "Anisotropic fixed points in Dirac and Weyl semimetals", Phys. Rev. **B98**, 115122 (2018).

[53] R. Shankar, "Renormalization-group approach to interacting fermions", Rev. Mod. Phys. **66**, 129–192 (1994).

[54] A. Schlief, P. Lunts, and S.-S. Lee, "Exact critical exponents for the antiferromagnetic quantum critical metal in two dimensions", Phys. Rev. X **7**, 021010 (2017).

[55] E. Torres, L. Classen, I. F. Herbut, and M. M. Scherer, "Fermion-induced quantum criticality with two length scales in dirac systems", Phys. Rev. B **97**, 125137 (2018).

[56] K. S. Novoselov, A. K. Geim, S. V. Morozov, D. Jiang, M. I. Katsnelson, I. V. Grigorieva, S. V. Dubonos, and A. A. Firsov, "Two-dimensional gas of massless Dirac fermions in graphene", Nature **438**, 197 (2005).

[57] A. H. Castro Neto, F. Guinea, N. M. R. Peres, K. S. Novoselov, and A. K. Geim, "The electronic properties of graphene", Rev. Mod. Phys. **81**, 109–162 (2009).

[58] S. Sorella and E. Tosatti, "Semi-Metal-Insulator Transition of the Hubbard Model in the Honeycomb Lattice", EPL (Europhysics Letters) **19**, 699 (1992).

[59] I. F. Herbut, "Interactions and Phase Transitions on Graphene's Honeycomb Lattice", Phys. Rev. Lett. **97**, 146401 (2006).

[60] C. Honerkamp, "Density Waves and Cooper Pairing on the Honeycomb Lattice", Phys. Rev. Lett. **100**, 146404 (2008).

[61] S. Raghu, X.-L. Qi, C. Honerkamp, and S.-C. Zhang, "Topological Mott Insulators", Phys. Rev. Lett. **100**, 156401 (2008).

[62] I. F. Herbut, V. Juričić, and B. Roy, "Theory of interacting electrons on the honeycomb lattice", Phys. Rev. B **79**, 085116 (2009).

[63] C. Weeks and M. Franz, "Interaction-driven instabilities of a Dirac semimetal", Phys. Rev. B **81**, 085105 (2010).

[64] D. S. de la Peña, J. Lichtenstein, C. Honerkamp, and M. M. Scherer, "Antiferromagnetism and competing charge instabilities of electrons in strained graphene from Coulomb interactions", Phys. Rev. B **96**, 205155 (2017).

[65] C.-Y. Hou, C. Chamon, and C. Mudry, "Electron Fractionalization in Two-Dimensional Graphenelike Structures", Phys. Rev. Lett. **98**, 186809 (2007).

[66] S. Ryu, C. Mudry, C.-Y. Hou, and C. Chamon, "Masses in graphenelike two-dimensional electronic systems: Topological defects in order parameters and their fractional exchange statistics", Phys. Rev. B **80**, 205319 (2009).

[67] B. Roy and I. F. Herbut, "Unconventional superconductivity on honeycomb lattice: Theory of Kekule order parameter", Phys. Rev. B **82**, 035429 (2010).

[68] L. Classen, M. M. Scherer, and C. Honerkamp, "Instabilities on graphene's honeycomb lattice with electron-phonon interactions", Phys. Rev. B **90**, 035122 (2014).

[69] K. K. Gomes, W. Mar, W.-H. Ko, F. Guinea, and H. C. Manoharan, "Designer Dirac fermions and topological phases in molecular graphene", Nature **483N7389**, 306–310 (2012).

[70] G. Gat, A. Kovner, and B. Rosenstein, "Chiral phase transitions in d = 3 and renormalizability of four Fermi interactions", Nucl. Phys. **B385**, 76–98 (1992).

[71] B. Rosenstein, H.-L. Yu, and A. Kovner, "Critical exponents of new universality classes", Phys. Lett. **B314**, 381–386 (1993).

[72] L. N. Mihaila, N. Zerf, B. Ihrig, I. F. Herbut, and M. M. Scherer, "Gross-Neveu-Yukawa model at three loops and Ising critical behavior of Dirac systems", Phys. Rev. B **96**, 165133 (2017).

[73] L. Iliesiu, F. Kos, D. Poland, S. S. Pufu, and D. Simmons-Duffin, "Bootstrapping 3D Fermions with Global Symmetries", JHEP **01**, 036 (2018).

[74] N. Zerf, L. N. Mihaila, P. Marquard, I. F. Herbut, and M. M. Scherer, "Four-loop critical exponents for the Gross-Neveu-Yukawa models", Phys. Rev. D **96**, 096010 (2017).

[75] S.-K. Jian and H. Yao, "Fermion-induced quantum critical points in three-dimensional Weyl semimetals", Phys. Rev. B **96**, 155112 (2017).

[76] K. G. Wilson and M. E. Fisher, "Critical Exponents in 3.99 Dimensions", Phys. Rev. Lett. **28**, 240–243 (1972).

[77] J. Zinn-Justin, "Precise determination of critical exponents and equation of state by field theory methods", Phys. Rept. **344**, 159–178 (2001).

[78] M. Gräter and C. Wetterich, "Kosterlitz-Thouless Phase Transition in the Two Dimensional Linear σ Model", Phys. Rev. Lett. **75**, 378–381 (1995).

[79] G. v. Gersdorff and C. Wetterich, "Nonperturbative renormalization flow and essential scaling for the Kosterlitz-Thouless transition", Phys. Rev. B **64**, 054513 (2001).

[80] A. Codello, "Scaling Solutions in Continuous Dimension", J. Phys. **A45**, 465006 (2012).

[81] A. Codello and G. D'Odorico, "O(N)-Universality Classes and the Mermin-Wagner Theorem", Phys. Rev. Lett. **110**, 141601 (2013).

[82] L. Janssen and I. F. Herbut, "Antiferromagnetic critical point on graphene's honeycomb lattice: A functional renormalization group approach", Phys. Rev. **B89**, 205403 (2014).

[83] J. Borchardt and A. Eichhorn, "Universal behavior of coupled order parameters below three dimensions", Phys. Rev. **E94**, 042105 (2016).

[84] R. J. Baxter, "Potts model at critical temperature", J. Phys. **C6**, L445–L448 (1973).

[85] F. Y. Wu, "The Potts model", Rev. Mod. Phys. **54**, 235–268 (1982).

[86] R. B. A. Zinati and A. Codello, "Functional RG approach to the Potts model", J. Stat. Mech. **1801**, 013206 (2018).

[87] F. Léonard and B. Delamotte, "Critical Exponents Can Be Different on the Two Sides of a Transition: A Generic Mechanism", Phys. Rev. Lett. **115**, 200601 (2015).

[88] J. Borchardt and B. Knorr, "Global solutions of functional fixed point equations via pseudospectral methods", Phys. Rev. **D91**, [Erratum: Phys. Rev.D93,no.8,089904(2016)], 105011 (2015).

[89] J. Borchardt and B. Knorr, "Solving functional flow equations with pseudo-spectral methods", Phys. Rev. **D94**, 025027 (2016).

[90] P. Ponte and S.-S. Lee, "Emergence of supersymmetry on the surface of three dimensional topological insulators", New J. Phys. **16**, 013044 (2014).

[91] T. Grover, D. N. Sheng, and A. Vishwanath, "Emergent Space-Time Supersymmetry at the Boundary of a Topological Phase", Science **344**, 280–283 (2014).

[92] Z.-X. Li, A. Vaezi, C. B. Mendl, and H. Yao, "Observation of Emergent Spacetime Supersymmetry at Superconducting Quantum Criticality", Sci. Adv. 4, eaau1463 (2018) (2017).

[93] B. Roy, "Multicritical behavior of $\mathbb{Z}_2 \oplus O(2)$ Gross-Neveu-Yukawa theory in graphene", Phys. Rev. B **84**, 113404 (2011).

[94] S.-C. Zhang, "A Unified Theory Based on $SO(5)$ Symmetry of Superconductivity and Antiferromagnetism", Science **275**, 1089–1096 (1997).

[95] C. Wang, A. Nahum, M. A. Metlitski, C. Xu, and T. Senthil, "Deconfined quantum critical points: symmetries and dualities", Phys. Rev. X **7**, 031051 (2017).

[96] H. Shao, W. Guo, and A. W. Sandvik, "Quantum criticality with two length scales", Science **352**, 213–216 (2016).

[97] E. Torres, L. Janssen, and M. M. Scherer, "Emergent symmetry and order-to-order transitions of Dirac fermions with two compatible order parameters.", In preparation (Mar 2019).

[98] A. Das and S. Okubo, *Lie groups and lie algebras for physicists* (WORLD SCIENTIFIC, 2014).

[99] A. Eichhorn, D. Mesterházy, and M. M. Scherer, "Multicritical behavior in models with two competing order parameters", Phys. Rev. E **88**, 042141 (2013).

[100] P. Calabrese, A. Pelissetto, and E. Vicari, "Multicritical phenomena in $O(n_1) \oplus O(n_2)$-symmetric theories", Phys. Rev. B **67**, 054505 (2003).

[101] M. Levin and T. Senthil, "Deconfined quantum criticality and néel order via dimer disorder", Phys. Rev. B **70**, 220403 (2004).

[102] I. Boettcher, J. M. Pawlowski, and S. Diehl, "Ultracold atoms and the functional renormalization group", Nuclear Physics B - Proceedings Supplements **228**, "Physics at all scales: The Renormalization Group" Proceedings of the 49th Internationale Universitätswochen für Theoretische Physik, 63 –135 (2012).

[103] N. Khan, J. M. Pawlowski, F. Rennecke, and M. M. Scherer, "The Phase Diagram of QC_2D from Functional Methods", arXiv e-prints, arXiv:1512.03673 (2015).

[104] J. Braun, H. Gies, and D. D. Scherer, "Asymptotic safety: a simple example", Phys. Rev. D **83**, 085012 (2011).

[105] L. Janssen, "Spontaneous breaking of Lorentz symmetry in $2 + \epsilon$-dimensional QED", Phys. Rev. D **94**, 094013 (2016).

[106] W. Wetzel, "Two-loop β-function for the Gross-Neveu model", Physics Letters B **153**, 297 –299 (1985).

[107] J. Gracey, "Three-loop calculations in the $O(N)$ gross-neveu model", Nuclear Physics B **341**, 403 –418 (1990).

[108] C. Luperini and P. Rossi, "Three-loop β-function(s) and effective potential in the Gross-Neveu model", Annals of Physics **212**, 371 –401 (1991).

[109] D. Roscher, E. Torres, and P. Strack, "Dual QED$_3$ at "$N_F = 1/2$" is an interacting CFT in the infrared", Journal of High Energy Physics **2016**, 17 (2016).

[110] J. Gracey, "Computation of critical exponent η at $O(1/N_f^2)$ in quantum electrodynamics in arbitrary dimensions", Nuclear Physics B **414**, 614 –648 (1994).

[111] W. Chen, M. P. A. Fisher, and Y.-S. Wu, "Mott transition in an anyon gas", Phys. Rev. B **48**, 13749–13761 (1993).

[112] R. K. Kaul and S. Sachdev, "Quantum criticality of $U(1)$ gauge theories with fermionic and bosonic matter in two spatial dimensions", Phys. Rev. B **77**, 155105 (2008).

[113] S. S. Pufu, "Anomalous dimensions of monopole operators in three-dimensional quantum electrodynamics", Phys. Rev. D **89**, 065016 (2014).

[114] Y. Huh and P. Strack, "Stress tensor and current correlators of interacting conformal field theories in 2+1 dimensions: fermionic Dirac matter coupled to $U(1)$ gauge field", Journal of High Energy Physics **2015**, 1–17 (2015).

[115] S. M. Chester and S. S. Pufu, "Anomalous dimensions of scalar operators in QED$_3$", Journal of High Energy Physics **2016**, 69 (2016).

[116] S. Giombi, G. Tarnopolsky, and I. R. Klebanov, "On C_J and C_T in conformal QED", Journal of High Energy Physics **2016**, 156 (2016).

[117] S. Giombi, I. R. Klebanov, and G. Tarnopolsky, "Conformal QED$_d$, F-theorem and the ϵ expansion", Journal of Physics A: Mathematical and Theoretical **49**, 135403 (2016).

[118] L. Di Pietro, Z. Komargodski, I. Shamir, and E. Stamou, "Quantum Electrodynamics in $d = 3$ from the ϵ Expansion", Phys. Rev. Lett. **116**, 131601 (2016).

[119] J. Polchinski, "Renormalization and effective lagrangians", Nuclear Physics B **231**, 269 –295 (1984).

[120] A. J. Niemi and G. W. Semenoff, "Axial-anomaly-induced fermion fractionization and effective gauge-theory actions in odd-dimensional space-times", Phys. Rev. Lett. **51**, 2077–2080 (1983).

[121] A. N. Redlich, "Gauge noninvariance and parity nonconservation of three-dimensional fermions", Phys. Rev. Lett. **52**, 18–21 (1984).

[122] A. N. Redlich, "Parity violation and gauge noninvariance of the effective gauge field action in three dimensions", Phys. Rev. D **29**, 2366–2374 (1984).

[123] M. Mulligan and F. J. Burnell, "Topological insulators avoid the parity anomaly", Phys. Rev. B **88**, 085104 (2013).

[124] J. Polchinski, "Dualities of fields and strings", Studies in History and Philosophy of Science Part B: Studies in History and Philosophy of Modern Physics **59**, Dualities in Physics, 6 –20 (2017).

[125] T. Senthil, D. T. Son, C. Wang, and C. Xu, "Duality between $(2 + 1)d$ Quantum Critical Points", (2018).

[126] A. Altland and B. D. Simons, *Condensed matter field theory*, 2nd ed. (Cambridge University Press, 2010).

[127] J. v. Delft and H. Schoeller, "Bosonization for beginners — refermionization for experts", Annalen der Physik **7**, 225–305 (1998).

[128] A. Gogolin, A. Nersesyan, and A. Tsvelik, *Bosonization and strongly correlated systems* (Cambridge University Press, 2004).

[129] C. Dasgupta and B. I. Halperin, "Phase transition in a lattice model of superconductivity", Phys. Rev. Lett. **47**, 1556–1560 (1981).

[130] D. F. Mross, J. Alicea, and O. I. Motrunich, "Explicit Derivation of Duality between a Free Dirac Cone and Quantum Electrodynamics in $(2+1)$ Dimensions", Phys. Rev. Lett. **117**, 016802 (2016).

[131] D. J. Gross and A. Neveu, "Dynamical symmetry breaking in asymptotically free field theories", Phys. Rev. D **10**, 3235–3253 (1974).

[132] J. Gracey, "Electron mass anomalous dimension at $O(1/N^2)$ in quantum electrodynamics", Physics Letters B **317**, 415 –420 (1993).

[133] W. Pan, W. Kang, K. W. Baldwin, K. W. West, L. N. Pfeiffer, and D. C. Tsui, "Berry phase and anomalous transport of the composite fermions at the half-filled Landau level", Nature Physics **13**, 1168–1172 (2017).

[134] M. Levin and D. T. Son, "Particle-hole symmetry and electromagnetic response of a half-filled landau level", Phys. Rev. B **95**, 125120 (2017).

[135] A. C. Potter, M. Serbyn, and A. Vishwanath, "Thermoelectric transport signatures of dirac composite fermions in the half-filled landau level", Phys. Rev. X **6**, 031026 (2016).

[136] D. F. Litim, "Optimization of the exact renormalization group", Phys. Lett. **B486**, 92–99 (2000).

[137] D. F. Litim, "Mind the gap", Int. J. Mod. Phys. **A16**, 2081–2088 (2001).

[138] D. F. Litim, "Critical exponents from optimized renormalization group flows", Nucl. Phys. **B631**, 128–158 (2002).

[139] J. M. Pawlowski, M. M. Scherer, R. Schmidt, and S. J. Wetzel, "Physics and the choice of regulators in functional renormalisation group flows", Annals of Physics **384**, 165 –197 (2017).

Acknowledgements

So many people to thank and so few of them will actually read this!

In the first place I want to use the opportunity to thank my advisor, Michael Scherer, for accepting the challenge of adopting a one year old orphan PhD student. Not only did he do a superb job as an advisor by being always ready to help and providing interesting projects to work on, but he was also full of patience when the projects were going at an excrutiatingly slow pace (sorry for that!), and always made sure I felt like a valuable member of the team. Danke auch dass du von Anfang an bereit warst mit mir über Physik auf deutsch zu reden, Ich weiß dass es wahrscheinlich nicht immer einfach war, und dafür bin ich sehr dankbar.

I want to thank Philipp Strack for giving me the opportunity to work with him, even though our collaboration was short lived. Thanks to Prof. Achim Rosch, not only for the time he took to help me with my projects during the transition period after my former advisor left, but also for agreeing to be the second examiner of this work. In this regard, my dearest thanks go to Henry Legg for proofreading long parts of this manuscript and to Florian Lange.

I have met some great colleagues during my time at the institute, and I would like to thank in particular all of the people that had the burden of sharing an office with me the last few years, for they all made the work hours just a bit more fun: Yoran, Jan, Florian and Francis. To my colleagues Federico and Henry in particular I am grateful for the many hours of not so productive conversations that still somehow always reminded me how much I enjoy the work we do. Thanks are also in order to the crew of the Renormierbar™ for the fun atmosphere they managed to create in the otherwise nonexistant landscape of social events of the institute.

An dieser Stelle möchte ich mich ganz herzlich bei meine Karate Familie bedanken: Erkan, Kaan und Filiz. Eure Unterstützung war mir enorm wichtig und nicht nur während die viele Trainings, Lehrgänge und Wettkämpfe, sondern auch außerhalb des Dojos. Ihr habt mich als Teil eure Familie angenommen und diese Arbeit wäre ohne eure Hilfe nicht möglich gewesen. Ich bin wirklich stolz der "andere Sohn" zu sein.

Y bueno, ahora que oficialmente acaba mi "periodo formativo", parece ser un buen momento para agradecerle a toda la gente que ha hecho de éste un camino tan placentero. A los físicos: Dani, Guti, Macla, Juli, Juanchito, Juanito, Mario, Nico y Anny. De tanto que la pasamos bueno, a veces todavía dudo que de hecho hayamos estudiado. A Monika por ser la persona más querida y ayudarme tanto durante y después de mi tiempo en el H. Special thanks go to Elenita for the many years of moral support.

Por último quiero agradecerle a mi familia: a mis hermanos y especialmente a mi madre por todo el apoyo incondicional y por creer en mi cuando me decidí embarcar en esta aventura. La contribución que han hecho a este trabajo es imposible de calcular.

Erklärung

Ich versichere, dass ich die von mir vorgelegte Dissertation selbständig angefertigt, die benutzten Quellen und Hilfsmittel vollständig angegeben und die Stellen der Arbeit - einschließlich Tabellen, Karten und Abbildungen -, die anderen Werken im Wortlaut oder dem Sinn nach entnommen sind, in jedem Einzelfall als Entlehnung kenntlich gemacht habe; dass diese Dissertation noch keiner anderen Fakultät oder Universität zur Prüfung vorgelegen hat; dass sie - abgesehen von unten angegebenen Teilpublikationen - noch nicht veröffentlicht worden ist sowie, dass ich eine solche Veröffentlichung vor Abschluss des Promotionsverfahrens nicht vornehmen werde. Die Bestimmung der Promotionsordnung sind mir bekannt. Die von mir vorgelegte Dissertation ist von PD Dr. Michael Scherer betreut worden

Teilpublikationen

- *Dual QED$_3$ at $N_\mathrm{f} = 1/2$ is an interacting CFT in the infrarred.*
  Dietrich Roscher, **Emilio Torres** and Philipp Strack.
  J. High Energ. Phys. (2016) 2016:17.
- *Fermion-induced quantum criticality with two length scales in Dirac systems.*
  Emilio Torres, Laura Classen, Igor H. Herbut and Michael M. Scherer.
  Phys. Rev. B, **97**,125137 (2018).
- *Emergent symmetry and order-to-order transitions of Dirac fermions with two compatible order parameters.*
  Emilio Torres, Lukas Janssen and Michael M. Scherer.
  In preparation (Jul. 2019).

Signed:

Date: